MATERIALS AND MANUFACTURING PROCESSES

Special Issue on
Hard Carbon Films

Volume 8 *Number 1* *1993*

MATERIALS AND MANUFACTURING PROCESSES

Aims and Scope. *Materials and Manufacturing Processes* is a journal in the English language providing an international forum for current developments and future direction in the area of materials and manufacturing processes. Manuscripts may fall into several categories including full articles, solicited reviews, or commentary, unsolicited reviews or commentary, and patent and book reviews.

Subscription Information. *Materials and Manufacturing Processes* (ISSN: 1042-6914) is published in six numbers by Marcel Dekker, Inc., 270 Madison Avenue, New York, New York 10016. The subscription rate for 1993 is as follows:

			Individual Professionals	Foreign Postage		
Volume	Frequency	Institutional Rate	and Student Rate	Surface	Airmail To Europe	Airmail To Asia
8	6 numbers	$495.00	$35.00	$21.00	$33.00	$39.00

Your order must be prepaid by personal check or may be charged to MasterCard, VISA, or American Express. Please mail payment with your order to: Marcel Dekker Journals, P.O. Box 5017, Monticello, New York 12701-5176.

CODEN: MMAPET 8(1) i-vi, 1-128 (1993)
ISSN: 1042-6914

MATERIALS AND MANUFACTURING PROCESSES

Editors

T.S. SUDARSHAN
Materials Modification, Inc.
2929-P1 Eskridge Center
Fairfax, Virginia 22031
phone # (703) 560-1371
fax # (703) 560-1372

T.S. SRIVATSAN
Department of Mechanical Engineering
The University of Akron
Akron, Ohio 44325
phone # (216) 972-6196
fax # (216) 972-6027

MATERIALS AND MANUFACTURING PROCESSES

Indexing and Abstracting Services. Articles published in *Materials and Manufacturing Processes* are selectively indexed or abstracted in:

■ Abstracts Journal of the Institute of Scientific Information of the USSR Academy of the Sciences ■ Academy of Sciences of the USSR ■ Advanced Ceramics Bulletin ■ Advanced Composites Bulletin ■ American Society for Metals ■ Applied Mechanics Reviews ■ Ceramics Bulletin ■ Chemical Abstracts ■ Corrosion Abstracts ■ Engineering Index ■ INSPEC ■ ISI-Materials Science Citation Index ■ Japan Abstracts ■ Japan Institute of Metals ■ Rapra Abstracts ■ UNIDO-Tech Monitor

Manuscript Preparation and Submission. See end of issue.

The Journals of Marcel Dekker, Inc. are available in microform from: RESEARCH PUBLICATIONS, 12 Lunar Drive, Drawer AB, Woodbridge, Connecticut, 06525, (203) 397-2600 or Toll Free 1-800-REACH-RP (732-2477). Outside North and South America: P.O. Box 45, Reading, RG1 8HF, England, 0734-583247.

Contributions to this journal are published free of charge.

This journal is printed on acid-free paper.

Typeset by SV Associates, Herndon, Virginia.

SPECIAL ISSUE ON
HARD CARBON FILMS

This is a special issue of *Materials and Manufacturing Processes*, Volume 8, Number 1, 1993.

MARCEL DEKKER, INC. New York, Basel, Hong Kong

MATERIALS & MANUFACTURING PROCESSES, 8(1), 1-8 (1993)

LASER PROCESSING OF DIAMOND AND DIAMOND-LIKE FILMS

V.P. Ageev, V.Yu. Armeyev, N.I. Chapliev,
A.V. Kuzmichov, S.M. Pimenov, and V.G. Ralchenko

Institute of General Physics
USSR Academy of Sciences
Vavilov str., 38
Moscow 117942, USSR

ABSTRACT

Laser processing of polycrystalline diamond and amorphous carbon films is shown to be a promising technology for micropatterning of these materials in electronics and other applications. By using excimer lasers, holes and pits have been formed in 10-60 μm thick diamond films by physical etching with ablation rates of up to 300 nm/pulse. The channels of micrometer scale width were created in diamond-like carbon films on silicon by chemical etching in oxygen by the scanning with a cw Ar^+ laser beam. At laser powers below the etching threshold, a transformation of amorphous carbon to graphitic carbon allows the formation of conductive lines of different geometry in dielectric carbon layers.

INTRODUCTION

The potential applications of diamond and diamond-like carbon (DLC) films in science and industry are based on unique properties of these films and relatively simple techniques of their deposition on different substrates (1-3). The very high hardness and wear resistance, inertness against aggressive chemical environment, low friction coefficient make carbon coatings invaluable in mechanical engineering. Electronic properties of diamond and related carbon materials combined with the extremely high values of thermal conductivity and breakdown voltage allow consideration of such films as active and passive elements in microelectronic devices. Wide optical range of transparency of diamond and the possibility of varying precisely the optical properties of DLC films in the course of the growth process are primary requisites for use of carbon films as protective and antireflection layers on optical elements.

Applications of carbon films in microelectronics require the development of methods of their treatment either directly during the growth process or after the film synthesis. For example, after deposition of isolated diamond or DLC layers on active elements of integrated circuits, it is necessary to make windows, metallization and patterning with submicron resolution. In the present paper we consider some approaches to use lasers for microprocessing of diamond and DLC films, that can be of interest in technology.

EXPERIMENTAL PROCEDURE

Experiments were conducted either in pulsed or in continuous wave modes of irradiation. In the latter case the laser beam was scanned over the surface to be treated. The lasers on excimer molecules XeCl and KrF emitting the pulses of 14-40 ns duration at 308 nm and 248 nm wavelengths, and also CO_2 laser operated at 10.6 μm wavelength with 1-2 μs pulse duration were used as pulsed radiation sources. Ar^+ ion laser emitting continuous wave light of 1.5 W power at 488 nm wavelength was used in direct writing mode.

The laser beam was focused onto a surface by the objectives with different focal length to obtain the beam spot of 1-1000 μm in diameter. The samples to be irradiated were placed on an x-y table within a vacuum chamber pumped off to 10^{-6} torr pressure, that could be filled then by oxygen or xenon. The output laser parameters as well as reflected and/or transmitted main (excimer, CO_2)or probe (He-Ne laser) beams were measured to characterize the energy absorbed and structural changes in material.

Polycrystalline diamond films of 10 to 60 μm thickness were deposited onto tungsten and silicon at the temperature of about 1000°C from DC arc discharge in a methane/hydrogen mixture. The coatings with either pyramid-like or globular structures could be produced by variation of deposition parameters. DLC films were grown on silicon wafers from r.f. glow discharge in benzene. The density of 1.3 μm thick films was about 2.4 g/cm^3 and hydrogen content up to 20% at., as determined by secondary ion mass spectrometry. Different methods were used to study the film structure before and after laser action, including an optical and scanning electron microscopy (SEM), Raman spectroscopy, and surface profile measurements. In some cases the samples were irradiated right inside the SEM vacuum chamber in order to monitor an evolution of surface structure in the process of multishot laser action.

RESULTS AND DISCUSSIONS

Physical etching of diamond films

The noticeable etching of diamond was observed only at laser fluences above some threshold value E_{th} dependent on the laser wavelength. For example, the threshold fluence is equal to E=1 J/cm^2 for pulses at 308 nm wavelength. The

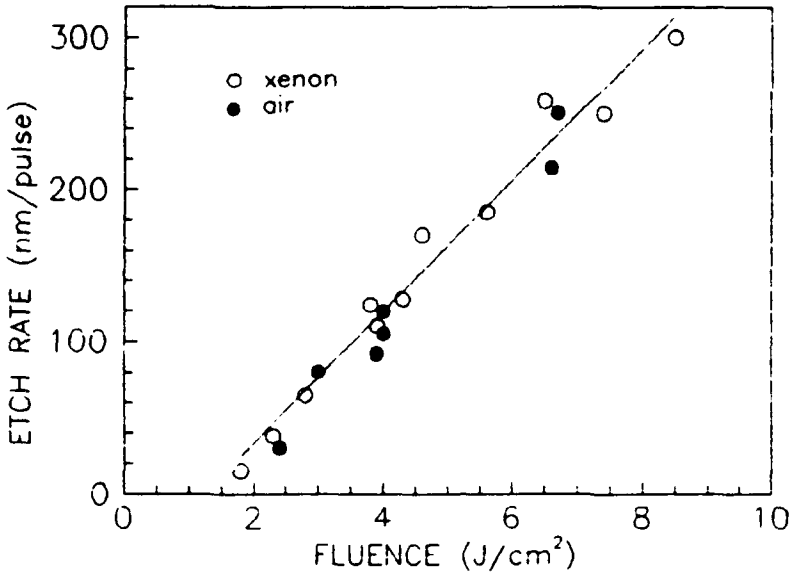

Figure 1. Etching rate of diamond film versus laser fluence in XeCl excimer laser pulse in air and xenon.

etching rate determined as the thickness of the layer removed by one pulse depends linearly on fluence in the entire range studied (E=0.1-18 J/cm^2), being the same in xenon and air as shown in Fig.1. The threshold of the etching as well as etching rate slightly depend on laser wavelength. The results obtained with KrF laser (wavelength 248 nm) are presented elsewhere (4).

We note the extremely high etching rate achieved, up to 300 nm/pulse, which is several orders of magnitude higher than the value of 200 nm/s reported for etching of natural diamond with NO_2 molecules assisted by Xe^+ ion beam (5).

The independence of etching rate on the surrounding gas indicates a physical rather than the chemical nature of the etching process. Thus, the temperature of T=3500°C, required for carbon sublimation, should be reached in every pulse. However, our estimates show that at etching threshold fluence E_{th}=1 J/cm^2 the maximum surface temperature doesn't exceed 1000°C because of low extinction coefficient (α=2000 cm^{-1}) and high thermal conductivity (k=4.1 W/cm•s•K) of the film (6,7). We suggest therefore that an initial part of the laser pulse transforms an outer layer of diamond to an opaque graphite-like phase with reduced thermal conductivity. Then the remaining part of the pulse easily heats and removes the graphitized layer. The next pulse triggers the same process, allowing a graphite piston to move deeper. This model was proposed by Rothschild et al. (8). The graphitization step is supported by Raman spectra and optical transmission measurements of irradiated free-standing films (6). Particularly, the structure of

material at the crater's bottom is similar to that of amorphous (glassy) carbon or graphite with extremely small (20-30 Å) grain size. The threshold fluence for graphitization is found to be not more than 0.02 J/cm^2 at 308 nm (6).

Patterning of diamond films

For fabrication of microelectronic devices it is necessary to create structures in diamond with submicron resolution. However, the formation of such fine structures was not the aim of present work, so we dealt usually with patterns of several micrometers size or more. The microstructures were produced by two methods, both based on material ablation. In the first case the beam of an excimer laser was projected onto the film surface through a metallic mesh with a cell size of 100 μm. Figure 2 shows an example of a structure (pit array), produced by such a technique (laser lithography). Earlier Rothschild et al (8,9) had achieved submicron resolution in etching of natural diamond and diamond-like films using a similar optical scheme at 193 nm wavelength.

Another method uses the formation of light-induced periodical structures (ripples) under the action of polarized laser beam. The ripples appear as a result of interference of incident and scattered waves, modulation of incident and absorbed laser intensity and, consequently, temperature and etch rate of the irradiated surface (10). In this case the periodicity of microrelief depends on wavelength, angle of incidence and polarization state. Figure 3 shows a SEM picture of the film area subjected to a series of CO_2 laser pulses with Gaussian intensity profile and linear polarization. The diffraction gratings produced with the period around 10 μm close to CO_2 laser wavelength can be used as deflectors in optics and in fabrication of diamond-based electronic devices.

One more approach to the formation of narrow channels with a desired configuration should be noted, namely a direct laser writing (9). In this mode the pulse-repetition or cw lasers can be used to evaporate a material by the finely focused beam, scanned along a computer-controlled path. Concerning the carbon materials this technique was used earlier to treat only DLC films with pulsed YAG and excimer lasers (9,11), but it can be applied obviously to diamond films too.

Chemical etching of DLC films.

Compared with diamond, the DLC films containing some quantity of graphitic bonds, are more chemically active and more opaque. According to Smith (12) an extinction coefficient of amorphous carbon in the visible is in the range 10^4 -10^5 cm^{-1}. These circumstances allow to use effectively the laser heating for etching of DLC films in air via carbon oxidation reaction, that occur at temperatures even lower than 1000°C. Using an Ar^+ ion laser beam 1 to 20 μm in diameter (d), and scanning velocity (V) in the range 5 - 400 μm/s we have formed the channels in the films. As an example, the channel produced at d=2 μm is shown in Fig.4.

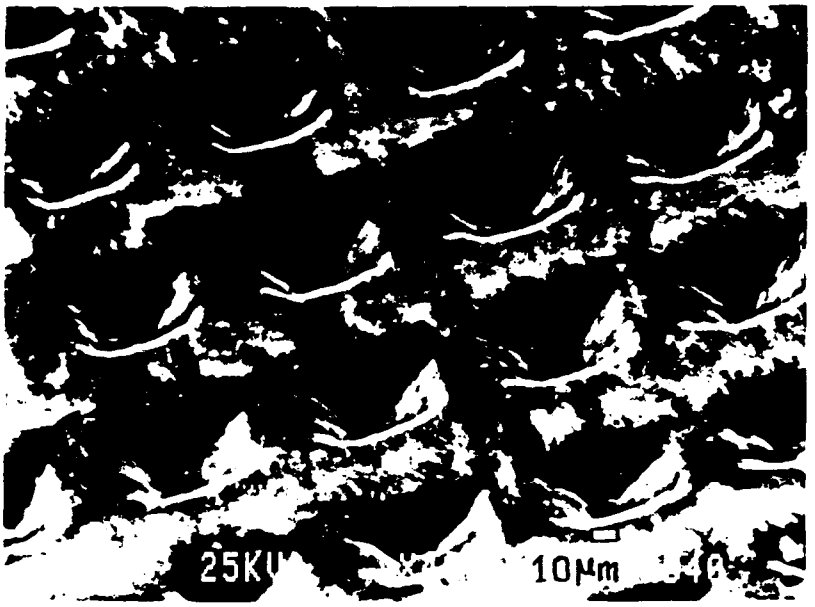

Figure 2. Pit array in diamond film produced by projecting technique with KrF laser in multishot mode.

Figure 3. Periodic structure on diamond film produced by microsecond pulses of linearly polarized CO_2 laser

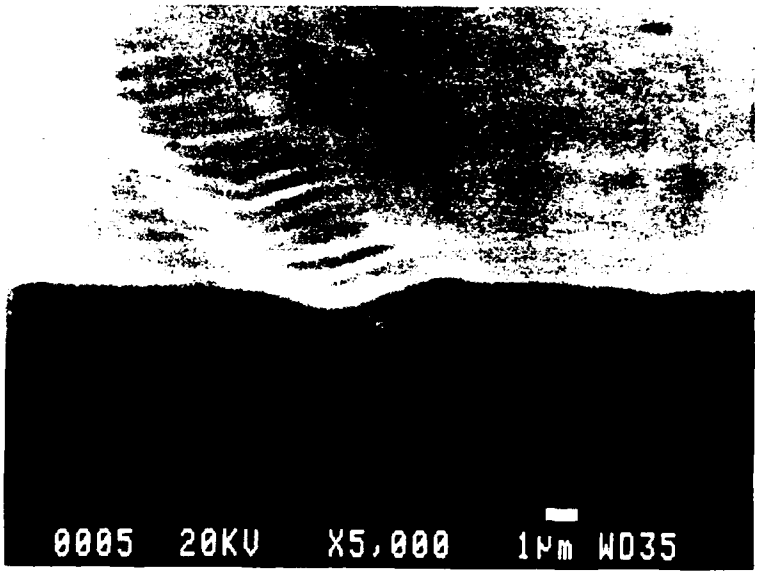

Figure 4. Channel in DLC film etched in air by direct writing with Ar^+ laser

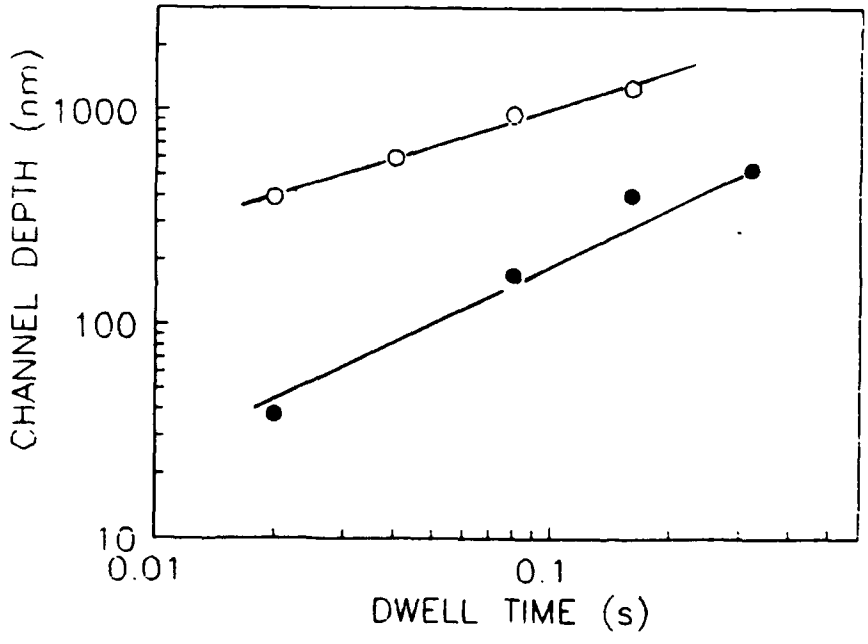

Figure 5. Depth of channel in DLC film etched in air versus exposure time at laser powers 310 mW (full circles) and 610 mW (open circles). Beam diameter d=8 μm.

For every set of irradiation parameters the threshold laser power (P_o), above which etching starts, was found. This value corresponds to the appearance of about 1 nm deep channel- the smallest one, that could be detected by our profilometer. Particularly, at V=400 μm/s the value of P_o was equal to 50 mW and 180 mW for beam diameters d=2 μm and d=8 μm, respectively. The corresponding threshold temperature was about 600°C as evidenced by thermogravimetric analysis of the film burnt in oxygen and by the temperature estimates, derived from the analysis of Raman spectra of the irradiated films (13).

Figure 5 shows that the depth of etched channels, (h) increases approximately linearly with exposure time τ=d/V, varied by the appropriate choice of scanning velocity. From Arrhenius law for carbon oxidation $h = Const \cdot \exp(-E_a/RT) \cdot \tau$, where E_a is activation energy, it follows, that the surface temperature distribution is the same for different values of τ. The maximum temperature within the beam spot is independent of scanning velocity, because of the exposure time $\tau = 10^{-2}$-1 s is much greater than the characteristic time $t \approx d^2/\sigma \approx 10^{-5} - 10^{-6}$ s (σ is thermal diffusivity of a film or a substrate), required to establish a steady-state temperature. The etching rates as high as 40 μm/s at d=8 μm have been measured in case of oxidation in air. Even higher values could be obtained by the increase of laser intensity and/or oxygen partial pressure.

Writing of conductive lines in DLC films.

The laser heating with power lower than the etching threshold value results in a structural transition from dielectric diamond-like state to conducting graphite-like one. We note that a graphitization process starts at temperatures T=400-450°C (1,13). Our optical scheme allowed us to observe in situ with microscope the contrast lines of 3-15 μm width appeared in the process of direct writing with Ar^+ laser beam with 20 μm spot size and power below etching threshold. The resistivity drop from 10^8 Ohm•cm (virgin film) to 10^{-2} - 10^{-1} Ohm•cm (graphitized line) have been detected by two probe technique, the latter value being low enough to use the laser annealed DLC film for fabrication of resistors, interconnections and adhesive, highly wear resistant and nonoxidizable electrical contacts of better quality than ones prepared by laser carbonization of polymer films (14).

CONCLUSIONS

The experiments conducted and discussed herein have shown that laser technology is useful in local processing of diamond and diamond-like carbon films. We demonstrated the effective physical etching of diamond films by excimer laser radiation, the etching rate reaching 300 nm per 40 ns pulse. The chemical etching of DLC films in oxygen with etching rates up to 40 μm/s was performed using the Ar^+ laser in direct writing mode. Lastly, the conductive lines of micrometer scale width were created within dielectric DLC films.

REFERENCES

1. Angus, J.C., P. Koidl, and S. Domitz, Plasma Deposited Thin Films, J. Morton and F. Jansen (eds), CRC Press, Boca Raton, Fla, p.89, (1986).

2. Yoshikawa, M., (ed), New Diamond, Ohmsha Ltd, Tokyo, (1988).

3. Spitsyn, B.V., L.L. Bouilov, and B.V. Derjaguin, Journal of Crystal Growth, Vol.52, p.219, (1981).

4. Chapliev, N.I., V.I. Konov, S.M. Pimenov, A.A. Smolin, B.V. Spitsyn, I.G. Teremetskaya, A. Blatter, U. Bogli, and H.P. Weber, Excimer Laser Etching and Polishing of Diamond Films. Paper presented at Second International Symposium on Diamond Materials, Washington, D.C. (to be published), May 6-10, (1991).

5. Efremow, N.N., M.W. Geis, D.C. Flanders, G.A. Lincoln, and N.P. Economou, Journal of Vacuum Science and Technology B, Vol.4, p.416, (1985).

6. Ageev, V.P., L.L. Bouilov, V.I. Konov, A.V. Kuzmichev, S.M. Pimenov, A.M. Prokhorov, V.G. Ralchenko, B.V. Spitsyn, and N.I. Chapliev, Soviet Physics - Doklady, Vol.33, p.840, (1988).

7. Bouilov, L.L., A.A. Aleksenko, A.A. Botev, and B.V. Spitsyn, Doklady AN SSSR, (in Russian), Vol.287, p.888, (1986).

8. Rothschild, M., C. Arnone, and D.J. Ehrlich, Journal of Vacuum Science and Technology B, Vol.4, p.310, (1986).

9. Rothschild, M., and D.J. Ehrlich, Journal of Vacuum Science and Technology B, Vol.5, p.389, (1987).

10. Siegman, A.E., and P.M. Fauchet, IEEE Journal of Quantum Electronics, Vol.QE-22, p.1384, (1986).

11. Prawer, S., R. Kalish, and M. Adel, Applied Physics Letters, Vol.48, p.1585, (1986).

12. Smith, F.W., Journal of Applied Physics, Vol.55, p.764, (1984).

13. Armeyev, V.Yu., V.I. Mikhailov, V.G. Ralchenko, and V.E. Strelnitsky, Soviet Physics-Lebedev Institute Reports, No.5, p.17, (1990).

14. Lyons, A.M., C.M. Wilkins, and F.T. Mendenhall, Laser and Particle-Beam Chemical Processing for Microelectronics, Ehrlich, D.J., G.S. Higashi, and M.M. Oprysko, (eds.), Materials Research Society Symposia Proceedings, Pittsburgh, Vol.101, p.67, (1988).

MATERIALS & MANUFACTURING PROCESSES, 8(1), 9-17 (1993)

DIRECT LASER WRITING OF MICROSTRUCTURES IN DIAMOND-LIKE CARBON FILMS

V.Yu. Armeyev, N.I. Chapliev, I.M. Chistyakov, V.I. Konov
V.G. Ralchenko, V.E. Strelnitsky, and V.Ya. Volkov

General Physics Institute
Academy of Sciences
Vavilov str., 38
117942 Moscow, CIS

ABSTRACT

The formation of conductive lines into a dielectric diamond-like carbon film via the graphitization of an amorphous phase under the action of a scanning Ar+ laser beam is reported. The nucleation of small (≤ 30 Å) graphite crystallites, as evidenced by Raman spectroscopy, results in a resistivity drop from 10^8 Ωcm to $5x10^{-2}$ Ωcm. Microchannels have been etched in the film via carbon oxidation in air. The dependence of the etching rate on the laser power reveals two distinct regions assigned to different activation energies.

INTRODUCTION

Diamond (D) and diamond-like carbon (DLC) films are recognized as very attractive materials for many applications due to their high electrical resistivity, extreme hardness and wear resistance, chemical resistance and optical transparency from UV to IR (1,2). The structure of DLC films is amorphous, consisting of a mixture of three-fold sp^2 *graphitic* bonds and four-fold sp^3 *diamond* bonds. Annealing of DLC films in the temperature range 300 - 600°C results in a conversion of sp^3 to sp^2 bonds with an appearance of the graphite microcrystals and loss of diamond-like properties (3,4). On the other hand the unique mechanical and chemical characteristics of D and DLC films require some sophisticated treatment technologies. In the field of microelectronics lasers offer the possibilities of forming the diverse structures in carbon materials, including submicrometer patterning both of D and DLC films (5,6), drilling and polishing of thick D films (7), and writing of conductive strips in DLC films (8).

All the previous studies of laser interaction with DLC films were performed with the aid of short pulse laser sources. In the present paper we have studied the annealing and etching of these films by continuous wave argon ion laser. In this case the cw laser action is assumed to be complicated because of: a) the heat affected zone spreads significantly, b) reactivity of ambient gas (e.g., oxygen) often becomes more important, and c) substrate-coating interaction may occur even for thick opaque films.

EXPERIMENTAL

The DLC films 1 μm thick were deposited onto Si wafers from r.f. glow discharge in benzene using a technique, similar to that described elsewhere (9). They have high density 2.4 g/cm^3, electrical resistivity 10^8 Ωcm and microhardness 35 GPa. According to SIMS analysis the hydrogen content was about 15% at. The Gaussian beam of a cw Ar+ laser emitting at λ = 488 nm wavelength was focused onto the film surface, the beam spot diameter, d, being varied from 1 μm to 30 μm. The samples were mounted on a translation stage, moving with a velocity of up to 400 μm/s. The electrical resistance of the strips formed was measured by the two-probe method. The surface relief in a heat affected zone was recorded with *Talystep* Taylor-Hobson profilometer. The structure transformations in the films irradiated were studied by Raman spectroscopy with Jobin-Ivon MOLE Microprobe. The green line at λ = 514.5 nm was used for the scattering excitation in a spot of $\approx$ 1 μm diameter.

RESULTS AND DISCUSSION

Writing of conductive lines

The resistance, R, of the lines of l = 6-8 mm length annealed at different laser power was measured using silver paste contacts. The data normalized per unit length (Ω/μm) are shown in Fig.1. Also shown is the resistivity, ρ, of the modified material, calculated as $\rho = (R/l)\cdot w\cdot h_o$, where h_o is the film thickness and w is the line width. We assume a transformation to occur homogeneously through the whole film depth as the temperature distribution in the depth is nearly uniform within a surface layer considered. The resistivity drops at a threshold power $P_{th} \approx 420$ mW, when the graphitization is assumed to start. With a further power increase the value of ρ decreases to the minimum level of 5×10^{-2} Ωcm, still remaining 2 orders of magnitude lower than that of well crystallized graphite. We conclude that the annealing of amorphous carbon results in some intermediate graphite-like structure, as observed previously (8) in case of pulsed laser treatment of DLC films.

Concerning the resistivity calculation used it is necessary to pay attention to the importance of correct measurement of the line width, w. We determined the value of w versus laser power by two ways. In the first case the profilometer was used to measure the surface relief in the heat affected zone. The data obtained are referred henceforth as *profile* width. In the second one the lines were directly observed and

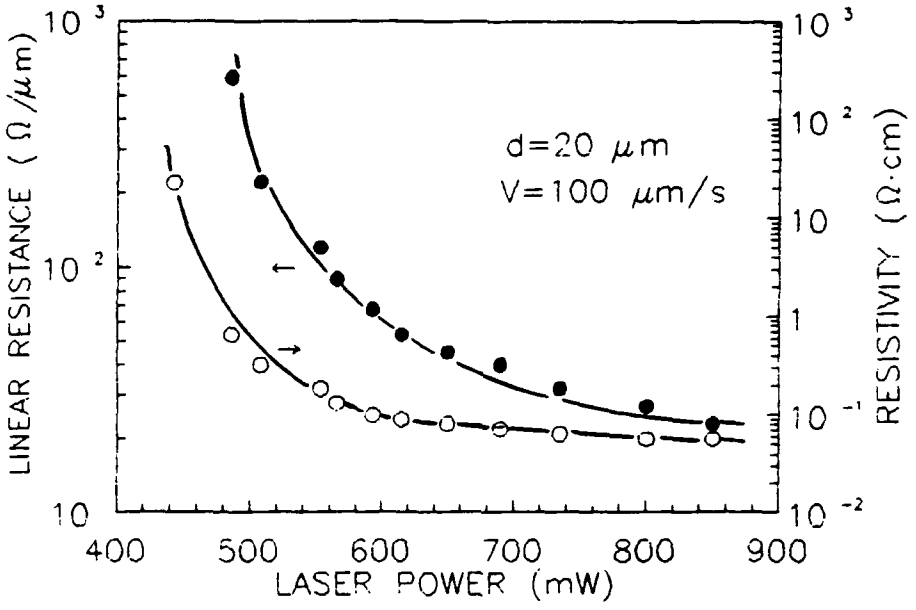

Figure 1. Linear resistance (full circles) and resistivity (open circles) of graphitized lines vs laser power.

measured with optical microscope. These data are referred to as *visual* width. Because of the fact that the as-deposited film density (2.4 g/cm^3) exceeds the density of monocrystalline graphite (2.26 g/cm^3) as well as the density of other forms of graphite, the material would expand under local annealing. A hill-like surface relief appears as a result with a typical form shown in Fig.2. A groove at the center of the protrusion is due to material etching via carbon oxidation at high laser power, as will be discussed later. When oxidation is absent, the surface profile displays a more or less perfect Gaussian form. In all cases we chose the FWHM value to be the *profile* width.

The line width versus laser power plots determined by two methods are shown on Fig.2. One can see that the *profile* width exceeds clearly the *visual* one, the latter appeared to be exactly equal to the groove width. Thus the zone of material transformation spreads really beyond the visually observed strip. Therefore, it was the *profile* width that we used to estimate the resistivity of lines.

In addition the amplitude of the surface corrugation has been found to grow also with the laser power. The density change, being inversely proportional to this amplitude, can be used, among other parameters, to characterize the structural transformation in DLC films under annealing. In particular a correlation between density and optical absorption changes has been reported (10). We observed in the power range from 420 to 600 mW the decrease of reflectivity (λ = 0.63 μm) from

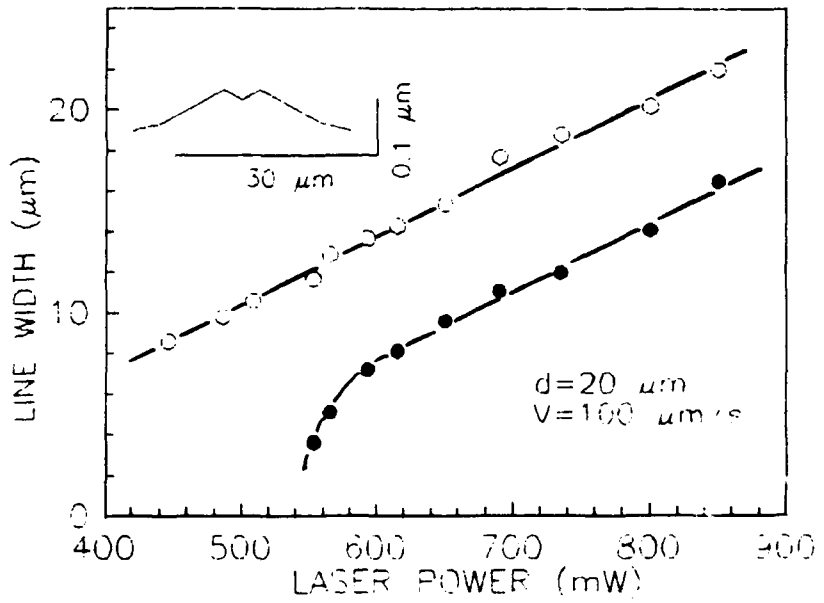

Figure 2. *Visual* (full circles) and *profile-based* (open circles) line width vs laser power. Insertion: typical surface relief across the laser trace.

15%, typical for the as-deposited film down to 7% for a graphitized strip. This gives an idea to use DLC thin films not only as protective coatings for magnetic (11) and optical (12) memory discs, but also as an active media for write-once optical recording based on a carbon crystallization mechanism.

Structural Changes

A more detailed analysis of laser induced structural changes was performed with Raman scattering, known as a very sensitive method for this aim (11,13). Figure 3 shows the evolution of Raman spectra with a laser power increase. The spectrum of the as-deposited film is typical for amorphous carbon (4): it displays the line centered at 1558 cm^{-1} (G peak) and a very broad disorder induced line at 1285 cm^{-1} (D peak). Both lines narrow gradually and shift towards higher wave numbers with laser power (and consequently with the temperature reached), G and D peaks approaching the asymptotic positions at 1605 cm^{-1} and 1360 cm^{-1}, respectively. This evidence suggests a graphitization process, if one takes into account, that the single crystal of graphite shows one single line at 1580 cm^{-1}, while polycrystalline graphite exhibits an additional line at 1355 cm^{-1} (14).

The spectrum parameter useful to characterize the degree of graphitization is a value of an integral intensity ratio, I(D)/I(G), of D and G lines (4,14). In particular,

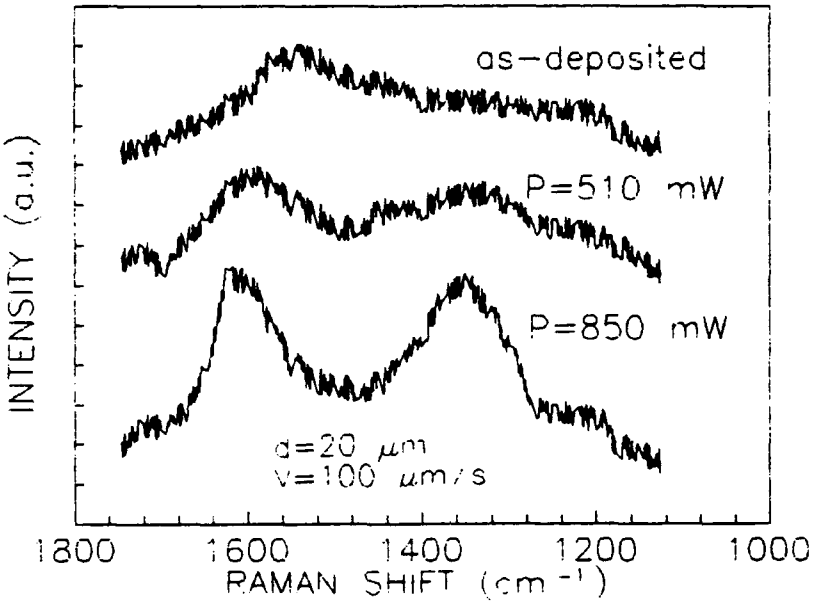

Figure 3. Raman spectra of DLC film annealed at different laser power.

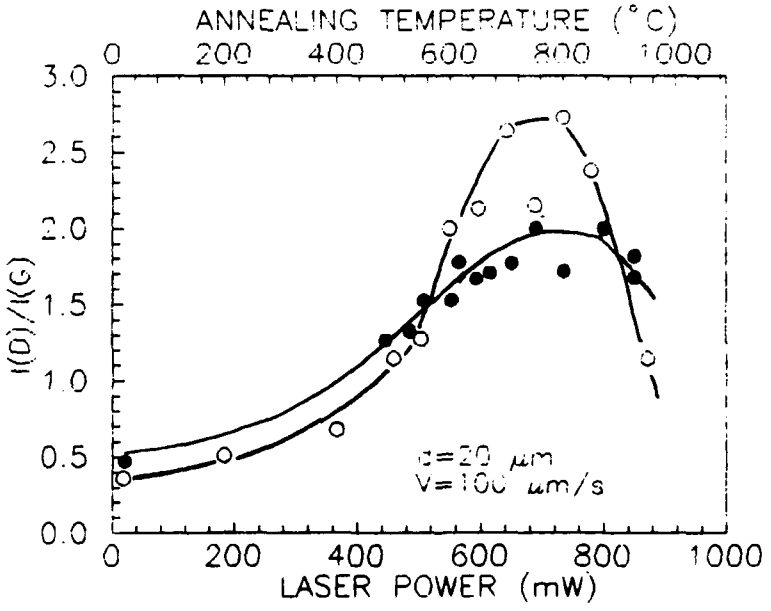

Figure 4. Intensity ratio vs laser power (full circles). Intensity ratio vs annealing temperature from Dillon et al. (4) (open circles) is shown for comparison.

this ratio has been found to be inversely proportional to a mean crystallite size L_a in the basal plane of graphite (14). The growth of I(D)/I(G) with a laser power increase occurs mainly in the range from 400 mW to 600 mW as shown in Fig.4. Following Dillon et al. (4) we attribute this to the increase of the number and size of graphite crystallites with the temperature increase. For comparison we present also the intensity ratio vs annealing temperature for a-C:H film annealed in N_2 and H_2 (4). The agreement between laser and furnace data becomes the best, if the laser induced temperature rise is calibrated against the power as T(°C) = 1.1 P (mW).

Using the relationship L_a (Å)=45.5·{I(D)/I(G)}$^{-1}$ from Tuinstra et al. (14), we have estimated the crystallite size to be $L_a \approx 27$ Å for the film annealed at P ≈ 800 mW. The value of L_a obtained is comparable with the previously reported data L_a = 20 Å (15) and L_a = 16 Å (4), found with the same calculation procedure at temperatures where I(D)/I(G) vs T curve reached a plateau. Further increase in crystallite size with temperature rise above 800-1000°C would lead to the decrease of I(D)/I(G) ratio (4,16). We didn't observe however this stage because of the insufficient laser power available.

Oxidation

As far as all experiments were performed in air environment we observed that the etching of DLC film starts at P ≈ 550 mW, as evidenced with profilometer measurements. Obviously the etching occurs via carbon oxidation due to the reaction C(s) + 1/2 O_2(g) --> CO(g). As a result the channels of ≈ 1 μm minimum width were formed in the film, when the laser beam was focused into spot of 1 μm diameter.

The etching rate was determined as $dh/d\tau = h/\tau$, where h is a channel depth and τ is some *effective* time of reaction not equal to the beam dwell time $\tau_o = d/V$. This value of τ is chosen from the condition, that the mass reacted during non-isothermal oxidation be equal to that reacted upon isothermal oxidation at maximum temperature To during some equivalent time interval τ. If an oxidation kinetics obeys Arrhenius' law dh/dt = Const·exp(-E_a/RT), E_a being an activation energy, then τ can be calculated (17) for a given non-isothermal process with a maximum temperature To reached at the moment t = t_o:

$$\tau = \left(2\pi \frac{RT_o^2}{E_a \left| \frac{d^2T}{dt^2} \right|} \right)^{0.5} \qquad (1)$$

Here the second derivative d^2T/dt^2 is taken at t = t_o. Assuming for the sake of simplicity the temperature history at low scanning velocity V to be a Gaussian one.

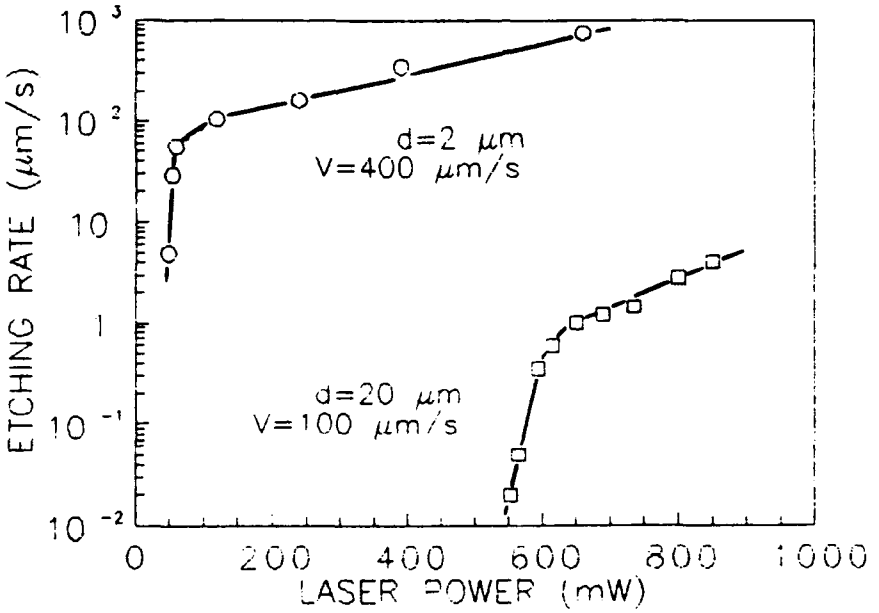

Figure 5. Etching rate vs laser power

$$T(t) - T_0 \exp\left(\frac{-V^2(t-t_0)^2}{\Delta^2}\right) \qquad (2)$$

We find d^2T/dt^2 ($t = t_o$) = $2T_oV^2/\Delta^2$. Using the first approximation the value E_a = 40 kcal/mol, reported for graphite oxidation (18), we have $\tau \approx 0.5\ \delta/V$ at T_o = 103°K. As the radius Δ (at i/e level) of laser induced temperature distribution is close to the laser spot diameter $\Delta \approx d$ (19), we obtain finally $\tau \approx 0.5\ d/V$.

With such an *effective* time of reaction the dependence of etching rate on laser power has been measured at 20 μm and 2 μm beam diameters, as shown in Fig.5. The maximum etching rate approaches 10^3 μm/s in case of sharper focusing. A striking feature of the both etching rate curves is the presence of a bend point where the slope of linear segments changes dramatically. Using the laser power - temperature relation as determined above from Raman spectra, the data in Fig.5 were converted to Arrhenius plot. Two linear segments appear again, yielding (at d = 20 μm) the activation energy $E_a \approx$ 90 kcal/mol at T = 580 - 660°C (stage I) and E_a=18 kcal/mol at T = 660 - 900°C (stage II).

The slope decrease in the kinetic curves and a tendency to reaction rate saturation for carbon oxidation is known in case when oxygen supply is limited by the

diffusion of O_2 molecules through a surrounding gas (18). However, our estimates (similar to those made for laser assisted metal combustion (20)) show that the oxygen flux towards the reacting surface still remains by several orders of magnitude lower than the saturation level. Thus the mechanism of kinetics change observed in laser induced DLC oxidation is not clear now. To explain this effect, probably the hydrogen behavior during annealing should be taken into account. Our preliminary experiments on the thermal desorption and DTA analysis show that the molecular hydrogen release from the film ceases just at the temperature (≈650°C), where the bend in Arrhenius plot is observed. It is not excluded, therefore, that the hydrogen released and adsorbed onto the surface is able to influence the carbon oxidation rate at stage I.

CONCLUSIONS

The annealing and oxidation in air of amorphous diamond-like carbon films have been studied using a finely focused scanning Ar+ laser beam as a heat source. The conductive lines with variable resistance have been written into a dielectric DLC film via its graphitization. The narrow channels of width as small as 1 μm were etched by means of carbon oxidation. The temperature dependence of the oxidation rate shows the two stages with different activation energy.

ACKNOWLEDGEMENTS

The authors are indebted to V.I. Mikhailov for Raman spectra measurements.

REFERENCES

1. Yoshikawa, M., (ed.), New Diamond, Ohmsha-Ltd., Tokyo, (1988).

2. Angus, J.C., P. Koidl, and S. Domitz, Plasma Deposited Thin Films, J. Morton and F. Jansen (eds), CRC Press, Boca Raton, FL, p.89, (1986).

3. Dischler, B., A. Bubenzer, and P. Koidl, Solid State Communications, Vol.48, p.105, (1983).

4. Dillon, R.O., J.A. Woollam, and V. Katkanant, Physical Review B, Vol.29, p.3482, (1984).

5. Rothschild, M., C. Arnone, and D.J. Ehrlich, Journal of Vacuum Science and Technology B, Vol.4, p.310, (1986).

6. Rothschild, M., and D.J. Ehrlich, Journal of Vacuum Science and Technology ..: Vol.5, p.389, (1987).

7. Ageev, V.P., L.L. Bouilov, V.I. Konov, A.V. Kuzmichov, S.M. Pimenov, A.M. Prokhorov, V.G. Ralchenko, B.V. Spitsyn, and N.I. Chapliev, Soviet Physics-Doklady, Vol.33, p.840, (1988).

8. Prawer, S., R. Kalish, and M. Adel, Applied Physics Letters, Vol.49, p.1585, (1986).

9. Anderson, D.A., Philosophical Magazine, Vol.35, p.17, (1977).

10. Smith, F.W., Journal of Applied Physics, Vol.55, p.764, (1984).

11. Tsai, H.C., and D.B. Bogy, Journal of Vacuum Science and Technology A, Vol.5, p.3287, (1987).

12. Moravec, T.J., D. Chen, and S. Shravagi, Proceedings of Topical Meeting on Optical Data Storage, Incline Village, N.Y., 17 Jan. 1983, Optical Society of America, Washington, D.C., WA 3/1-4, (1983).

13. Adar, F., Microchemical Journal, Vol.38, p.50, (1988).

14. Tuinstra, F., and J.L. Koenig, Journal of Chemical Physics, Vol.53, p. 1126, (1970).

15. Wada, N., P.J. Gaczi, and S.A. Solin, Journal of Non-Crystalline Solids, Vol.35-36, p.543, (1980).

16. Vidano, R., and D.B. Fischbach, Journal of the American Ceramic Society, Vol.61, p.13, (1978).

17. Bonch-Bruevich, A.M., and M.N. Libenson, Bulletin of Academy of Science of USSR, Physical Series, Vol.46, p.1104, (1982).

18. Walker, P.L., F. Rusinko, and L.G. Austin, Advances in Catalysis, Vol.11, p.133, 1959.

19. Chen I., and S. Lee, Journal of Applied Physics, Vol.54, p.1062, (1983).

20. Konov, V.I., I.N. Mihailescu, and V.G. Ralchenco, Proceedings of Laser Advanced Material Processing, Osaka, pp.477-484, (1987).

MATERIALS & MANUFACTURING PROCESSES, 8(1), 19-58 (1993)

DEPOSITION OF DIAMOND-LIKE AND OTHER SPECIAL COATINGS BY PULSED LASER ABLATION AND THEIR POST-SYNTHESIS PROCESSING

S.B. Ogale, A.P. Malshe, and S.M. Kanetkar
Center for Advanced studies in Materials Science
and Solid State Physics
Department of Physics
University of Poona
Pune 411 007, India.

ABSTRACT

Use of pulsed laser ablation technique for deposition of diamond-like and other special coatings is discussed here at length, establishing the correlation between the process parameters and the film quality. Process parameters dealt with sufficient detail are the laser wavelength, laser pulse width and energy density, nature of ambient and the corresponding partial pressure, substrate temperature and the electric field, if any, applied during deposition. The optimum parameter space for deposition of films having high performance features are identified in the case of diamond-like films and films of cubic boron nitride, titanium nitride and tungsten carbide. In this context, results on the characterization of the films deposited under different conditions are discussed. These include data obtained by Raman spectroscopy, IR spectroscopy, X-ray diffraction, ellipsometry, UV-VIS transmission, scanning electron microscopy. The post-synthesis of the laser deposited films using ion and laser beams from the standpoint of enhancing their quality or etching of dielectric features therein are also discussed.

INTRODUCTION

It is only during the past few decades that their is a growing realization of the potential of diamond in the interest of modern technological utilization (1-3). There is a realization of the necessity of synthesizing diamonds and diamond-like forms in a controlled way so as to enable reproducibility and tailorability with reference to a specific application. At this moment, synthesis of diamond and diamond-like carbon (DLC) coatings is perhaps a unique area which is at the cutting-edge of both science as well as technology and which surpasses most other areas of advanced materials

research in scope, content, acitivty and future prospects. In addition to diamond and diamond-like carbon coatings, other coatings based on special-property materials such as BN, TiN and WC (Table 1) are being actively considered for technological utilization in their traditionally unencountered spheres of application (3-7). Breakthroughs have already been achieved in synthesizing crystalline diamond and cubic boron nitride (c-BN) phases at low temperature (600°C - 900°C) and low pressure (tens of Torrs of H_2 + CH_4 for diamond deposition) and this has made tremendous impact on scientific and technological perspectives related to modern materials science (2,4). Interestingly, the properties of such coatings are highly sensitive to their microchemical (stoichiometry, bond order, inhomogeneity etc.) and microstructural (degree of disorder, microcrystallinity etc.) features and as such they depend on the technique used for their synthesis.

A wide variety of techniques have been explored and employed to synthesize diamond, DLC, and other special coating materials mentioned above. Major ones amongst these to synthesize diamond are d.c./r.f./microwave/hot filament plasma chemical vapour deposition (CVD) from hydrocarbon gas, ion beam deposition, ion beam assisted deposition, and electron cyclotron resonance (ECR) plasma CVD and major one to synthesize DLC are ionized evaporations of hydrocarbon gas, r.f. sputtering of graphite target, laser deposition (8). The advances in deposition methods have provided greater control on the film properties and it is becoming increasingly feasible to synthesize films having properties tailored to the required specifications. Although most of these techniques have been able to produce good quality films, the growth rates have not been found to be very substantial and improvements are being sought on a continued basis. For example, with ion beam methods the growth rates achieved in the early phase of research were extremely low, however with the development of high fluence ion sources the growth rates of DLC films were brought upto 360 Å/cm^2/hr (9). Subsequently, growth rates of almost 500 Å/hr over 20 cm^2 area, could be achieved using a sputtered source of carbon ions (10). Such enhancements in process capabilities are in progress in the context of all the available techniques.

In recent years, the technique of Laser-induced Physical Vapour Deposition (L-PVD), one of the new generation of thin film deposition techniques, is being increasingly employed to produce a number of special coatings (11,12). The advantages of the laser deposition technique lie in its simple implementation, near-stoichiometric deposition of constituents, precise control of the stoichiometry of the gas phase components by control of ambient partial pressure, and ability to achieve non-equilibrium reactions at the target and growth surface. In this review, we discuss the synthesis of DLC, c-BN, TiN, and WC films by the L-PVD technique. In the case of DLC films, we bring out and discuss a number of issues such as optimization of process parameters, criterion for identifying *good quality* DLC film, interpretation of Raman spectra of DLC films obtained under various deposition conditions, and dynamics/kinematics of the deposition process in the light of the results obtained in different laboratories. *Film Quality* is a term that depends on the nature of application. We will refer DLC film quality in terms of the ratio of sp^3 bonded carbon atoms to other allotropes, particularly the sp^2 bonded carbon atoms.

TABLE 1
Some properties of materials used as special coatings.

	Diamond	Diamond like Carbon (DLC)	cubic BN	TiN	WC
Density & colour	3.51 g/cc, colourless in purest form	1.89-2.0 g/cc tan to yellowish tan	3.48 g/cc greyish black	5.22 g/cc golden yellow	15.63 g/cc grey
Hardness	7000-10,000 Kg/mm^2	900-3000 Kg/mm^2	4100-7100 Kg/mm^2	2000 Kg/mm^2	2100 Kg/mm^2
Chemical stability	Inert	Inert	Inert	Sl.soluble in HF+hot water	Soluble in $HF+HNO_3$ +water
Thermal stability & Coeff. of thermal expansion	20 W/(cm.K) $4.8x10^{-6}$ /°C		6 W/(cm.K) $5.6x10^{-6}$ /°C	$9.35x10^{-6}$ /°C	a-$5.0x10^{-6}$ c-$4.2x10^{-6}$ /°C
Refractive Index	2.42	1.8-2.2	1.5-1.7		
Energy gap	5.5 eV	2-3 eV	3-5 eV		
Electrical resistivity	> 10^{16} ohm-cm	10^7-10^{13} ohm-cm	> 10^{11} ohm-cm	26 μohm-cm	19.2+0.3 μohm-cm
Crystal structure	Diamond Cubic, sp^3 bonding	Amorphous composite of sp^3 + sp^2	Cubic diamond sp^3	Cubic FCC	Hexagonal
Melting point	> 3550°C		sublimes 3000°C	2930°C	~2870°C

LASER-INDUCED ABLATION-DEPOSITION AND RELATED HYBRID TECHNIQUES

L-PVD and the Corresponding Experimental Approach

A characteristic trend in contemporary *modern materials science* is the development of new and novel techniques with the aim of preparing phases and structures not accessible by means of the conventional routes. Towards this end the key aspect is control of spatial and time scales in processing and control of energy flow into the systems and subsystems. Unlike electron or ion beams, the monochromaticity, pulsing features and high power capability associated with laser beams offer an adequate parameter space to achieve these objectives and hence lasers are being looked upon as an attractive tools for modern materials processing (13).

The laser induced vaporization was observed at much early stages in the field of laser processing. However, this was primarily used only for laser drilling or cutting. Although it has been known since 1965 that material deposition can be achieved by high power laser evaporation of solid materials in vacuum (14), the recognition of this process of *Laser-induced Physical Vapour Deposition (L-PVD)* as a prolific technique for synthesis of materials in thin film form is of very recent origin. In L-PVD, the aspect of pulsed laser induced non-equilibrium vaporization of material is meaningfully utilized to synthesize thin film forms of stable and metastable phases of materials via collection of the evaporated flux of material on adjacent substrates. In a typical experiment of L-PVD, a solid target is irradiated by high power laser pulses in a background pressure of a selected gaseous species in the range between 10^{-6} Torr to few hundred millitorr, and the laser generated plasma is allowed to condense on the substrates (Fig.1). The substrate kept in front of the target material may be maintained at an elevated temperature to enhance adhesion or to facilitate organization of deposited species so that a good quality thin film can be obtained. Depending upon the processing parameters, particularly, the laser energy density, laser wavelength, laser pulse width and ambient gas pressure, films can be deposited at the rate of a few tens to a few hundreds of angstroms per pulse. The types of materials which can be laser deposited are not limited unless the material itself is transparent to the laser wavelength or is highly reflecting. The pulsed laser ablation-deposition process can be viewed as process consisting of three separate stages, namely: i) the interaction of the laser beam with the target surface, ii) an initial isothermal expansion of the laser induced plasma, and iii) a final adiabatic plasma expansion leading to the deposition of films (15). The irradiation of targets by laser beams with different wavelengths and energies has an effect on the characteristics of the deposited films. Lasers with different characteristic features have been used either in continuous wave (CW) or in pulsed mode for the deposition of the thin film. In order to study the predominant species in the laser induced plasma plume various diagnostic instrumentation such as Optical emission and absorption spectroscopies, and mass spectrometry have been utilized (16).

An important parameter in laser ablation-deposition is the laser energy density (15). The energy density appears to control the maximum plasma temperature, which

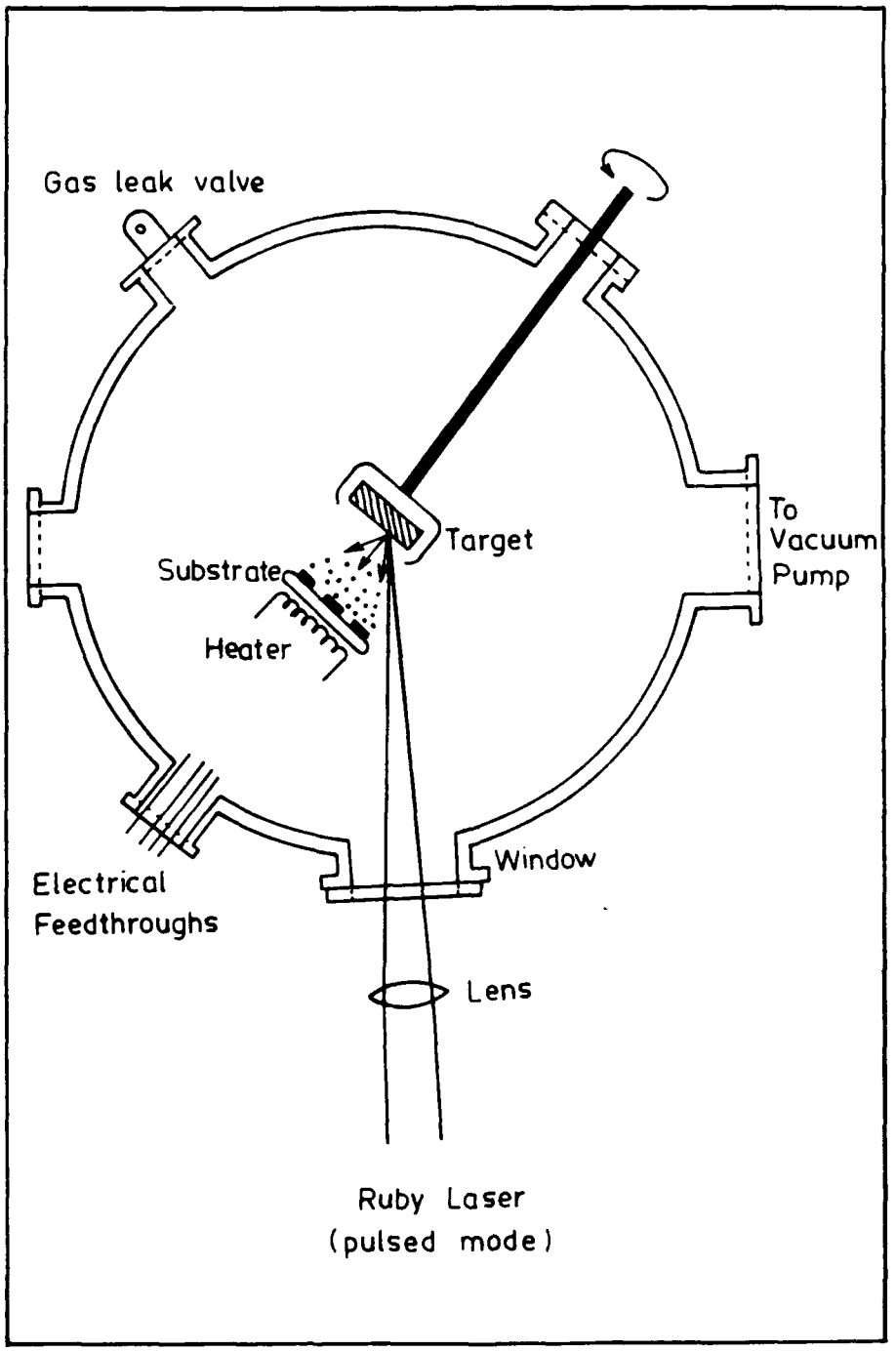

Figure 1. Schematic of pulsed laser deposition setup.

determines the expansion velocity of the plasma. At relatively low energy densities, it is found that the composite target material does not evaporate congruently. As the energy density is increased, the composition of the film more closely approaches that of the target. At very high energy densities, the ejection of molten matter from the target as micron-sized particles is inevitable (17). The collection of these particulate matter on the substrates could pose serious problems in device quality structures. The laser irradiation on the target during the ablation process significantly modifies the surface topography. Depending on the laser power and wavelength, extreme variations in target composition could occur at various points in the laser induced etch pit. The associated compositional changes would be reflected in the stoichiometry of the deposited films. It has been shown that there exist two distinct regions in the deposited films with different thicknesses and compositions (18). This is correlated with two components which appear in the angular distribution of the flux of the ablated species, i.e., a narrowly and widely dispersed component around the surface target normal. The widely dispersed ablated flux component (attributed to thermal evaporation) does not yield stoichiometric composition of the target. On the other hand, the forward peaked component appears to give rise to a film composition closer to that of the target. Within a few nanoseconds of laser irradiation of the target surface, the material rapidly evaporates. This results in a subsequent forward ejection of that material due to a secondary process. The possible secondary processes are (16): 1) surface shock waves generated by rapid surface evaporation (19), 2) a subsurface explosion generated by a combination of a hot subsurface region, capable of building a high vapour pressure zone, and a cooler surface produced by a rapid evaporation of the material from the surface (20), and 3) the production of a high density region of ablated material in front of the laser-impacted surface (Knudsen layer) (21), which could lead to large number of collisions among the ablated species resulting in a recondensation process and particles emission in a forward peaked direction.

In addition to the study of the basic phenomena discussed above, an accurate understanding of the evolution of the ablated plume from the target and the transport of the ablated species towards the substrate is necessary to optimize the deposition process, and thus the film characteristics. The studies of the evolution of the laser generated plasma plume (initial isothermal and subsequent adiabatic expansion) (15) reveal that the energy distribution of the ablated species can in principle be explained in terms of the theory of supersonic molecular beams (15,16), where the velocity distribution function of the laser ablated atoms from a solid can be expressed as:

$$f(v) = Av^{3}\exp(-m(v-v_o)^2/2kT_s)$$

where v is the velocity of the atoms, v_o is the stream velocity, m is the mass of the atoms, k is Boltzman constant, T_s is the temperature parameter describing the velocity spread, and A is a normalization constant. The velocities of these species tend to equilibrate at a specific distance (about 7 cm depending on laser energy density) from the target surface (22). The best quality films are obtained when the substrate is positioned at that particular distance (22). The Laser Ionization Mass

Spectrometry (LIMS) and Post-Ablation Ionization (PAI) studies have ruled out the possibility of the ejection of stoichiometric clusters. Different laser wavelengths, coherence, fluence, photon rates, energy, duty cycle, target and vacuum conditions, etc., may render the comparison of data obtained in separate systems unreliable. In spite of the uncertainties still existing in relation to the type of ablated species under different experimental conditions, the ablated species reaching the substrate appear to be very energetic (several tens of eV), which stands out as one of the key factors contributing to the high quality of laser deposited films.

Hybrid Techniques

In addition to its intrinsic advantageous features, the L-PVD process is also accessible to independently controllable modifications. This notion has given rise to the introduction of several hybrid techniques by different workers. In their hybrid method for deposition of DLC films Fujimori et al. (23) employed for the first time a combination of laser and ion beams. They used a CW-CO_2 laser ($\lambda = 10.6\ \mu m$) to evaporate graphite and during the deposition the substrate was bombarded by argon ions produced from a cold-cathode ion source (Fig.2a). The evaporation of the target material was achieved at a power density of 4×10^3 W/cm^2 and at various ion acceleration voltages. The films deposited by this hybrid technique showed significant rise in electrical resistivity, optical transmittance and hardness as compared to the films prepared without ion bombardment during deposition. Subsequently, Wagal et al. (24) reported a hybrid method in which the growth rate was enhanced by use of high fluence carbon ions that were extracted from a laser-generated plasma plume from a cold graphite target. Here a Nd-Glass ($\lambda = 1.06\ \mu m$) laser was used for the ablation of the target material and the ions were drawn out of the plume and accelerated by static fields applied between grounded graphite target and negatively biased grid structure (Fig.2b).

Typically, accelerating potentials in the range 300 V to 2000 V were used. DLC films produced by this technique were found to be mirror smooth with uniformity of optical quality. Further improvement in this laser plasma source was reported by Collins et al. (25). The experimental arrangement was similar to the one reported by Wagal et al. (24), except for the incorporation of an auxiliary discharge electrode to increase the plasma temperature further by Joule heating in the small volume of the ablation plume (Fig.3a). Here a Nd-YAG laser ($\lambda = 1.06\ \mu m$) was used for ablation and the laser power density used was 5×10^{11} W/cm^2 exceeding the so called *Nagel criterion*, as termed by these authors. The current which passed from electrode to the ablation plume was measured with Rogowski coil. A discharge current of 10 A was used to heat the plume and no effect of the discharge current was observed unless it is passed through the small volume at the laser focus. With this type of plasma source Collins et al. could achieve growth rates of DLC of 0.5 micrometer/h over an area of 20 sq cm. Subsequently, Krishnaswamy et al. (26) reported a capacitive-discharge laser-ablation hybrid technique which involved irradiation of a graphite target with a laser pulse (Excimer at 308 nm) and superimposing capacitively stored energy (2.3 J at 3 KV) onto the laser ablated spot in synchronization with the laser

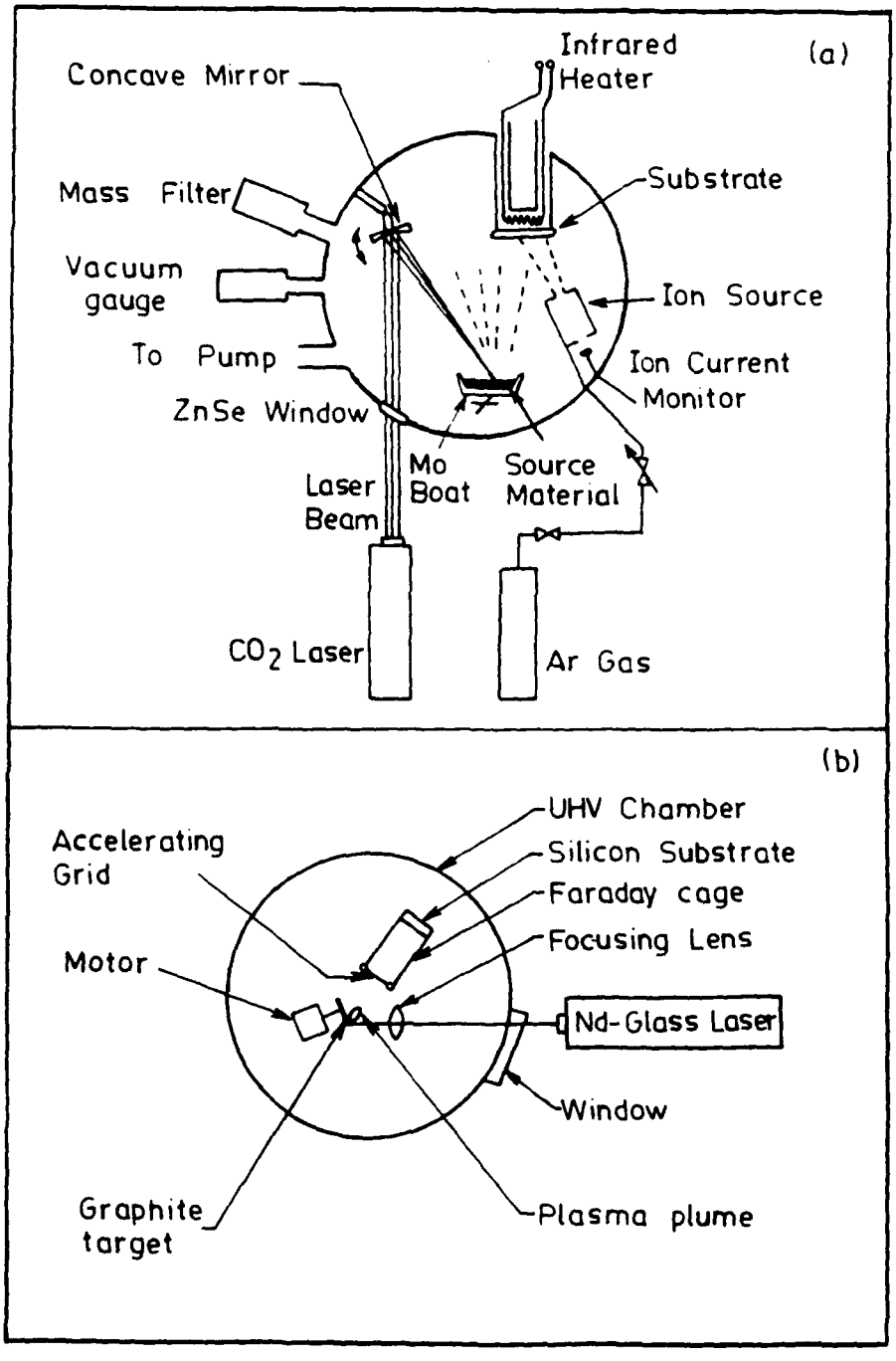

Figure 2. Schematic of hybrid-pulsed laser deposition setups. (Figures from Ref. 23 and 24).

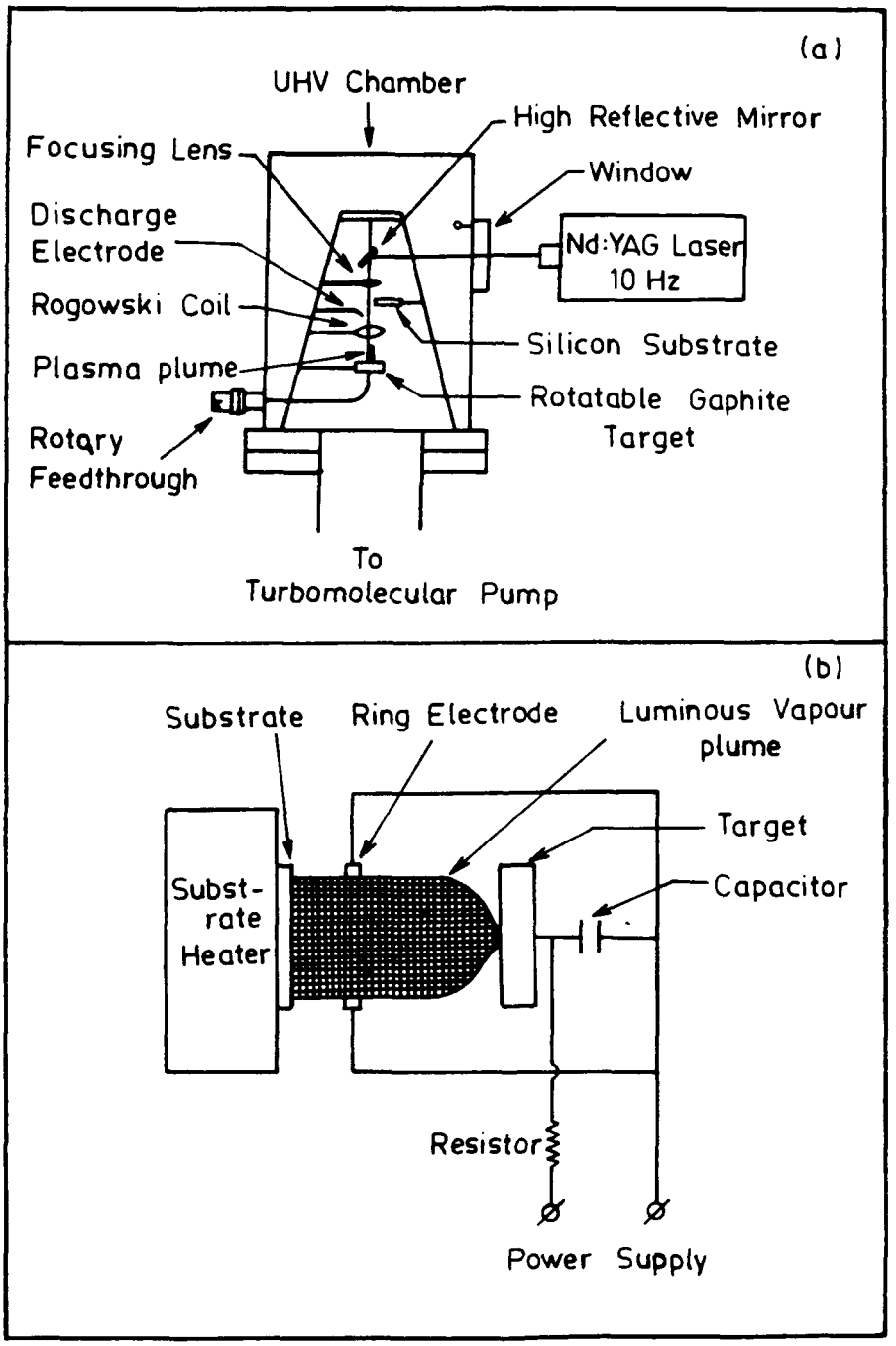

Figure 3. Schematic of hybrid-pulsed laser deposition setups. (Figures from Ref. 25 and 26).

pulse (Fig.3b). These authors claimed improvements in microhardness, uniformity and homogeneity in DLC films. In all these hybrid methods, the basic idea is to put in more energy in the plasma plume. More energetic ionic species thus produced are found to be useful for achieving high growth rates and better quality films. Large area deposition, better adhesion, improved optical, electrical and mechanical properties have been shown to be the other significant advantages of hybrid methods.

PROPERTIES OF LASER DEPOSITED DIAMOND-LIKE CARBON (DLC) FILMS

The structural states of carbon have been a subject of immense interest for quite sometime in view of their implications for our understanding of the connection between the nature of chemical bonding and the short-, medium-, and long- range order in the solid state physics. It is known that depending on the preparation method and conditions, carbon can exist in various thermodynamically stable/metastable forms such as diamond, graphite, microcrystalline carbon, diamond-like hydrogenated/non-hydrogenated carbon, glassy carbon, amorphous carbon, and recently discovered *Buckminsterfullerene* (Buckyball) (27); and these forms exhibit significantly different optical, chemical, and mechanical properties. It is generally believed that these variations in the properties are a consequence of the relative population of sp^3, sp^2, and sp^1 hybridized orbital states of carbon atoms (Table 2), the last one being the least probable (28). It is of interest to examine whether the relative population of these bonding states can be controlled and the structural state of carbon can be tailored by resorting to newer, especially far from equilibrium, thin film deposition methods. Different attempts at the synthesis of carbon films by non-conventional routes have resulted in a wide variety of DLC films with material properties ranging from highly hydrogenated polymer-like films with optical gap of 2.5 eV, through very hard films with optical gaps as small as 0.5 eV, to amorphous materials with diamond micro-crystallites embedded therein (29,30). These results indicate that there is significant influence of deposition conditions on both local bonding and intermediate range order in DLC films. In spite of all these efforts, the unique criterion for *good quality* DLC material does not seem to have emerged. Recently, Davanloo et al. (31,32) have suggested that the imaginary part of the index of refraction, K specified at $\lambda = 6328$ Å can serve as a measure with which to quantify the changes in the merits of the films. However, Yoshikawa (33) and several other workers (34) have found that the ratio of sp^3/sp^2 bonding configurations to be a more appropriate indicator to describe the quality of DLC films.

Hydrogen-free DLC Films

In the initial phase of research on hard carbon coatings, the deposited material used to be identified as a-C irrespective of its electrical, optical, properties. It is only in early 1980 that researchers became aware of the distinction between a-C with and without diamond-like properties. First attempt to synthesize hydrogen-free DLC film by L-PVD approach was reported by Fujimori et al. (23) in 1982. They used a CO_2

TABLE 2
Classification of various forms of deposited carbon according to carbon bonding, and crystal structure. (25).

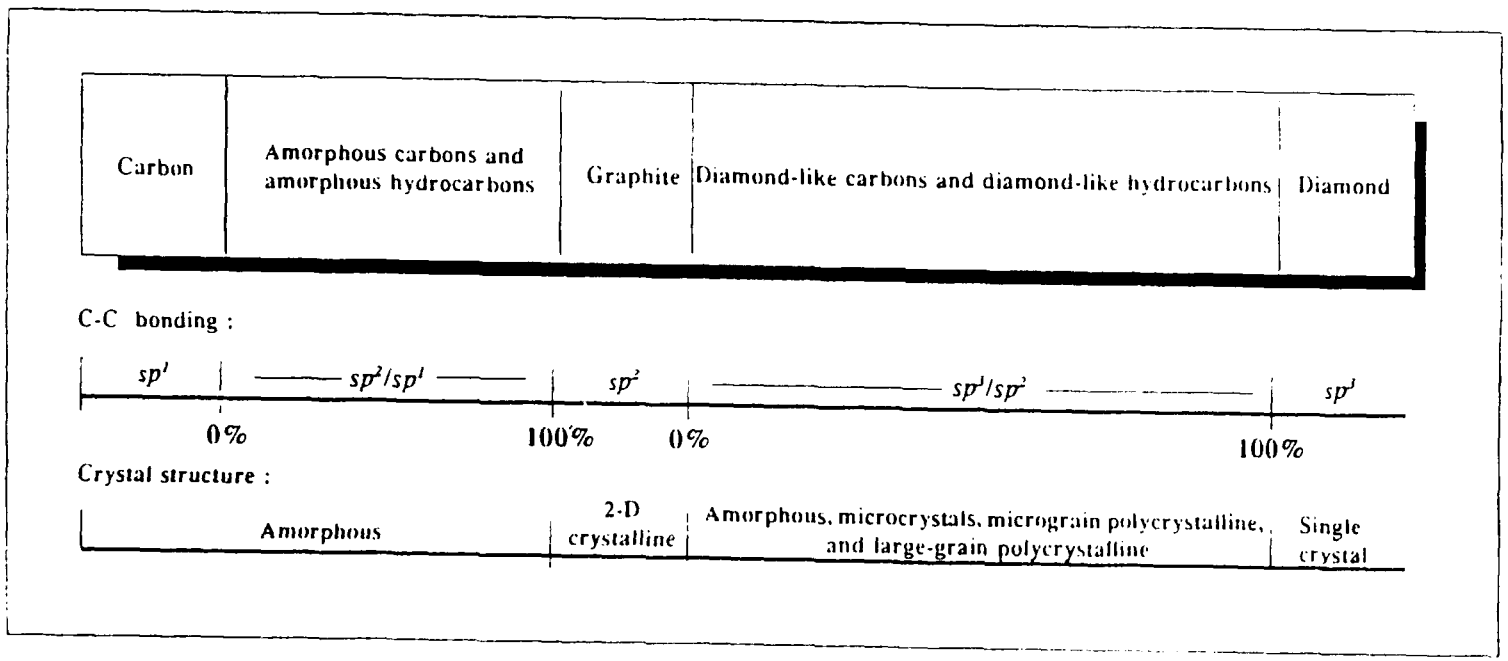

laser (continuous wave, maximum output power 80 W) for the ablation of carbonaceous material. Since carbon is difficult to vaporize due to its high sublimation point and high thermal conductivity, powdered graphite and powdered diamond were used as source materials. The films were deposited on fused quartz plates with laser power density 5 x 10^3 W/cm^2. The films were characterized for their electrical resistivity, optical transmittance and hardness. It was observed that the films prepared from powdered diamond exhibited high electrical resistivity of 10^3 ohm.cm and high optical transmittance whereas those synthesized from powdered graphite showed predominantly graphitic structure. Fujimori et al. also tried hybrid technique wherein the substrate was subjected to ion bombardment during the deposition and such an attempt resulted in marked increase in resistivity, transmittance and hardness, as stated earlier. Thus, though the hybrid technique appeared promising to deposit DLC films even from powdered graphite source, significant efforts were needed to get excellent quality DLC films through L-PVD technique.

Marquardt et al. (35) carried out L-PVD experiment and varied the temperature of plasma by changing the laser power density. Unlike the experiment carried out by Fujimori et al. (23), here Q-switched Nd-YAG laser was used to evaporate spectroscopic grade solid carbon rod surface. The X-UV plasma emission spectra during deposition were analysed by a 1-meter *grazing incidence spectrograph*. These spectra were used to estimate plasma electron temperature. These investigations clearly revealed the dependence of electrical and mechanical properties of the films on the carbon ion/atom energies. Particularly, the hardness was seen to increase significantly with the enhanced plasma temperature. However, the optical gap was always found to be ~ 0.4 eV for all a-C films. The transition from soft to hard carbon was found to occur for increase in laser pulse power density over ~ 5 x 10^{10} W/cm^2 (Fig.4). It is difficult to say whether the transition is sharp but the above mentioned value of threshold laser power density emphasises the importance of this laser processing parameter to obtain DLC films. Collins et al. (25) have subsequently termed this *threshold energy density for hard carbon* as *Nagel Criterion* for obtaining good quality DLC films. Marquardt et al. also indicated that the plasma electron temperature of ~ 40 eV corresponding to the threshold laser power density closely matches with the estimated desirable values for DLC formation suggested by *shock synthesis model* (36) and the model based upon *preferential sputtering of the more weakly bonded carbon atoms* (37) as a mechanisms of hard carbon formation.

Pompe et al. (38) studied some important problems related to nucleation and growth issues using Q-switched Nd-YAG laser for carbon film deposition. The laser power density used was slightly below Nagel criterion. Solid graphitic carbon material was used as a target. This, also happened to be the first instance of application of Raman spectroscopy in the investigations of DLC films to bring out the presence of sp^2 and sp^3 bonded carbon atoms. On the basis of frequency shift of D band (around 1350 cm^{-1}) and G band (around 1550 cm^{-1}) in Raman spectra of these films, transition from amorphous to crystalline carbon phases could be studied. Though this report does not mention explicitly about the formation of DLC films, it does show the production of hard carbon films at sufficiently high laser power density. High hardness is indeed a necessary condition for DLC films but high electrical resistivity

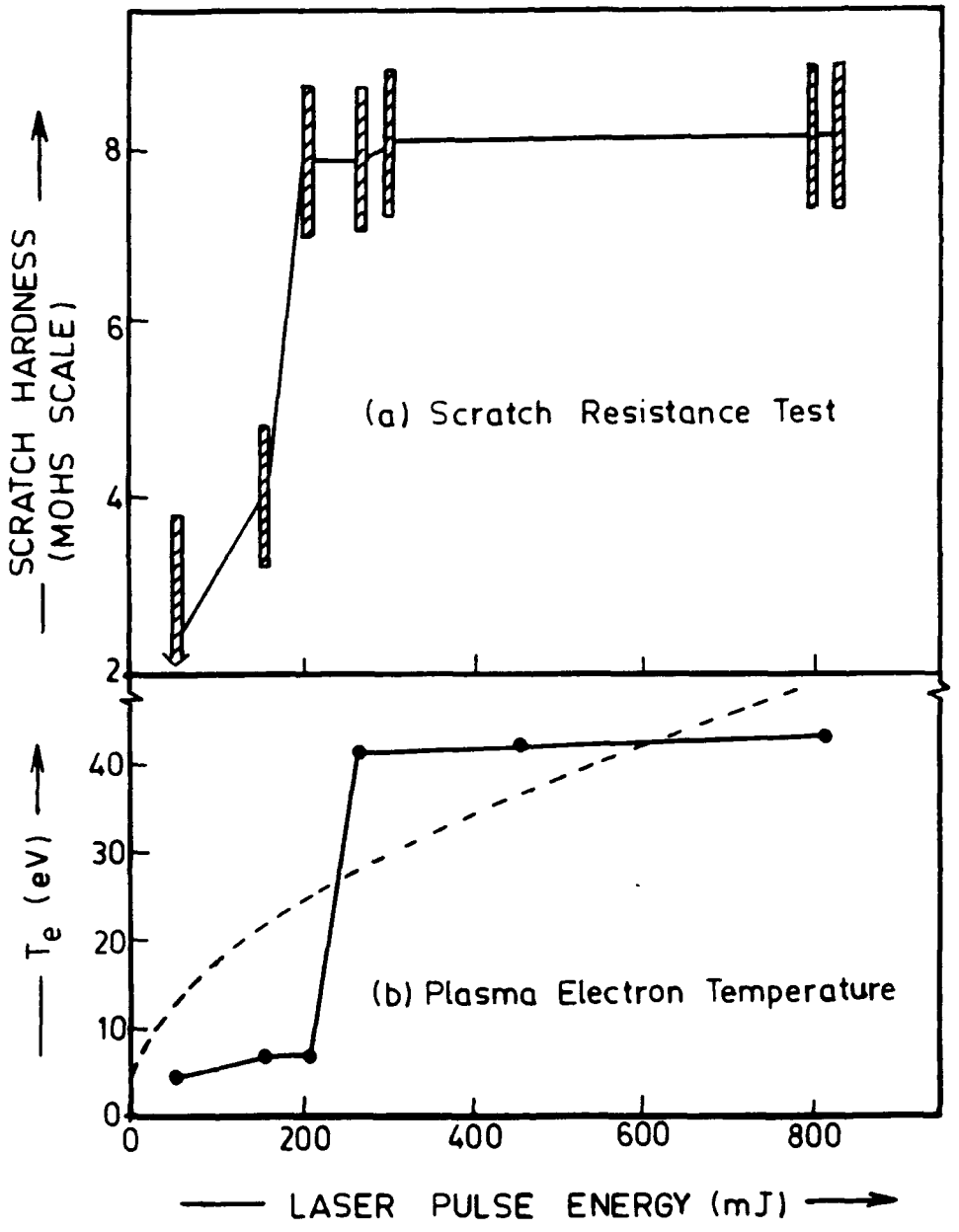

Figure 4. Scratch Hardness (a), and (b) plasma electron temperature as a function of laser pulse energy. Data points shown in (b) are estimates of T_e from X-UV spectra; dashed curve shows dependence anticipated from theory. (Figure from ref. 35).

and high optical transmittance are also essential to identify them as DLC films. Unfortunately, Pompe et al. (38) did not report on the electrical and optical properties of the films and therefore it is difficult to comment upon the precise DLC character of their films. They could bring out that residual compressive stress and a high local mass density favour nucleation of crystalline carbon phase. This problem of nucleation and kinetics of layer growth was also further investigated by Richter and Pompe in their subsequent article (39).

The issue of synthesis of DLC films by L-PVD was readdressed by Sato et al. (40) in 1987. Unlike other investigators, they used a XeCl excimer laser (308 nm) with typical peak power density of 3×10^8 W/cm^2. The target was high purity (4N) graphite and the films were deposited on single crystal Si and quartz substrates. Keeping laser power density constant, carbon films were deposited at various substrate temperatures to observe the effect of thermal input upon the film growth. Such investigations were not reported earlier on the laser deposited carbon films. It was observed by these workers that the carbon films deposited at a substrate temperature of 50°C exhibited diamond-like properties. Structurally the films were amorphous, their refractive index was found to be in the range of 2.1 to 2.2, the band gap was 1.4 eV, they were found to be chemically inert, and their electrical resistivity was of the order of 10^8 ohm.cm. Interestingly, Raman spectrum of these films showed only one broad peak at 1520 cm^{-1} and the authors did not report on the hardness of the films. Later reports on the detailed studies of Raman spectra of various forms of a-C film prepared by different techniques showed that the DLC films exhibit intense line at 1530 cm^{-1} with a shoulder at 1400 cm^{-1} and the relative intensity ratio of these two lines could be used to estimate the sp^2/sp^3 bonding percentage (33). Presence of small contribution of 1400 cm^{-1} band in the Raman spectrum reported by Sato et al. (40) supports the formation of DLC films in their case. Lower value of optical band gap was attributed to the absence of hydrogen in the film. In addition to above mentioned results another interesting observation was also reported by Sato et al. They observed that higher the laser power density, larger is the density of particles on the deposited film. At a power density of $\sim 6 \times 10^8$ W/cm^2 particle density as large as 1×10^6 cm^{-2} was observed on the films. Though Sato et al. never mentioned the Nagel criterion, their work suggests that one should be careful while using this criterion to avoid high particulate density which may deteriorate the morphology of films. Soon thereafter, working slightly below Nagel criterion, Wagal et al. (24) demonstrated the synthesis of DLC films on large area substrates at a high growth rate of 20 micrometer/hr using hybrid L-PVD technique discussed earlier. Using this L-PVD hybrid setup they could obtain large ratio of ions to neutrals as compared to the conventional setup. Films obtained were smooth and scratch proof having chemical inertness towards common acids and organic reagents.

Recently, Malshe et al. (41) have employed Q-switched pulsed Ruby laser (λ=694 nm) to vaporize pyrolytic graphite to deposit hydrogen free DLC films. They used an approach similar to that by Sato et al. (40) and characterized the laser deposited films using low-angle XRD, Raman spectroscopy, Ellipsometry, IR transmittance, optical band gap (UV-VIS transmittance and reflection) measurements. Use of Raman and ellipsometry techniques was an added feature of

this work. The laser deposition was carried out at three different substrate temperatures, viz. 25°C, 50°C, and 100°C. The film deposited at 50°C exhibited high electrical resistivity 10^7 ohm.cm and large transmittance particularly in IR region (Fig.5). The optical band gap was found to be 1 eV (Fig.6) and the detailed analysis of Raman spectrum in terms of the intensity and position variation of D (1350 cm^{-1}) and G (1550 cm^{-1}) bands indicated significant contribution of sp^3 bonds in the films in addition to sp^2 bonds (Fig.7). All these properties are the signatures of DLC films, however in the absence of hardness measurement the authors preferred to call these films as a-C films. Subsequently, Collins et al. (25) and Krishnaswamy et al. (26) employed hybrid techniques for the synthesis of DLC films from graphite source. Krishnaswamy et al. (26) could obtain superior quality DLC films by plasma discharge and laser ablation hybrid technique as compared to those deposited by conventional L-PVD. The film hardness was 25 GPa and optical band gap was 1.25 eV for the film deposited at 25°C. Due to the spreading of the plasma the uniformity of the films was found to be significantly improved. The overall improvement in the quality of the DLC films was attributed to spreading of plasma as well as the modified particle energy distribution associated with the plasma plume generated by laser ablation. Recently more detailed studies of deposition of DLC films using laser ablation and plasma hybrid technique have been carried out by Rengan et al. (42). Formation of amorphic diamond, a term defined by Davanloo et al., is yet another significant development achieved through the hybrid techniques. Davanloo et al. (31,32) have claimed to have synthesized *amorphous diamond phase* characteristically distinct from the DLC phase by their hybrid technique. This is the first report of its kind wherein the XRD of the film shows the amorphous structure whereas the measurements of optical properties, mass densities and STM support the identification of this amorphic diamond as a conglomerate of very fine grains of 100-200 Å size. These authors did not report Raman results and emphasised that laser power density should be of the order of 10^{11} W/cm^2 to obtain good quality films.

Finally, it is important to mention about a very recent attempt to grow ultrathin epitaxial DLC films on Si<100> by L-PVD technique (43). The deposition was carried by using a Nd-YAG frequency doubled laser. The films were characterized by surface techniques and STM was used to confirm crystalline morphology over 100 x 100 Å surface of the film. The surface lattice was observed to be hexagonal with nearest neighbour distance 2.52 Å to 2.46 Å. This investigation clearly demonstrated that during the initial growth of few tens of A thickness of DLC film on Si, long range crystalline order is produced and a hexagonal lattice pattern is maintained. Further growth of the film generates the DLC properties but the structure transforms to amorphous state. All these studies of L-PVD and hybrid techniques carried out in the last decade show substantial progress in the deposition techniques and in the properties of the deposited films.

Hydrogenated Diamond-like Carbon Films

It is known that hydrogen can be incorporated into the amorphous carbon network by reacting with dangling bonds and by formation of hydrocarbons and thus,

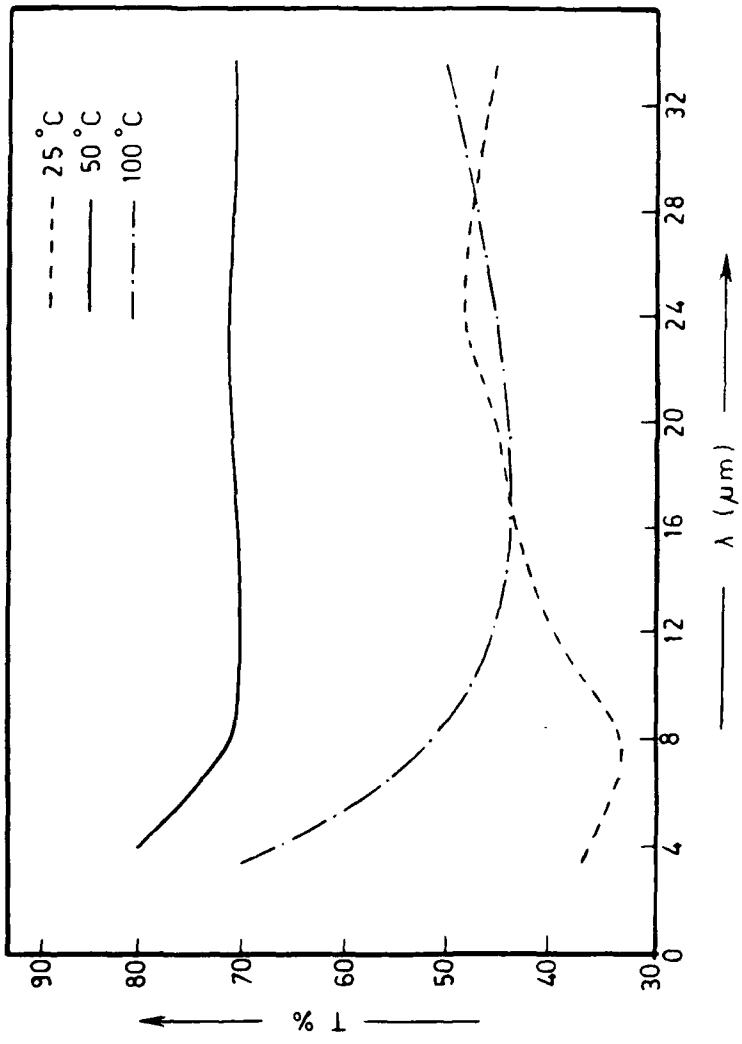

Figure 5. Infrared transmission (T%) for pulsed ruby laser deposited carbon films for various substrate temperatures.

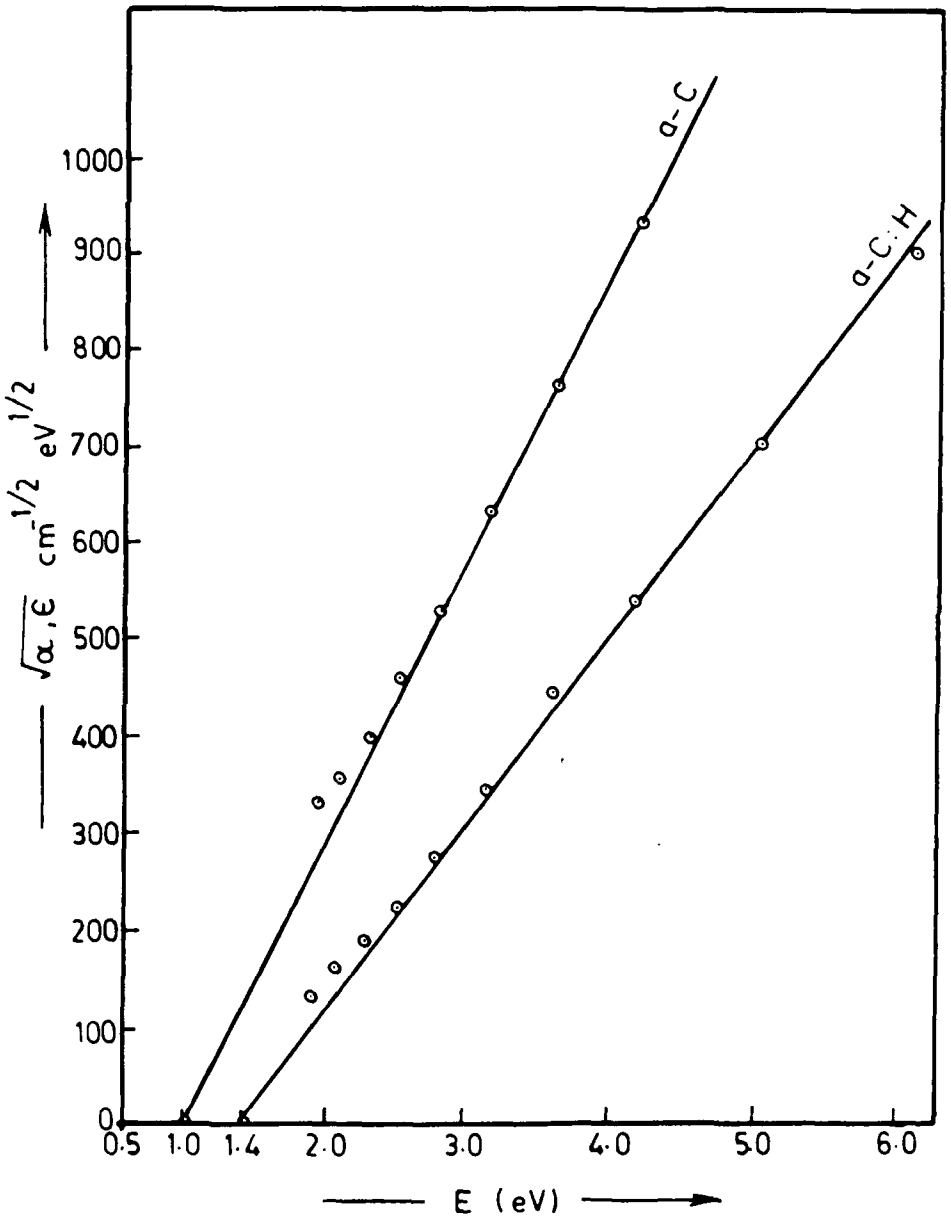

Figure 6. Tauc's function $(\alpha.E)^{1/2}$ as a function of photon energy (E) for laser deposited a-C and a-C:H deposited on quartz.

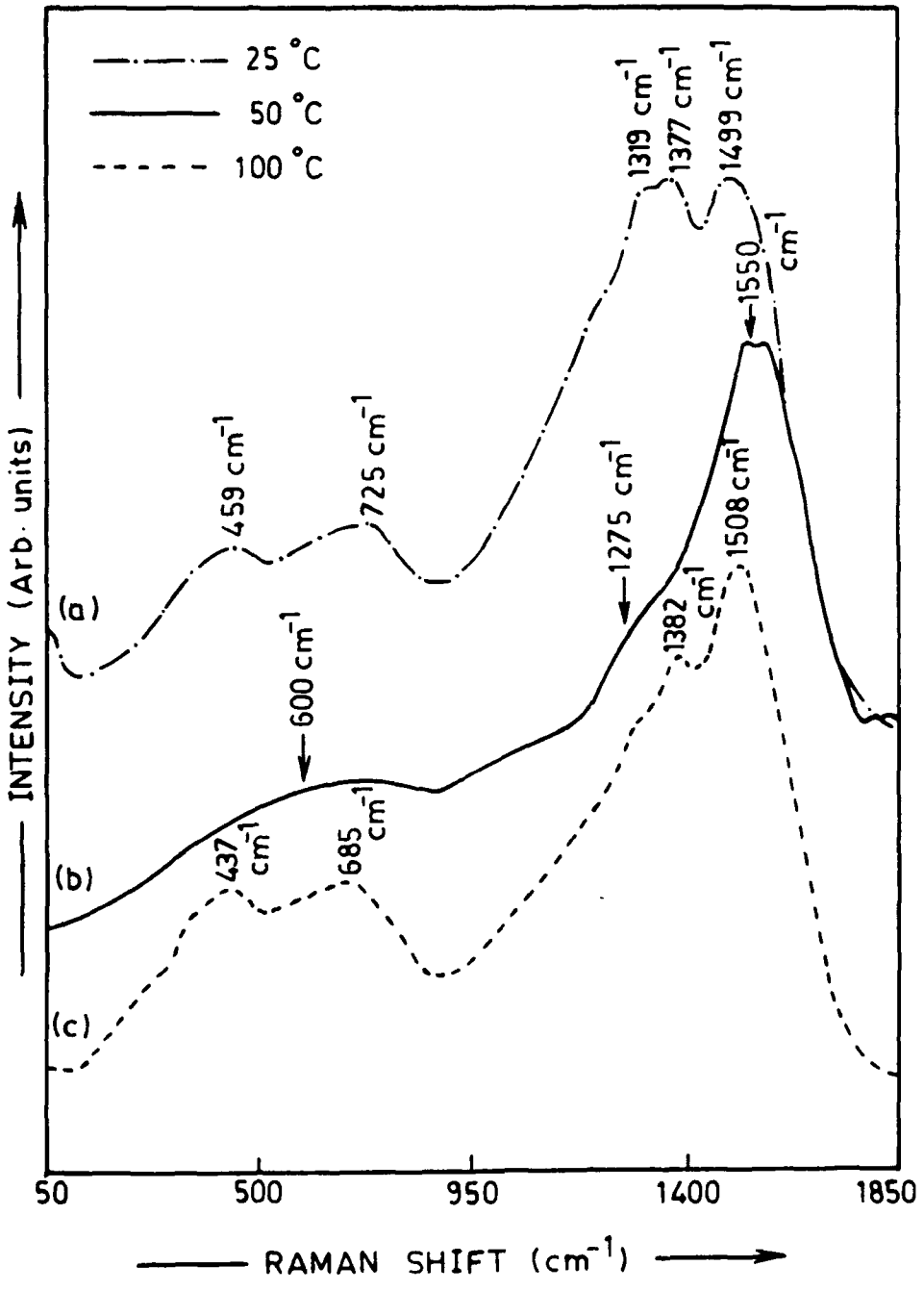

Figure 7. Raman scattering intensity of pulsed ruby laser deposited carbon films at substrate temperature, (a) 25°C, (b) 50°C, and (c) 100°C as a function of Raman shift.

hydrogenation introduces many sp^3 sites in the carbon films (33). A number of attempts have been made to disclose complex deposition parameter-structure-property relationships in hydrogenated a-C films produced by different methods. These studies have revealed that the a-C:H material represents a broad range in structure, being primarily amorphous with variable proportion of sp^2 and sp^3 bonding, broadly governed by hydrogen concentration. The role of hydrogen in stabilizing the tetrahedral (sp^3) bonding has also been well identified. However, the control on the hydrogen incorporation in the film and hence the sp^3 bonding and also the rates of deposition achieved by these techniques, are still comparatively poor. Additionally, the conventional deposition techniques generally use high substrate temperatures (T_s), thereby having limited scope in producing antireflection and corrosion-resistant coatings on delicate active semiconductor devices.

Hydrogen is known to react with carbon in the higher temperature regime (>800°C) (44). Since the laser ablation process can generate such hot carbon ions/clusters, use of L-PVD in a hydrogen atmosphere can be expected to help in reducing the sp^2 centers in the deposited carbon films to a great extent without a need for raising the substrate temperature. Also, it has been shown by Chen and Mazumder (45) that atomic hydrogen is generated during laser irradiation of graphite in H_2 ambient. Such atomic hydrogen is known to be extremely helpful in growth and stabilization of not only DLC but also diamond phase. With this background, Malshe et al. (46) studied for the first time the L-PVD process in hydrogen atmosphere. In their investigations, pyrolytic graphite was used as a target and the temperature of the substrate was maintained at 50°C, an optimized value obtained through our previous synthesis of hydrogen-free DLC films (41). High purity hydrogen gas was introduced in the laser deposition chamber at 0.45 Torr. The films thus deposited on silicon and quartz substrates were analysed using IR spectrometer, optical band gap (UV-VIS transmission and reflection) measurements, Raman spectrometry and Talystep measurements. These a-C:H films were observed to be extremely smooth (roughness was typically below 1000 Å) and highly reflecting in the visible range with a faint yellow tinge compared to the dark tan colour of L-PVD deposited hydrogen-free a-C film. Another remarkable feature observed was a significant enhancement in the deposition rate. The deposition rate in hydrogen-free atmosphere was found to be 6 Å / pulse (41) whereas in hydrogen ambient it was found to increase to 25 Å/pulse. The increase in the deposition rate was attributed to the self sputtering effect which occurs at graphite surface in the hydrogen ambient during laser: graphite interaction. The hydrogen incorporation in a-C film was also helpful to raise the optical gap value to 1.4 eV which indicates an increase in the percentage of sp^3 bonding (Fig.6). This value of energy gap is very close to those of hydrogenated DLC film produced by plasma CVD method (47).

A careful analysis of frequency shifts and intensity changes of D and G bands of Raman spectrum of these films indicated predominant contribution of sp^3 bonding configuration in the films (Fig.8). These results were further supported through IR measurements and they also brought out that hydrogen gets reactively incorporated in the a-C films deposited by the transient L-PVD technique and stabilizes sp^3 co-ordination. In subsequent investigations Malshe (48) has studied the role of hydrogen

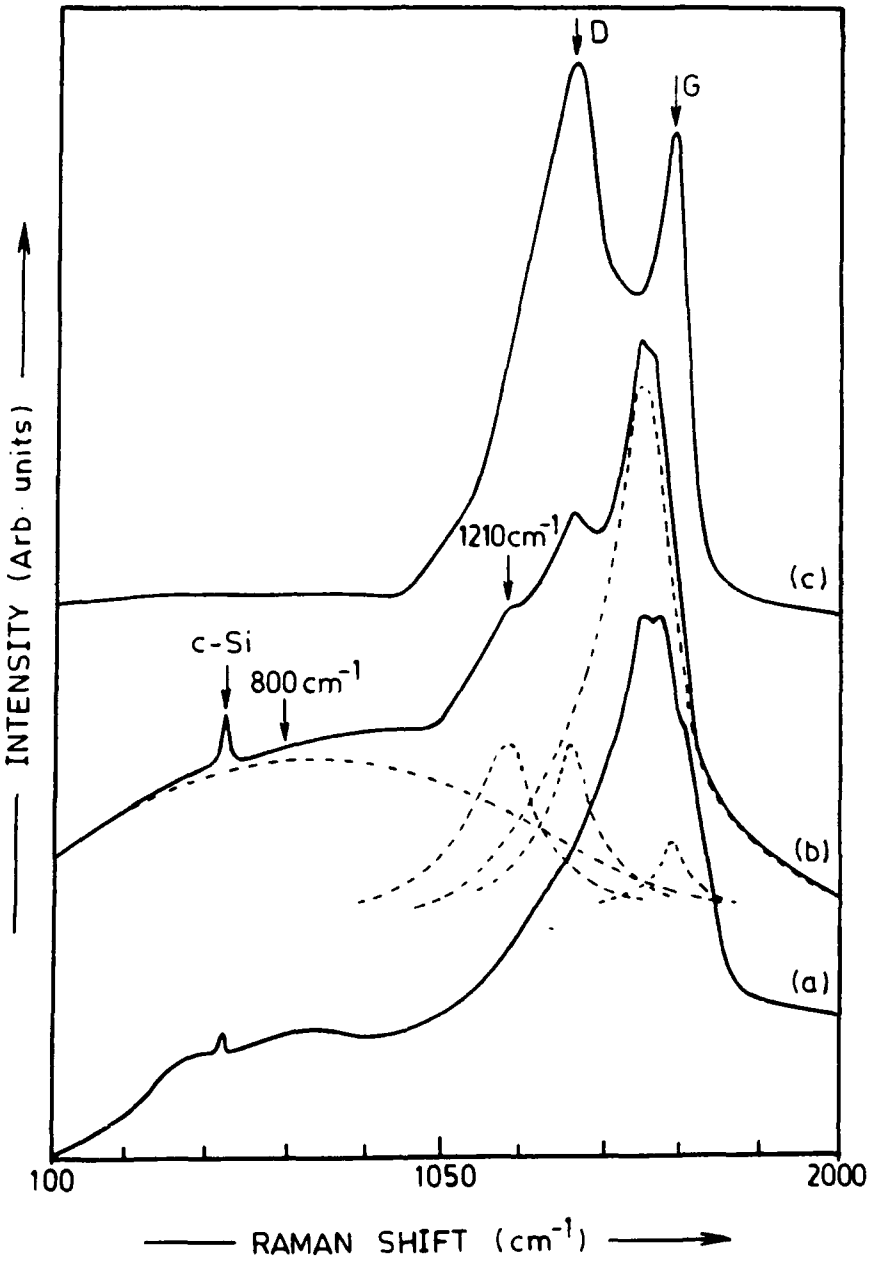

Figure 8. First-order Raman spectra of laser deposited (a) a-C, (b) a- C:H, and a-C:H films after annealing at 600°C. The hand-resolved broken-line bands centered at 800, 1210, 1500, and 1580 cm^{-1} furnished an approximate fit to the Raman spectrum (b) of laser deposited a-C:H films.

partial pressure on the properties of L-PVD deposited DLC (a-C:H) films. It was concluded that for laser energy density of 20 J/cm^2, good quality hydrogenated DLC films are obtained at an optimum hydrogen pressure of about 1.5 Torr (Fig.9). Recently Rengan et al. (49) have also carried out synthesis of a-C:H films using laser ablation and plasma hybrid technique in a hydrogen ambient. An interesting feature of this study is the presence of C_{60} clusters, stable molecules having a soccer ball geometry. As mentioned earlier, various techniques have been used to synthesize DLC films with varying degree of properties (Table 3). However, these early investigations show a great promise for synthesis of novel carbon related deposits by L-PVD technique.

L-PVD OF c-BN AND OTHER SPECIAL COATINGS

Bulk boron nitride crystallizes in two forms, hexagonal and cubic. Hexagonal boron nitride (h-BN) is the stable polymorph at standard temperature and pressure whereas cubic boron nitride (c-BN) is metastable. These two polymorphs are often compared to graphitic and diamond forms of carbon. h-BN is highly anisotropic and the compound has strong intralayer and weak interlayer B-N bonds. The sp^2 interlayer bonds are characteristic of h-BN and sp^3 bonds are the signatures of c-BN. Therefore, the BN polymorphs are distinguished from each other by large differences in optical, electrical, mechanical and chemical behaviour. Particularly, c-BN has diamond like properties and therefore it has been considered as a viable alternative to diamond films for many applications. The attraction stems from the fact that the lattice mismatch between c-BN and Si <100> is 5% which suggests that c-BN could be introduced in semiconductor device fabrication with an acceptable degree of strain. The high value of the hardness of c-BN is useful for coating of cutting tools whereas highly radiation resistant property makes c-BN an appropriate material for mask fabrication required in X-ray lithography. Unfortunately, the metastable nature of c-BN poses a great problem in synthesizing it in bulk or thin film forms. c-BN in bulk form was first generated in 1951 by Wentorf (50) by exposing h-BN to a very high pressure and temperature. Subsequently, more densely packed c-BN in bulk form was synthesized using different techniques. However, producing c-BN in *high quality* thin film form is still regarded as a challenging problem. We will refer c-BN *film quality* in terms of structural, particularly epitaxial structural ordering, compositional and morphological uniformity of the c-BN films.

Several ion beam techniques and CVD methods have been used to obtain h-BN or c-BN in thin film form. Recently, scientists have succeeded in producing metastable c-BN thin film. Due to its inherent nonequilibrium processing nature, L-PVD technique has proved to be useful in synthesizing c-BN films. The deposition of BN thin film by L-PVD route was first reported by Kessler et al. (51) in 1986. They used Q-switched ruby laser to ablate h-BN target. The laser deposition was carried out in nitrogen ambient partial pressure of 20 Pa and the deposited films were characterized by TEM, IR and EDAX measurements. From all these measurements, the films were found to be h-BN. Recently Paul et al. (52,53) have published reports describing the laser deposition of BN film on InP for MIS

TABLE 3

Formation and Properties of Carbon Films Deposited by various conventional and non-conventional deposition techniques. (38).

	Preparation Method	Max. Particle energy (eV)	Growth rate	Substrate temperature	Resitivity (Ohm.cm)	Vickers' hardness (MPa) (load ($\times 10^{-2}$M))	Film Structure	Refs.
(I)	D.C. glow discharge	300-5000	5-10 $\times 10^{-1}$ nm.s^{-1}	Upto 550K	10^{5} - 10^{6}	27500(5) 18500(20)	Amorphous; components of amorphous diamond, amorphous graphite, amorphous polymers and voids.	76-78
(II)	R.f. glow discharge	About 1000	0.1-20 $\times 10^{-1}$ nm.s^{-1}	From 298K to 400K	10^{6} - 10^{12}	Upto 56000 (Knoop)	Amorphous	79-81
(III)	Reactive r.f. sputtering	-	0.02-1 $\times 10^{-1}$ nm.s^{-1}	From 298K to 450K	About 10^{12}	10000(100) 20000(50)	Amorphous with a high content of sp^3 bonds.	83
(IV)	Sputtering of Graphite cathodes, accelerating of the generated C ions	Upto 1000	Upto 80 $\times 10^{-1}$ nm.s^{-1}	298K	10^{10}	24000(200)	Amorphous and crystalline carbon phases including a dense phase C_8	76
(V)	Ion Beam sputtering	About 1-100	0.01-0.2 $\times 10^{-1}$ nm.s^{-1}	>298K	10^{4} - 10^{5}	-	Amorphous with small contents of crystalline graphite-and diamond-type phases	36, 75
(VI)	Ion beam sputtering with additional ion bombardment of the growing film	1200	0.1 $\times 10^{-1}$	>298K	(1-50) $\times 10^{6}$	-	Amorphous with crystalline phases	36, 75

TABLE 3 (continued)

	Preparation Method	Max. Particle energy (eV)	Growth rate	Substrate temperature	Resitivity (Ohm.cm)	Vickers' hardness (MPa) (load ($\times 10^{-2}$M))	Film Structure	Refs.
(VII)	Evaporation (thermal and electron beam)	0.1-0.5	0.1-50 $\times 10^{-1}$ nm.s^{-1}	298K or cooled with LN_2 or ice	10^{-1}	-	Amorphous : random network of graphite-like and diamond-like bonded atoms	71-74
(VIII)	**Laser Vapour Deposition**							
	1. Laser evaporation : CW CO_2 laser (10.6 μm)	0.1-1.0	0.1-20 $\times 10^{-1}$ nm.s^{-1}	298K	10^{2}-10^{3}	-	Amorphous network with graphaite-type/diamond-type bonds	69,70
	2. Laser evaporation with additional ion bombardment : CW CO_2 laser (10.6 μm)	<1000 (Ar ions)	0.1 $\times 10^{-1}$ nm.s^{-1}	298K	10^{-1}	-	Amorphous, graphite like short-range order with strong cross-linkage	69,70
	3. Pulsed laser deposition :							
	a) Nd-YAG laser (1.06 μm)	-	0.1-0.2 Å/pulse	-	-	2-8 Mohs scale*	Amorphous network	35
#	b) Ruby laser (694 nm)	-	7 Å/pulse	323K	10^{5}	-	Amorphous network with low sp^3 content	41
	c) Excimer laser (308 nm)	-	200 Å/min	298K	10^{8}	-	Amorphous network	40

(continued)

TABLE 3 (continued)

Preparation Method	Max. Particle energy (eV)	Growth rate	Substrate temperature	Resitivity (Ohm.cm)	Vickers' hardness (MPa) (load ($\times 10^{-2}$M))	Film Structure	Refs.
4. *Pulsed Laser Deposition* With applied electric bias :							
a) Nd-YAG laser (1.06 μm)	50	0.5μm/hr.	298K	-	13 GPa*	Amorphous network with high sp^3 content	31
b) Excimer laser (308 nm)	-	0.7 Å/pulse	298K	-	18.1±10% GPa*	Like VIII(4(a))	26
# 5. *Pulsed Laser Deposition with* in-situ H_2 partial pressure :							
Ruby laser (694 nm)	-	25 Å/pulse	323K	10^{6} - 10^{7}	-	Amorphous network	46
(IX) Ion plating	Upto 3000	5-10 x 10^{1} nm.s^{-1}	>298K	10^{7} - 10^{15}	30000-60000(50)	Amorphous, graphite-like short-range order with strong cross-linkage	75,83
(X) Ion Beam Deposition	40-100	50 x 10^{1} nm.s^{-1}	298K	10^{11} - 10^{12}	-	Amorphous; polycrystalline diamond (particle size 5-10 nm)	85,86

* Hardness value is in given units

\# Authors Results

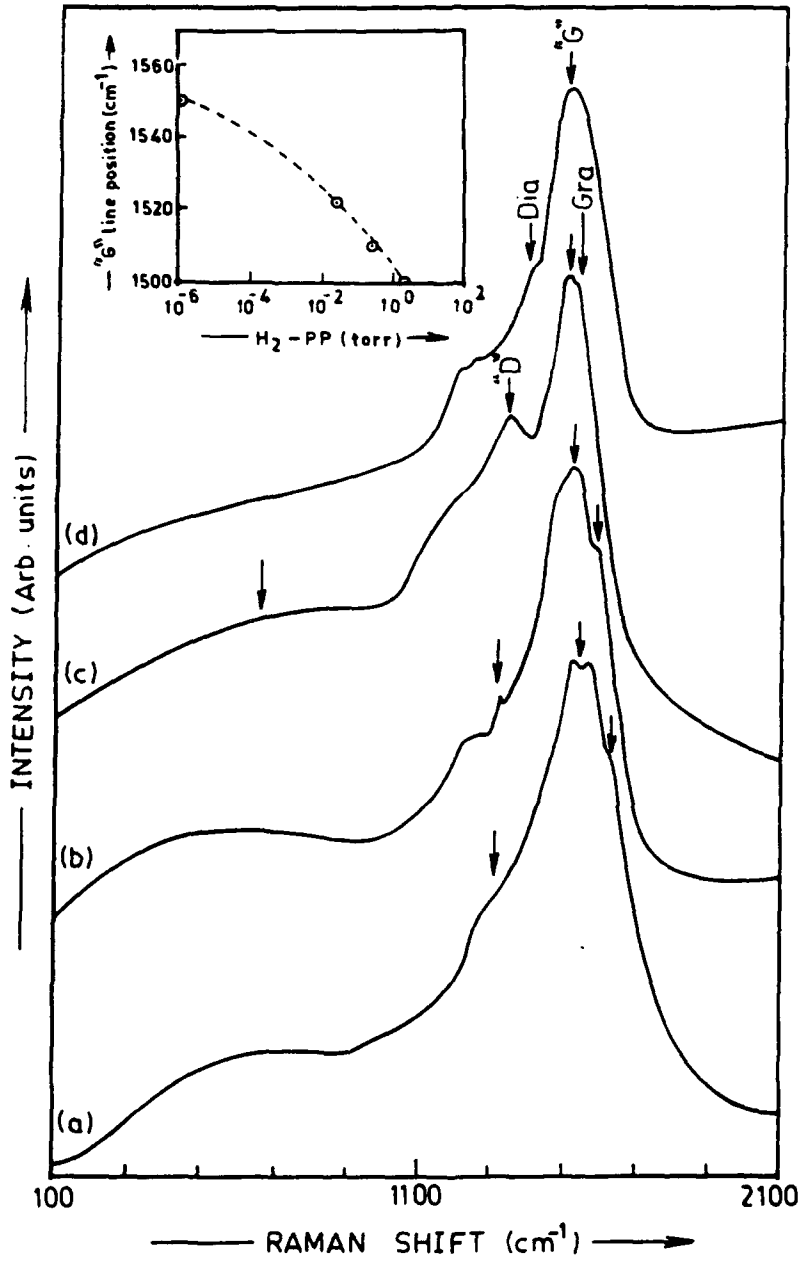

Figure 9. First-order Raman spectra of laser deposited (a) a-C, without (b) a-C:H, at 0.045 Torr (c) a-C:H, at 0.45 Torr and (d) a-C:H, at 1.5 Torr, of hydrogen partial pressure. The inset shows position of G-line as a function of hydrogen partial pressure.

applications. Again, a Q-switched ruby laser was employed to ablate h-BN target and BN films of thickness 500-1000 Å could be deposited on n-inP <100> substrates. At an energy density of 2 J/cm^2, the deposition rate was found to be 7 Å/pulse. XRD studies of the films indicated the formation of h-BN and the same was further confirmed through XPS analysis. The optical absorption studies revealed indirect nature of the gap at E_g = 4.1 eV. This value is well within the range of values reported in the literature which vary from 3.3 eV to 6.2 eV for h-BN thin films. The resistivity estimated from I-V curves was found to be ~ 10^{11} ohm.cm. The dielectric constant of 3.28 was observed to be within the range of values 2.7 - 7.7 reported by earlier workers. These authors could also successfully deposit h-BN on n-type Si substrate. Thus L-PVD technique was demonstrated to be a versatile method for deposition of insulating BN films on semiconductors where low-temperature processing is necessary.

Only very recently, Doll et al. (54) and Kanetkar et al. (55) reported successful growth of c-BN on Si <100> substrate using L-PVD technique. This can be considered as a significant development because BN may prove to be an attractive buffer layer for diamond growth on Si <100> due to small mismatch in their lattice constants (56). Doll et al. used an excimer laser (λ=248 nm) and the target was h-BN produced by Union Carbide. Depositions were made at laser fluence ranging 1.5 to 5.2 J/cm^2 and it was observed that for the ablation of h-BN threshold energy density of 0.34 J/cm^2 was required. The deposition was carried out using laser fluence of 3.9 J/cm^2 in N^2 ambient at pressure $3x10^{-2}$ Torr and the n-type Si <100> substrate was held at 600°C temperature.

The important feature of this investigation was the formation of a c-BN phase under the above mentioned deposition conditions which was confirmed through XRD (Fig.10) and Raman measurements. It was observed that there was preferred orientation of c-BN with respect to the Si substrate. The authors also studied the optical emission spectrum of laser generated plasma plume and observed the presence of B^+ and B^{++} species with no clear evidence of molecular BN (Fig.11). Thus, it could be inferred that BN forms atomically on the substrate surface. According to the authors a key factor in obtaining the c-BN appears to be the wavelength of the laser. The relationship between the photon energy and the formation of particular phase is not clear. However, it is likely that high photon energies may be useful for complete or partial dissociation of BN while at lower photon energies BN may be evaporating in molecular form. A higher photon energy can increase the kinetic energy of the ionic species and Doll et al. have observed in their time of flight analysis a velocity of B+ species of ~ 10^6 cm/sec which might have provided considerable surface mobility for the growth of BN on Si substrate. Using h-BN target and excimer laser (KrF 248 nm) source for ablation, Kanetkar et al. (55) have also reported successful growth of c-BN on Si <100> substrate. The substrate temperature was held at 400°C and the depositions were carried out in vacuum (5 x 10^{-7} Torr), in 120 mTorr of nitrogen and argon ambient with substrate biased at -300 V with respect to the target. Films deposited in vacuum had boron along with small amount of h-BN. For the films synthesised in nitrogen ambient, there was growth of small amount of c-BN phase, and Boron component was reduced

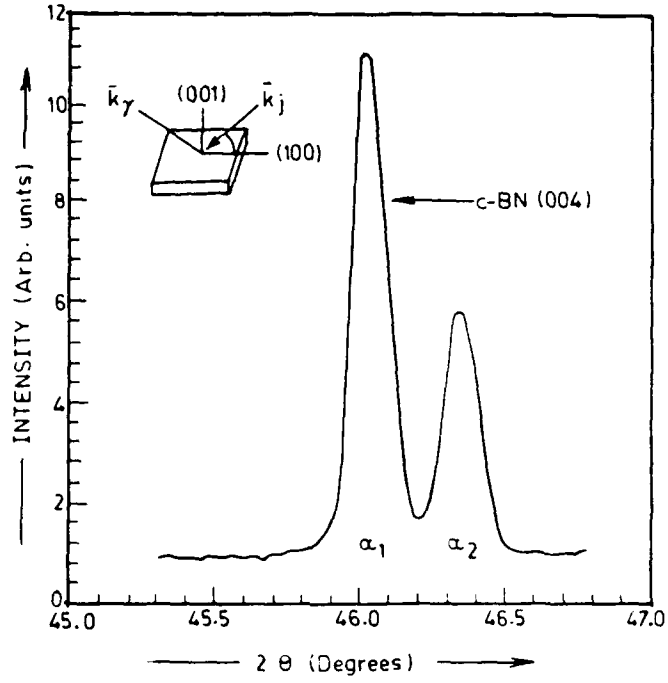

Figure 10. X-ray diffraction scan of a BN film grown on Si(001) for the scattering geometry shown in the inset. The position of the peak ($K_\alpha 1, K_\alpha 2$, wavelength doublet) is consistent with diffraction arising from a (004) line of a cubic zincblende film having a lattice constant of 3.619 Å. (Figure from ref. 54).

substantially. Interestingly, the films deposited in argon atmosphere with bias exhibited the growth of c-BN phase. The XRD of this film showed clear emergence of <400> c-BN peak. Such effect of bias in argon ambient has been observed by Mieno et al. (57) in the growth of c-BN using r.f. sputtering technique. Thus, the activation of deposition surface seems to be a key factor in obtaining c-BN thin films.

Titanium nitride (TiN) is yet another special type of coating which has wide ranging applications from erosion resistant coating for cutting tools to diffusion barrier in microelectronic device technology. N. Biunno et al. (58) investigated the formation of epitaxial TiN films on <100> oriented MgO substrates using pulsed excimer laser (λ=308 nm). The films were deposited by laser ablation of TiN pellet in high vacuum (10^{-7} Torr) at substrate temperature of ~ 450°C. The epitaxial relationship between MgO and TiN was confirmed through cross-sectional TEM measurements and RBS technique (Fig.12). The distinguishing features of these films were low deposition temperature, low impurity content, and their equiaxed grain structure.

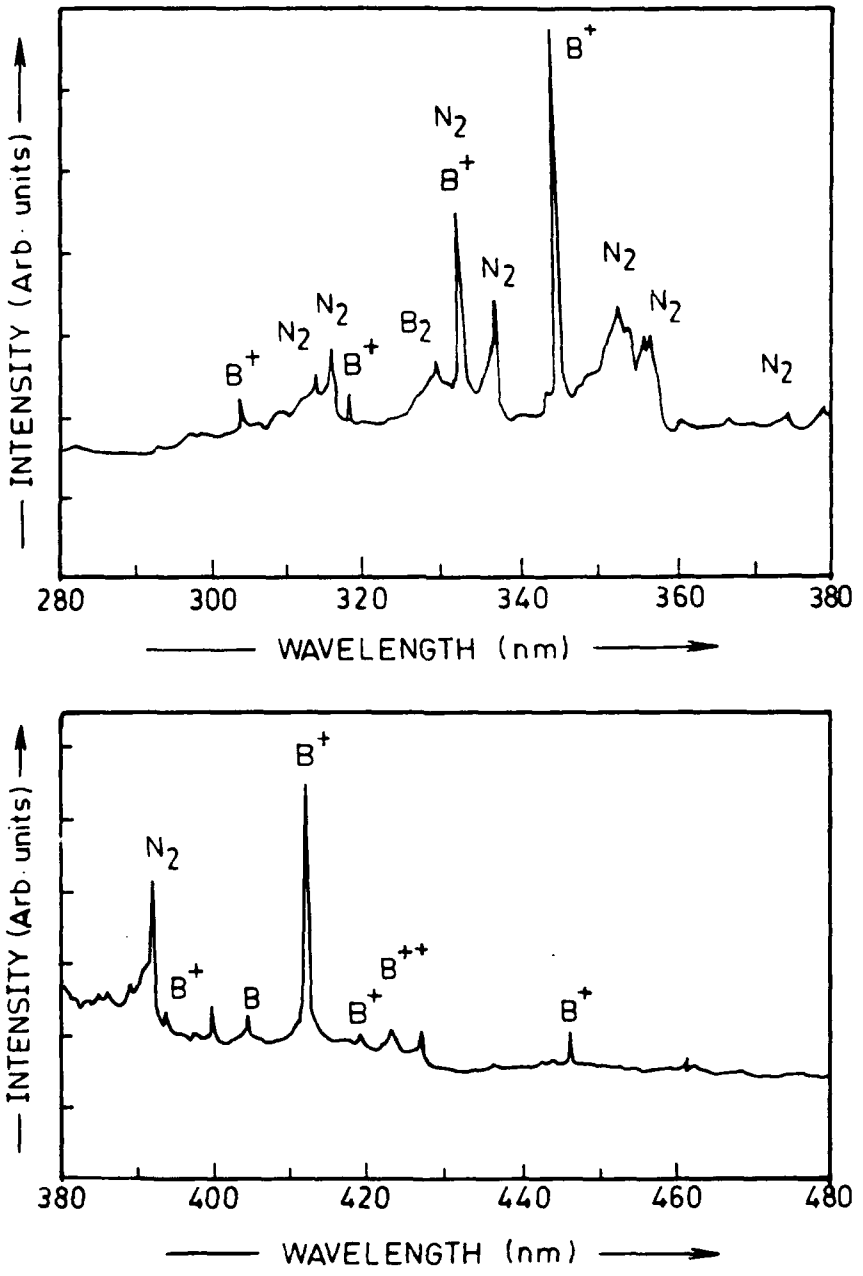

Figure 11. Optical emission spectra obtained during the laser ablation of boron nitride using KrF radiation (248 nm) in 50 mTorr of N_2. The fluence was 8.1 J/cm^2, the spectrometer viewed a point 4 mm above the target surface, and the 50 ns boxcar gate was positioned approximately 0.4 ns after the excimer pulse. (Figure from Ref. 54).

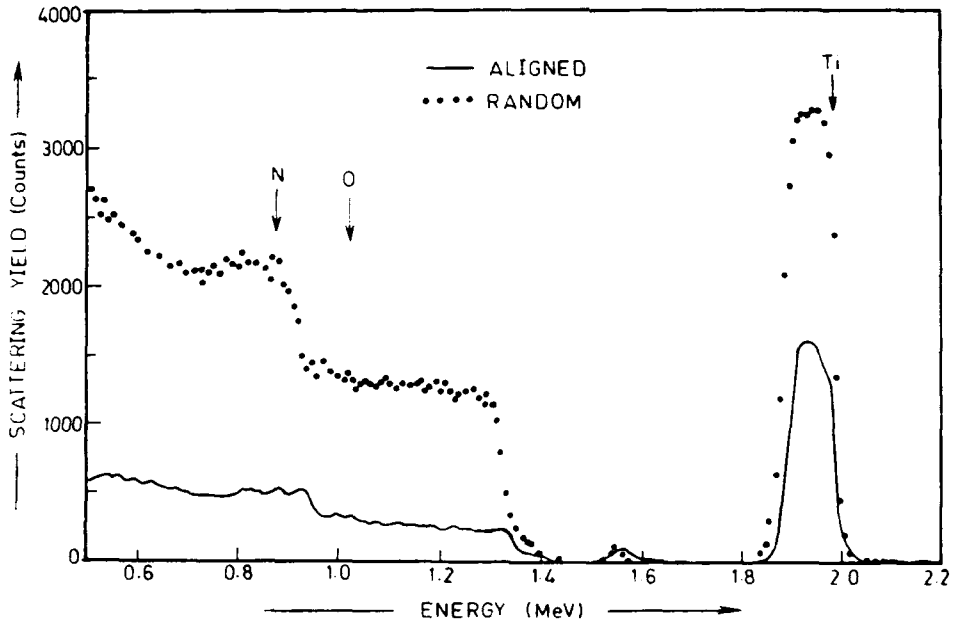

Figure 12. RBS channeling spectra of a <100> TiN film, 1000 A thick, deposited at 5-6 J/cm2 and 650°C on (100) MgO with /min < 50%. (Figure from Ref. 58).

The authors have envisaged that in-situ laser cleaning of silicon substrate prior to deposition might have led to excellent quality of epitaxial growth of TiN films on MgO substrate. The electrical resistivity of the best films was found to be ~ 50 ohm.cm. The resistivity was found to decrease linearly with temperature in the range of 25°-173°C indicating typical metallic behaviour. Auciello et al. (59) synthesized TiN films at room temperature using L-PVD technique. This is a significant achievement since in microelectronic application, it is always desirable to keep the processing temperature as low as possible. They used pulsed excimer laser operating at a shorter wavelength of 193 nm (ArF). Stoichiometric TiN pellet was used as a target. The ablated material was deposited on Si substrate and the films thus produced were characterized by Rutherford Backscattering (RBS), Auger Electron spectroscopy (AES), Transmission Electron Microscopy (TEM) and X-ray diffraction (XRD) techniques. Best quality TiN films with characteristic golden colour and good adhesion could be obtained when the laser deposition was carried out in nitrogen ambient.

It was shown by dynamic mass spectroscopy of species evolving from the target during laser ablation that in absence of nitrogen atmosphere, dissociated oxygen from oxygen containing molecules (e.g. H_2O, CO), could get incorporated in films. The

presence of oxygen was also checked by AES measurements. Oxygen contamination is a major problem in the deposition of TiN films, and this investigation demonstrates that a judicious pre-deposition conditioning of the target chamber and the proper control of ambient can lead to better quality of TiN films. Recently, pulsed excimer laser (λ=248 nm) synthesis of TiN on Si <100> has been reported by Kanetkar et al. (55). The films were deposited in vacuum (~ 10^{-7} Torr) at a substrate temperature of 250°C using TiN target. The films were characterized by SEM,TEM, and XRD techniques. Cross-sectional TEM studies revealed that the interface of these golden coloured polycrystalline films was smooth with minimal interdiffusion. The problem of oxygen contamination was not discussed by these authors, however, it is necessary to mention at this point that in certain application, such as TiN acting as diffusion barrier, it has been observed oxygen in TiN plays a dominant role for its stability (59).

Tungsten carbide (WC) is another well known material in the class of hard materials. Just like TiN, tungsten carbide also exhibits high thermal and chemical stability and therefore it is expected that WC should be useful as diffusion barrier in silicon devices. Recently, in our laboratory amorphous WC film could be deposited on Si substrate using pulsed ruby laser using a pure WC target (60). The substrate temperature was 400°C and the laser energy density was 60 J/cm^2. The performance of laser deposited WC film as diffusion barrier in the Al/WC/Si metallization scheme has also been studied. It was found that laser deposited amorphous tungsten carbide acts as a good diffusion barrier in the range 100°C to 500°C. In subsequent investigations use was made of an unreacted pressed mixture of W and C (2:1 molar proportion) as a target instead of a sintered compound for laser ablation (61). The depositions were carried out in vacuum at two different energy densities viz. 20 J/cm^2 and 40 J/cm^2. It was shown that depending upon the laser fluence, one could synthesize stoichiometric or nonstoichiometric tungsten carbide films through the reactive vaporization of pressed sintered W-C pellet.

POST-SYNTHESIS PROCESSING OF LASER DEPOSITED THIN FILMS

The very nature of the entire field of nano- and micro- technology in modern materials science demands tailorability of the properties of thin films and surface layers of materials to the required specifications with a control on the lateral and the vertical length scales over nanometer to submicron dimensions. It is clear that the conventional methods of materials processing such as furnace annealing, thermal diffusion etc. can not meet these requirements, not simply because of their intrinsic limitations in the context of region selectivity but also due to very limited parametric freedom these have to offer. Therefore, considerable efforts have been made during the past three decades towards developing newer materials processing techniques with novel consequences. Foremost amongst these are directed energy processing techniques, particularly the ones using ion and laser beams. Since, the field of film deposition by laser ablation is itself of relatively recent origin, there have been only a few attempts so far towards post-synthesis processing of these films. Here, we discuss some of these results.

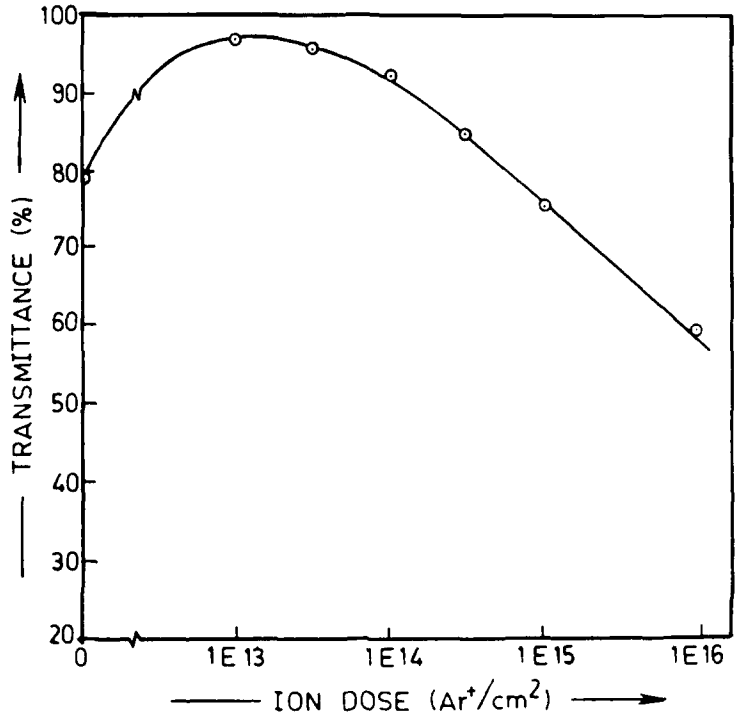

Figure 13. IR transmittance (in 2.5-4.0 micrometer range) vs. ion dose measurent spectrum of ion implanted a-C.

Ion Beam Induced Post-synthesis Modification of DLC Films

Ion Beam Processing involves bombardment of solid surfaces with selected ionic species (inert or reactive) having energy in the range of few tens to few hundreds of keV. This process offers unique abilities to control the properties of thin films to required specifications. As described in the earlier sections, the properties of DLC phase (a-C/a-C:H) are sensitive related to their microstructure and thus, ion beams offer a possibility of modification of DLC film properties leading to broadening the scope of their applicability. Prawer et al. (62,63) and Orzeszko et al. (64) have shown that hydrogen evolution is a crucial step in ion implantation of a-C:H DLC films. They have also pointed out that after hydrogen evolution radiation induced damage distribution plays an important role in modifying the properties of the hydrogenated DLC films.

Recently, Malshe et al. (65) have investigated argon ion implantation effects on laser deposited hydrogen-free DLC (a-C) films. As the film is hydrogen-free, the route of ion beam-induced modification will be different than that of hydrogenated DLC films. Our investigations show that for hydrogen-free DLC films there exists a

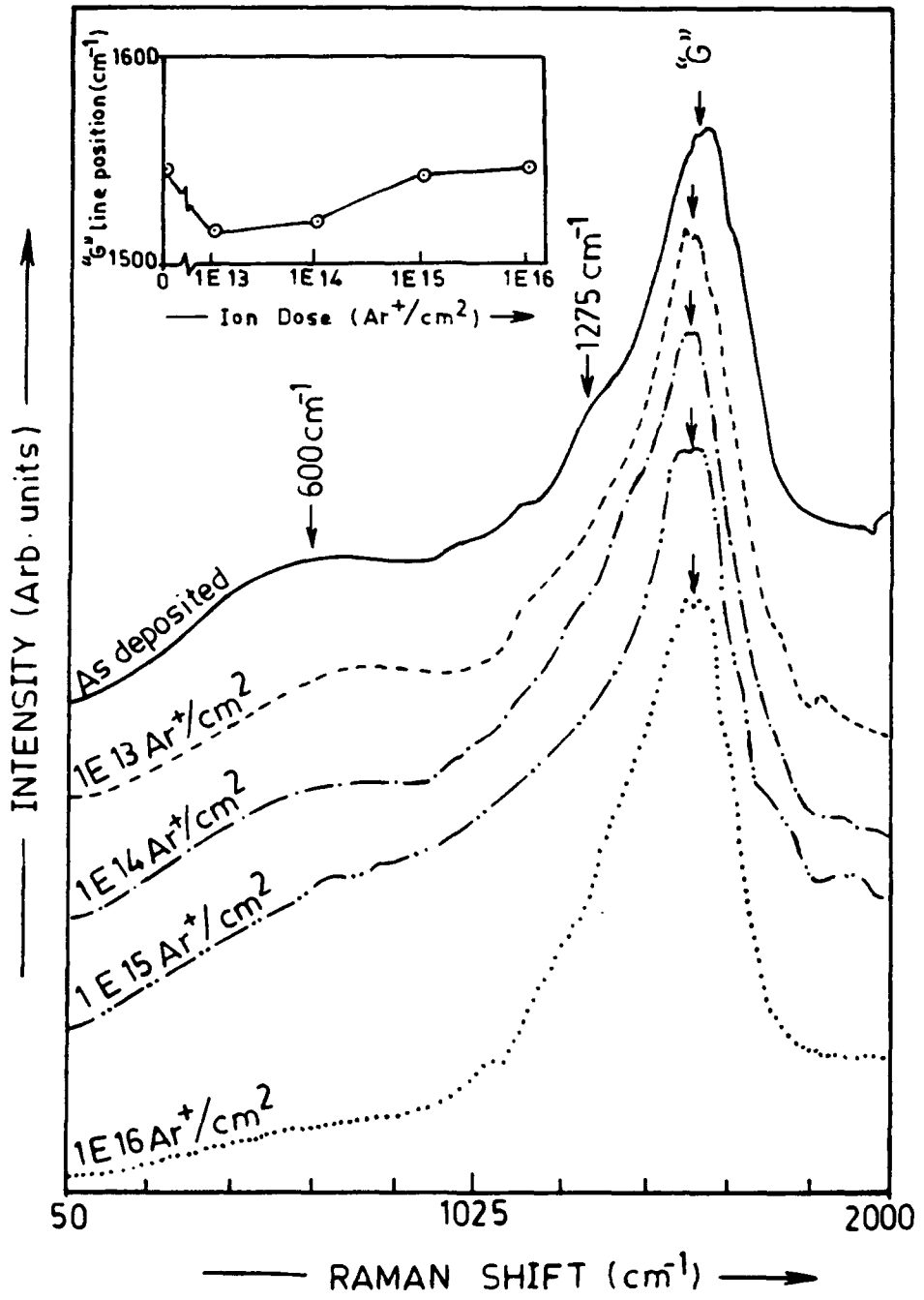

Figure 14. First-order Raman spectra of ion-implanted a-C films at various doses compared with that of the as deposited a-C films. The inset shows the position of the G-line as a function of ion dose.

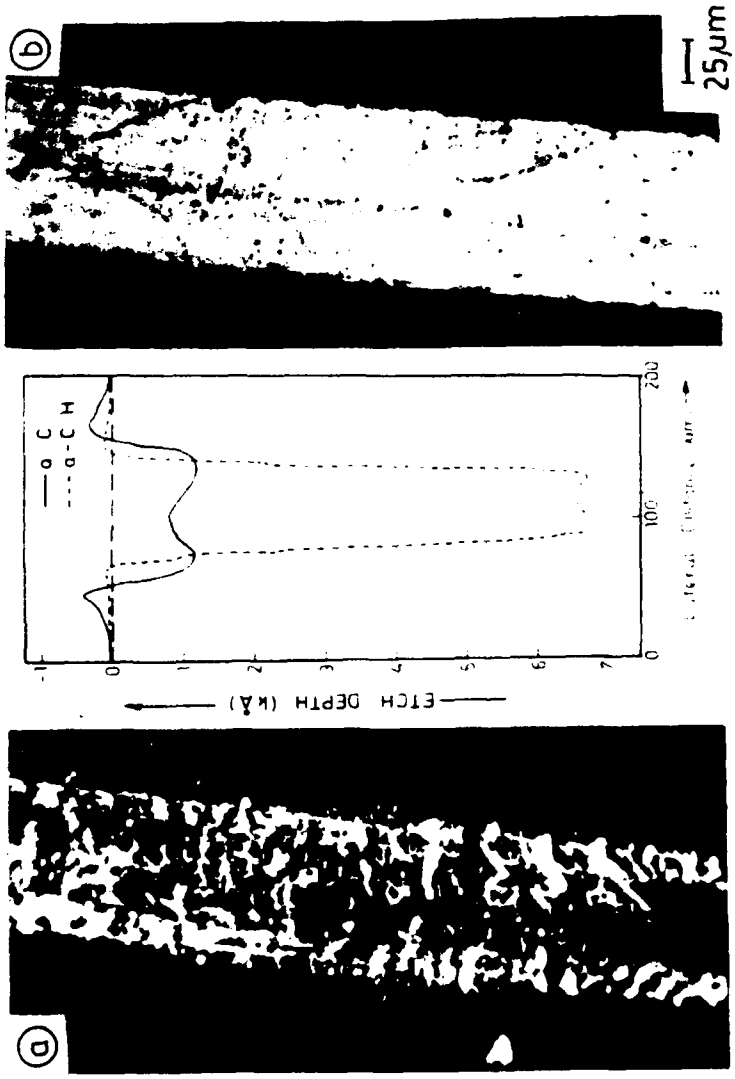

Figure 15. Scanning Electron Micrographs of laser etched a-C films (fig. 15a) and a-C:H films (fig. 15b) ($E = 325$ J/cm^2, $N = 25$). Inset shows overlap of thickness profile of a-C and a-C:H etched films.

dose value (typically in the range of $5x10^{13}$ ions/cm^2 to $1x10^{14}$ ions/cm^2), although not sharp as in the case of a-C:H, above which there is significant change in the optical and electrical properties of the DLC films. Interestingly enough, at very low ion dose values, particularly $1x10^{13}$ ions/cm^2, the IR transmittance of the a-C film increases drastically (Fig.13) and in congruence of this result it has been shown by Raman spectroscopy that the increase in transmittance can be attributed to the increase in the sp^3/sp^2 ratio in the implanted DLC matrix (Fig.14). It is important to mention that Zou et al. (66) have also reported similar increase in the microhardness and internal stress of the ion implanted (ion energy in MeV range) a-C:H films at lower dose values ($< 10^{13}$ ions/cm^2).

It is known that at lower dose values, particularly $< 1 \times 10^{13}$ ions/cm^2, ion generated cascades do not overlap and an ion typically in KeV range deposits about few eV/atom of energy in the ion cascade in the time scale of 10^{-11} sec. Thus, conditions are favourable for $sp^2 \rightarrow sp^3$ metastable transformation in the ion generated cascade. However, this planar to three dimensional structural transformation may lead to increase in internal stresses in the film. This increase in the strain energy of the lattice along with the radiation induced damage, particularly at higher dose values, may lead again to $sp^3 \rightarrow sp^2$ transformation and is indeed observed in the Raman spectrum of the films implanted at higher dose values ($> 1 \times 10^{15}$ ions/cm^2).

Laser Beam Induced Post-synthesis processing of L-PVD DLC Films

Rothschild et al. (67) were the first to carry out laser-induced controlled etching of amorphous diamond-like carbon films employing excimer laser ($\lambda = 193$ nm). They have indicated efficient use of DLC as positive photoresist. Recently, Malshe et al. (68) have done comparative study of KrF excimer laser induced etching of laser deposited a-C and hydrogenated DLC films. It has been shown that excimer laser etching rate of DLC a-C:H phase is much higher than DLC a-C phase. It has also been demonstrated that the etching of the former phase is cleaner than the latter one (Fig.15). It has further been brought out that hydrogen in the a-C:H films plays an influential role in the etching process. These investigations may help in defining the role of DLC films as photoresist materials.

CONCLUSION

The current status of research in the area of synthesis of thin films of Diamond, Diamond-like Carbon (DLC) and other materials such as BN, TiN, and WC by pulsed Laser ablation method is presented. It is brought out that the quality of Laser deposited films predominantly depends upon the deposition parameters such as laser fluence, laser wavelength, ambient gas pressure, and substrate temperature. Few cases of hybrid techniques involving Laser ablation in conjugation with a suitable method for further energizing of Laser generated plasma are also discussed and the corresponding implications for film properties are brought out. Also, hydrogenation

of films during deposition by pulsed Laser ablation is shown to improve the properties of DLC films significantly. Examples of post-synthesis processing of DLC films have also been discussed.

ACKNOWLEDGEMENT

The authors wish to acknowledge the financial support for this work from the Department of Electronics (DOE), India and INDO-US collaboration under the Department of Science and Technology (DST), India. One of the authors (A.P.M.) likes to thank the Council of Scientific and Industrial Research (CSIR), India for their financial support. The authors would also like to thank Dr. S.T. Kshirsagar, National Chemical Laboratory, Pune for the Raman measurements and for his fruitful contributions in the analysis of Raman spectra.

REFERENCES

1. Bachmann, P.K., and R. Messier, Chemical and Engineering News, p.24, (May 15, 1989).

2. Spear, K.E., Journal of American Ceramic Society, Vol.72, p.171, (1989).

3. "New Diamond", Japan Review in New Diamond (1990). (Papers therein).

4. Arya, S.P.S., and A. D'Amico, Thin Solid Films, Vol.157, p.267, (1988).

5. Witmer, M., B. Studer, and M. Melchiar, Journal of Applied Physics, Vol.52, p.5722, (1981).

6. Zega, B., M. Kornmann, and J. Amignet, Thin Solid Films, Vol.54, p.577, (1977).

7. Velkonen, E., T. Karlsson, B. Karlsson, and B.O. Johansson, Proceeding SPIE 1983 International Conference, Vol.401, p.41, (1983).

8. Angus, J.C., P. Koidl, and S. Domitz, p.89, J. Mort and F. Jansen (eds.), Plasma Deposited Thin Films, Ed.1, CRC Press, BOCA Raton, Florida, (1986).

9. Miyazawa, T., S. Misawa, S. Yoshida, and S. Gonda, Journal of Applied Physics, Vol.55, p.118, (1984).

10. Savvides, N., and B. Window, Journal of Vacuum Science and Technology A, Vol.3, p.2386, (1985).

11. Sankur, H., and J.T. Cheung, Applied Physics A, Vol.47, p.271, (1988).

12. Sudarshan, T.S., and V.V. Subramaniam, Fourth International Conference on Surface Modification Technology, France, (1990).

13. Lugomer, S., Laser Technology, Ed.1, Prentice Hall, New Jersey, (1990).

14. Smith, H.M., and A.F. Turner, Applied Optics, Vol.4, p.147, (1965).

15. Singh, R.K., and J. Narayan, Physical Review B, Vol.41, p.8843, (1990).

16. Auciello, O., A.R. Krauss, A.I. Kingon, and M.S. Ameen, Scanning Microscopy, Vol.4, p.203, (1990).

17. Nawathe, R., R.D. Vispute, S.M. Chaudhari, S.M. Kanetkar, A. Mitra, S.K. Date, and S.B. Ogale, Journal of Applied Physics, Vol.65, p.3197, (1989).

18. Venkatesan, T., W.D. Wu, A. Inam, and J.B. Wachtman, Applied Physics Letters, Vol.52, p.1193, (1988).

19. Bonch-Bruerich, A.M., and Ya A. Imas, Soviet Physics Technical Physics, Vol.12, p.1407, (1968).

20. Gangliano, F.P., and U.C. Paek, Applied Opitcs, Vol.13, p.274, (1974).

21. Kelly, R., and R.W. Dreyfus, Nuclear Instrumentation and Methods Physics Review, Vol.B32, p.341, (1988).

22. Zheng, J.P., Z.Q. Huang, D.T. Shaw, and H.S. Kwok, Applied Physics Letters, Vol.54, p.280, (1989).

23. Fujimori, S., T. Kasai, and T. Inamura, Thin Solid Films, Vol.92, p.71, (1982).

24. Wagal, S.S., E.M. Juengerman, and C.B. Collins, Applied Physics Letters, Vol.53, p.187, (1988).

25. Collins, C.B., F. Davanloo, E.M. Juengerman, W.R. Osborn, and D.R. Jander, Applied Physics Letters, Vol.54, p.216, (1989).

26. Krishnaswamy, J., A. Rengan, J. Narayan, K. Vedam, and C.J. McHarge, Applied Physics Letters, Vol.54, p.2455, (1989).

27. Baggott, J., New Scientist, p.16, (1990).

28. Dentchman, A.H., R.J. Partyka, Advanced Materials and Processes, Vol.6, p.29, (1989).

29. Weissmantel, C., K. Bewilogua, K. Breuer, D. Dietrich, U. Ebersbach, Ch. Erler, B. Rav and G. Reiss, Thin Solid Films, Vol.96, p.31, (1982).

30. Miyasato, T., Y. Kawakami, T. Kawano, and A. Hiraki, Japanese Journal of Applied Physics, Vol.23, p.L234, (1984).

31. Davanloo, F., E.M. Jungerman, D.R. Jander, T.J. Lee, and C.B. Collins, Journal of Applied Physics, Vol.67, p.2081, (1990).

32. Davanloo, F., E.M. Jungerman, D.R. Jander, T.J. Lee, and C.B. Collins, Journal of Materials Research, Vol.5, p.2398, (1990).

33. Yoshikawa, M., Materials Science Forum, Vol.52/53, p.365, (1989).

34. Robertson, J., Advances in Physics., Vol.35, p.317, (1986).

35. Marquardt, C.L., R.T. Williams, and D.J. Nagel, Materials Research Society Symposium Proceedings, Vol.38, p.325, (1985).

36. Weissmantel, C., K. Bevilogua, D. Dietrich, H.J. Erler, H.J. Hinnenberg, S. Klose, W. Nowick, and G. Reisse, Thin Solid Film, Vol.72, p.19, (1980).

37. Spencer, E.G., P.H. Schmidt, D.C. Joy, and F.J. Sansalone, Applied Physics Letters, Vol.29, no.118, (1976).

38. Pompe, W., H.J. Scheibe, A. Richeter, H.D. Baner, K. Bewilogua, and C. Weissmantel, Thin Solid Films, Vol.144, p.77, (1986).

39. Richter, A., and W. Pompe, Journal of Non-crystalline Solids, Vol.97/98, p.1443, (1987).

40. Sato, T., S. Furuno, S. Iguchi, and M. Hanabura, Japanese Journal of Applied Physics, Vol.26, p.L1487, (1987).

41. Malshe, A.P., S.M. Chaudhari, S.M. Kanetkar, S.B. Ogale, S.V. Rajarshi and S.T. Kshirsagar, Journal of Materials Research, Vol.4, p.1238, (1989).

42. Rengan, A., S.M. Kanetkar, J. Narayan, J.L. Park, Li Ming, and S. Bedge, (Unpublished).

43. Martin, J.A., L. Vazquez, P. Bernard, F. Comin, and S. Ferrer, Applied Physics Letters, Vol.57, p.1742, (1990).

44. Mantell, C.L., Carbon and Graphite Handbook, Interscience/Wiley, New York, (1988).

45. Chen, X., and J. Mazumder, (Unpublished).

46. Malshe, A.P., S.M. Kanetkar, S.B. Ogale, S.T. Kshirsagar, Journal of Applied Physics, Vol.68, p.5648, (1990).

47. Tamor, M.A., J.A. Haire, C.H. Wu, and K.C. Hass, Applied Physics Letters, Vo'.54, p.123, (1989).

48. Malshe, A.P., Ph.D. Thesis, University of Poona, (1991).

49. Rengan, A., S.M. Kanetkar, J. Narayan, J.L. Park, Li Ming, and J. Le, (Unpublished).

50. Wentorf, R.H., Journal of Chemical Physics, Vol.26, p.956, (1951).

51. Kessler, G., H.D. Baner, W. Pompe, and H.J. Scheiber, Thin Solid Films, Vol.147, p.L45, (1987).

52. Paul, T.K., P. Bhattacharya, and D.N. Bose, Electronics Letters, Vol.25, p.1602, (1989).

53. Paul, T.K., P. Bhattacharya and D.N. Bose, Applied Physics Letters, Vol.56, p.2648, (1990).

54. Doll, G.L., J.A. Sell, A. Wims, C.A. Taylor II and R. Clarke, Physical Review B, Vol.43, p.6816, (1991).

55. Kanetkar, S.M., S. Sharan, P. Tiwari, J. Matera and J. Narayan, MRS Proceedings on Surface Chemistry and Beam Solid Interaction, Vol.201, (1990).

56. Kanetkar, S.M., G. Matera, X. Chen, S. Pramanick, P. Tiwari, J. Narayan, G. Pfeiffer, and M. Paesler, Journal of Electronic Materials, Vol.20, p.141, (1991).

57. Mieno, M., and T. Yoshida, Japanese Journal of Applied Physics, Vol.29, p.1175, (1990).

58. Biunno, N., J. Narayan, A.R. Srivatsa, and O.W. Holland, Applied Physics Letters, Vol.55, p.405, (1989).

59. Auciello, O., T. Barues, S. Chevacharoendkul and G.E. McGuire, Thin Solid Films, Vol.181, p.65, (1989).

60. Ghaisas, S., Journal of Applied Physics (In press).

61. Ghaisas,S., R.D. Vispute, S.B. Ogale, S.M. Chaudhari, S.M. Kanetkar, S. Badrinarayan and S. V Ghaisas, Journal of Materials Research (Submitted).

62. Prawer, S., R. Kalish, M. Adel, and V. Richter, Applied Physics Letters, Vol.49, p.1157, (1986).

63. Prawer, S., R. Kalish, M. Adel, and V. Richter, Journal of Applied Physics, Vol.61, p.4492, (1987).

64. Orzeszko, S., J.A. Woollam, D.C. Ingram, and A.W. McCormic, Journal of Applied Physics, Vol.64, p.2611, (1988).

65. Malshe, A.P., S.M. Chaudhari, S.M. Kanetkar, S.B. Ogale, and S.T. Kshirsagar, Thin Solid Films, Vol.193/194, p.588, (1990).

66. Zou J.W., K. Schmidt, K. Reichelt, and B. Stritzker, Journal of Vacuum Science and Technology A, Vol.6, p.3103, (1988).

67. Rothschild, M., and D.J. Ehrlich, Journal of Vacuum Science and Technology B, Vol.5, p.389, (1987).

68. Malshe, A.P., S.B. Ogale, S.T. Kshirsagar, and K.S. Chari, Materials Letters, Vol.11, p.175, (1991).

69. Fujimori, S., and K. Nagai, Japanese Journal of Applied Physics, Vol.20, p.L194, (1981).

70. Fujimori, S., T. Kasai, and T. Inamura, Proceedings of Fifth Symposium on Ion Sources and Ion-assisted Technology, Tokoy, Ed. T. Takagi, p.319, (1981).

71. Wada, N., P.J. Gaczi, and S.A. Solin, Journal of Non-Crystalline Solids, Vol.35-36, p.543, (1980).

72. Kakinoki, J., K. Katada, T. Hanawa, and T. Ino, Acta Crystallography, Vol.13, p.171, (1960).

73. Morgan, M., Thin Solid Films, Vol.7, p.313, (1971).

74. Shiojiri, M., Y. Saito, M. Okada, and H. Sasaki, Japanese Journal of Applied Physics, Vol.18, p.1931, (1979).

75. Reisse, G., C. Schurer, D. Ebersbach, K. Bewilogana, K. Breuer, H.-J. Erler, and C. Weissmantel, Wiss. Z. Techn. Hochsch. Karl-Marx-Stadt, Vol.22, p.653, (1980).

76. Bakai, A.C., and W.E. Strelnizkij, Strukturnijei fisitscheskie swoistwa uglerodnich kondensatow, ZNIJ atominform Moscow, p.47, (1984).

77. Smith, F.W., Japanese Journal of Applied Physics, Vol.55, p.764, (1984).

78. Whitmell, D.S., and R. Williamson, Thin Solid Films, Vol.35, p.255, (1976).

79. Meyerson, B., and F.W. Smith, Journal of Non-Crystalline Solids, Vol.35-36, p.435, (1980).

80. Anderson, D.A., Philosophical Magazine, Vol.35, p.17, (1977).

81. Euke, K., Thin Solid Films, Vol.80, p.227, (1981).

82. Holland, L., Journal of Vacuum Science and Technology, Vol.14, p.5, (1977).

83. Bewilogua, K., D. Dietrich, G. Holzhuter, and C. Weissmantel, Physics Status Solodi A, Vol.71, p.K57, (1981).

84. Miyasato, T., Y. Kawakami, T. Kawano, and A. Hiraki, Japanese Journal of Applied Physics, Vol.23, p.L234, (1984).

85. Aisenberg, S., and R. Cabot, Journal of Applied Physics, Vol.42, p.2953, (1971).

86. Spencer, E.G., P.H. Schmidt, D.C. Joy, and F.J. Sansalone, Applied Physics Letters, Vol.29, p.118, (1976).

MATERIALS & MANUFACTURING PROCESSES, 8(1), 59-73 (1993)

DEPOSITION OF DIAMOND FOR CUTTING TOOL APPLICATIONS

K. Saijo, M. Yagi, K. Shibuki, and S. Takatsu
Toshiba Tungaloy Co. Ltd., 1-7 Tukagoshi, Saiwai Kawasaki 210, Japan

ABSTRACT

The poor adhesion of diamond film to substrates is one of the major problems for practical use in a cutting tool (1-4). In this study, sintered tungsten carbide (WC) body without Co metal, not cemented carbide, was used as the substrate (5), and the effects of surface decarburization of the substrate for improvement in the adhesion of diamond films were investigated. The surface decarburization and diamond coating were carried out in a microwave plasma CVD system. From the results of several adhesion tests, including the cutting tests, it is concluded that the good adhesion is obtained by surface decarburization of the substrate before diamond coating. The reasons for improvement in adhesion are considered by observing the interface structure between the film and the substrate. The damage mechanism of diamond coating on cutting an Al-18%Si alloy with increasing cutting speed is also discussed.

INTRODUCTION

Since Kamo et al. (6) of NIRIM developed the thermal filament CVD method, and the microwave plasma CVD method (7,8) in 1982, studies of the synthesis of diamond from gas phase have accelerated. Plasma jet method (9) and combustion flame method (10), etc., have also been developed for diamond film synthesis. These facts mean that diamond synthesis from gas phase has high possibility for large area coating (11), inexpensive production costs and shape flexibility of coating, etc., compared with high pressure diamond.

However, there are many problems to be solved for practical use of diamond film; for example, the poor adhesion on cutting tools, and the existence of non-diamond carbon in films for application to semiconductor fields. In the former case, two main reasons for poor adhesion may be considered. Firstly, the nucleation density of diamond is extremely low compared with that of other ceramic coatings. This results in a small contact area between the film and the substrate. Secondly,

non-diamond carbon phases, such as graphite and amorphous carbon, are deposited at the interface between the film and the substrate. Many countermeasures to improve the adhesion such as selection of substrate, fine scratch marks by diamond powder (12), removal of cobalt from the surface of cemented carbide (13), selection of coating condition (4,14,15), etc., have been tried. These treatments are effective in improving adhesion to some extent, but, no definitive method has been found yet.

In the present study, sintered WC body without cobalt was used as the substrate, and the effects of surface decarburizing of the substrate on the adhesion of diamond film were investigated (16). The cutting performance of the diamond coating was also examined.

EXPERIMENTAL DETAILS

First of all, a sintered WC body produced by hot pressing method at 1700°C in vacuum was used as the substrate. Ground surface of substrate was prepared in the as-sintered state (17) by re-sintering treatment, which it was done in vacuum at 1430°C. This treatment provides the necessary surface morphology of the substrate for adhesion of diamond film.

A microwave plasma CVD system was used for surface decarburization of the substrate and for diamond coating. Surface decarburizing of the substrate was done in H_2-2%O_2 gas under the conditions shown in Table 1(a). And then, the surface of decarburized substrate was scratched with 8 to 16 mm diamond powder dispersed in ethanol using an ultrasonic oscillator. After this treatment, diamond coating was done under the conditions consisting of 2 stages as shown in Table 1(b).

The first stage was done in H_2-2%CH_4 at 930°C to increase the nucleation density of diamond. In the second stage, CH_4 concentration and substrate temperature were changed to 3%CH_4 and 1060°C respectively to increase the growth rate of film and improve the crystallinity of diamond. For comparison, diamond coating without surface decarburizing was also produced.

These diamond coatings were characterized by a scanning electron microscope (SEM), X-ray diffraction, Raman spectroscopy, and by transmission electron microscope (TEM). The adhesion of diamond films was determined by an indentation test with a Rockwell hardness diamond cone. The cutting performance of diamond coatings was tested in turning an Al-10%Si alloy and milling a hard carbon and an Al-18%Si alloy using inserts of ISO SPGN120308 and HEHN532FN. The damage to diamond films after cutting was examined by SEM and micro-laser Raman spectroscopy. Hard carbon is graphite material including a little ceramic additives. It is hard to cut by a cemented carbide insert.

TABLE 1
The experimental conditions for surface decarburization (a) of substrate and diamond coating (b)

Factors	(a)	(b)	
		1st	2nd
Temperature (°C)	930	930	1060
Pressure (Torr)	60	60	80
O_2 in H_2 (vol %)	2	0	0
CH_4 in H_2 (vol %)	0	2	3
Time (min)	30	30	120

RESULTS AND DISCUSSION

Characterization of diamond coatings

The surface morphology of WC substrate before and after re-sintering treatment is shown in Fig.1. WC particle near the surface are slightly coarser due to re-sintering. Preparing the surface morphology of substrate is effective to increase the adhesion of diamond film, as it had been confirmed that the adhesion of diamond film on the as-sintered state is higher than that on lapped or ground ones (17). One of the reasons is that the film is mechanically locked among the coarse WC grains on the substrate surface.

Figure 2 shows the surface morphology of diamond film. It is preferentially consists of the crystals with (111) facets and the thickness is about 5 μm. The Raman spectrum of diamond film is shown in Fig.3. There is no remarkable difference in the profile whether the substrate was decarburized or not. The spectrum has a sharp diamond peak at 1333 cm^{-1} and a weak and broad peak of amorphous carbon from 1450 cm^{-1} to 1650 cm^{-1}. The changes in X-ray diffraction patterns of the substrate by surface decarburizing and diamond coating are shown in Fig.4.

Before surface decarburizing, all peaks from the substrate consist of WC (Fig.4(a)). After surface decarburizing, three sharp W peaks are observed (Fig.4(b)). After diamond coating on decarburized substrate, W peaks have disappeared, and strong WC peaks are observed again (Fig.4(c)). The carburization rate of decarburized substrate depends on the deposition temperature and time. W_2C peak was not observed after diamond coating at 1060°C for 2 hrs. These results mean that the recarburization of decarburized substrate is completed during diamond coating.

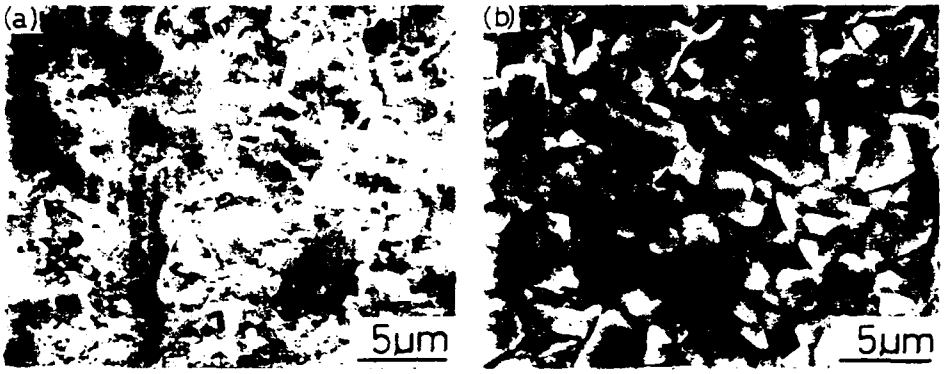

Figure 1. Surface morphology of WC substrate before and after re-sintering. (a) As-ground state (before re-sintering). (b) As-sintered state(after re-sintering).

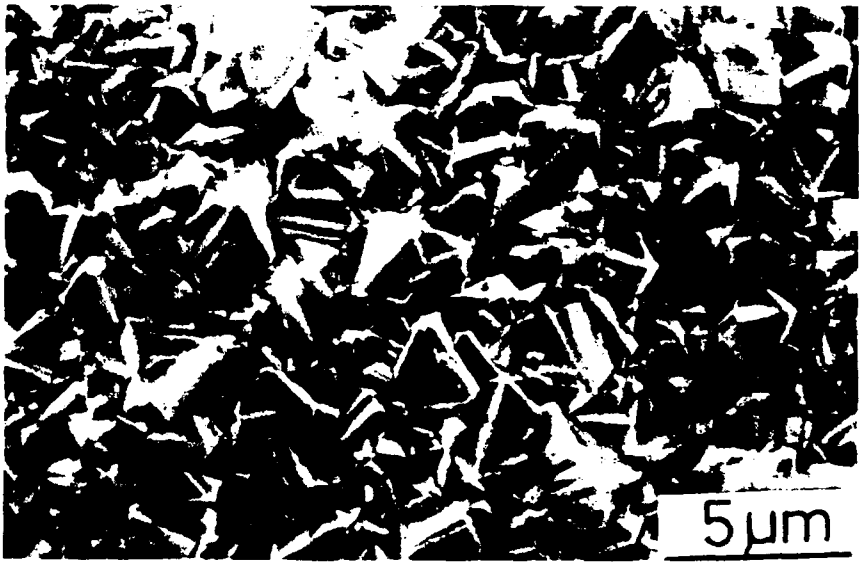

Figure 2. Surface morphology of diamond film.

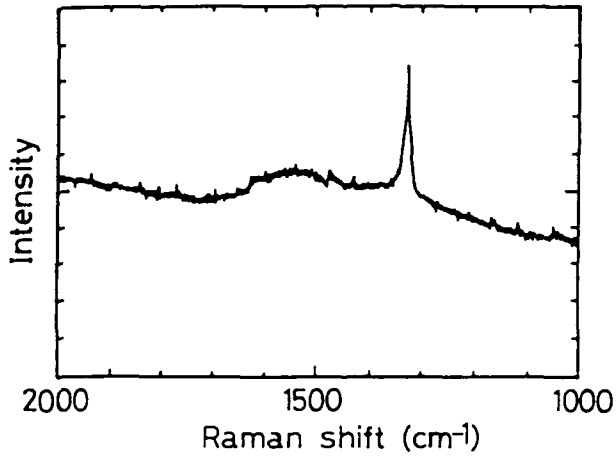

Figure 3. Raman spectrum of diamond film.

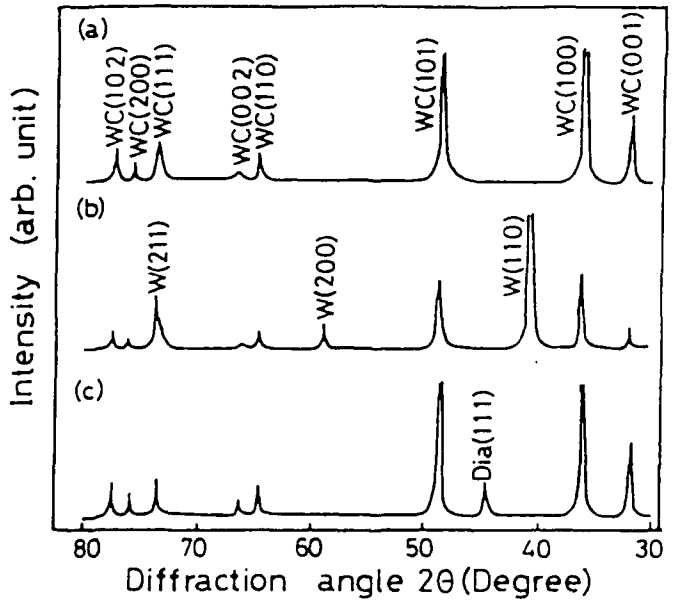

Figure 4. X-ray diffraction patterns of WC substrate. (a) Before decarburizing. (b) After decarburizing. (c) After diamond coating.

Evaluation of the adhesion of diamond film

The adhesion of diamond film was evaluated by an indentation test using a diamond cone with a top radius of 0.2 mm. The results are shown in Fig.5. By

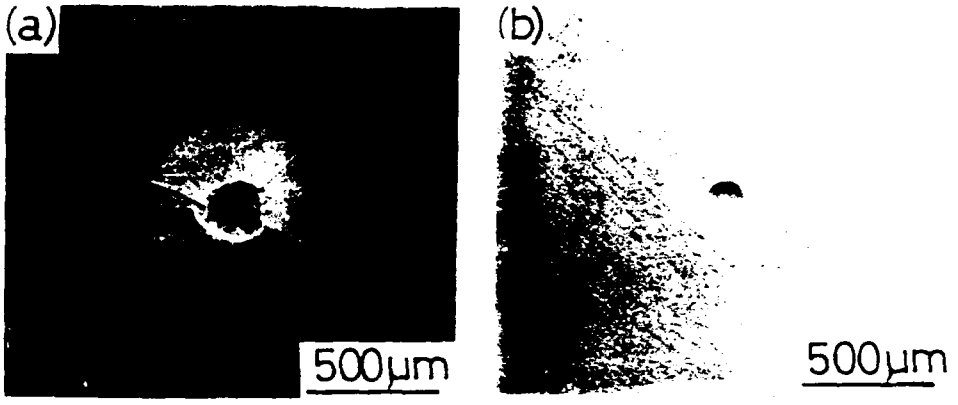

Figure 5. Diamond film after indentation test (load:60kgf). (a) On untreated substrate. (b) On decarburized substrate.

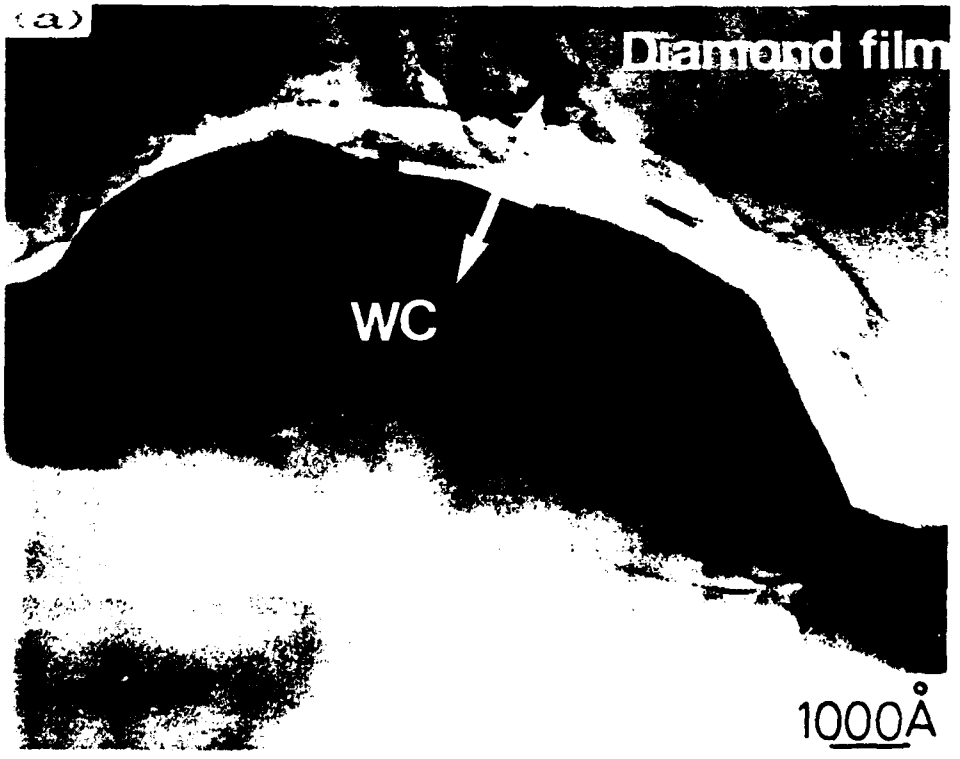

Figure 6a. TEM cross section image of diamond coatings on untreated substrate.

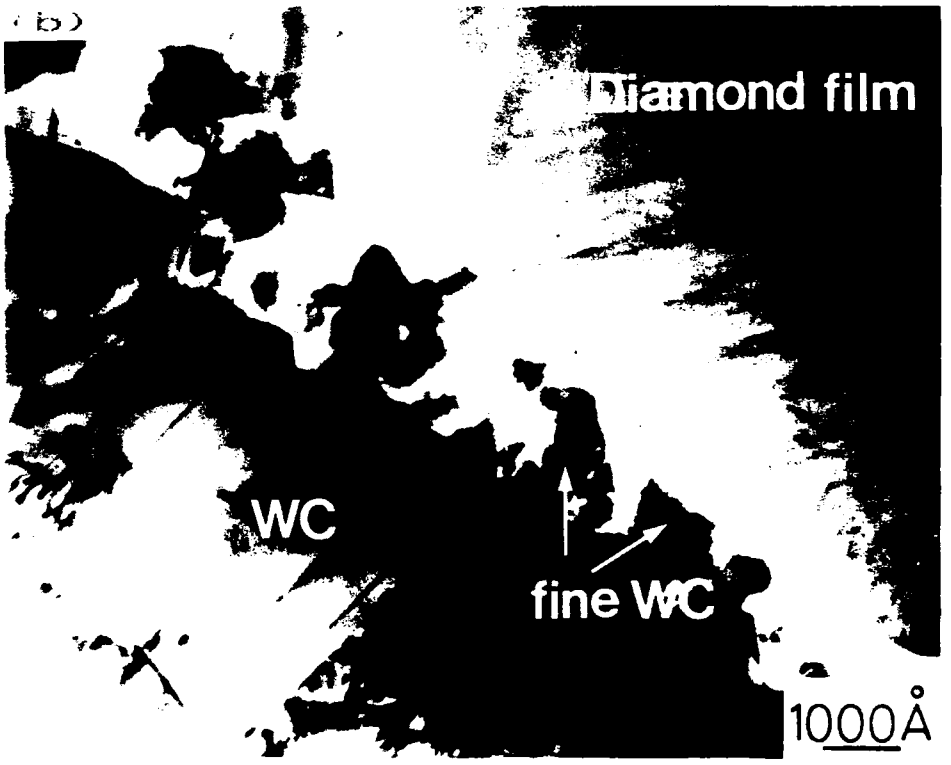

Figure 6b. TEM cross section image of diamond coatings on decarburized substrate.

indentation at a load of 60 kgf, flaking of the film is observed on diamond coating without surface decarburizing (Fig.5(a)), while the diamond coating on decarburized substrate shows better adhesion without film flaking (Fig.5(b)).

Observation of the interface structure by TEM

The interface structure of diamond coatings with and without decarburizing of substrate observed by transmission electron microscope (TEM) is shown in Fig.6. Very fine WC grains compared with original WC grains in the substrate are generated at the interface between the film and the decarburized substrate (Fig.6(b)). The grain size of fine WC is less than 0.1 μm. One of the reasons for generation of these fine WC grains is thought to be the generation of many defects induced in W layer by plasma decarburizing, which function as nucleation sites for WC when diamond was deposited. On the other hand, these fine WC grains are not observed between the film and the untreated substrate (Fig.6(a)). From these observations, the main reasons for improvement of the adhesion are increased contact area between

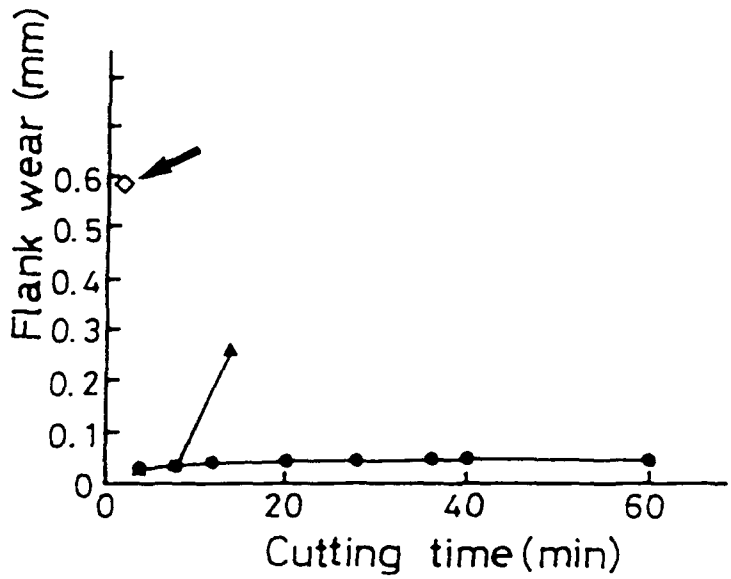

Figure 7. Flank wear in milling a hard carbon. ▲:diamond coating on untreated substrate. •:diamond coating on decarburized substrate. o:uncoated cemented carbide.

the film and the substrate by generating a lot of fine WC grains on decarburized substrate, and the embedding of film in the shape of wedges among the fine WC grain boundaries. And also, the carbon diffusion process into substrate may have some positive effects on adhesion.

Cutting performance of diamond coatings

The diamond coated inserts with and without the surface decarburizing of substrate were produced for cutting tests. As a comparison, an uncoated cemented carbide insert corresponding to ISO K10 grade and sintered diamond insert were also used.

Milling a hard carbon under dry condition

The results of milling a hard carbon at a cutting speed of 326 m/min, a depth of cut of 0.5 mm and a feed rate of 0.058 mm/tooth are shown in Fig.7. The hardness of work material is HRB102 (HRB: Rockwell hardness B scale). The thickness of diamond film is about 10 μm. The results indicate that the uncoated cemented carbide insert can not be used under this cutting condition, and the tool life of diamond coating on decarburized substrate is more than 7 times longer compared

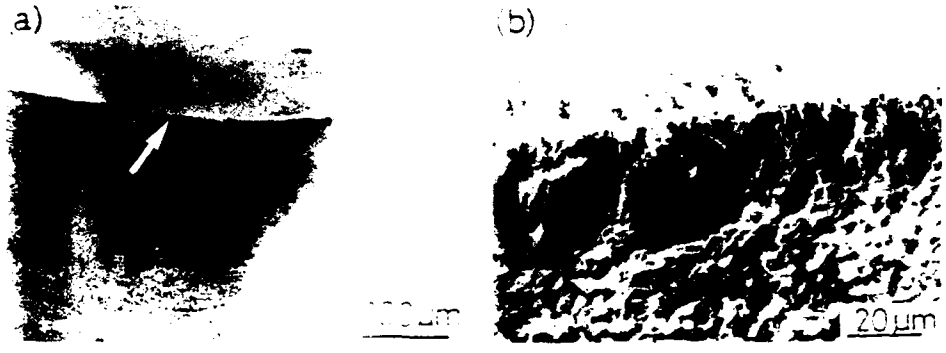

Figure 8. The cutting edge of diamond coating on decarburized substrate after milling for 60 min. (b) shows area indicated by arrow in (a).

with that of diamond coating on untreated substrate. Figure 8 shows the cutting edge of diamond coating on decarburized substrate after milling for 60 min. The wear of diamond film is negligibly small, even after cutting for 60 min. The result of micro-laser Raman spectrum analysis of diamond film on the cutting edge before and after cutting is shown in Fig.9. It indicates that neither the transformation of diamond to graphite, nor the contamination of graphite from the work material are detected after cutting a hard carbon.

Turning an Al-10%Si alloy under dry condition

Figure 10 shows the results of turning an Al-10%Si alloy at a cutting speed of 1000 m/min, a depth of cut of 0.5 mm and a feed rate of 0.1 mm/rev. The thickness of diamond film is about 6 μm. The wear of uncoated cemented carbide is increased very fast under this cutting condition. The tool life of diamond coating on decarburized substrate is more than 9 times longer as compared with that of uncoated cemented carbide. The cutting edge of diamond coating on decarburized substrate before and after cutting is shown in Fig.11. The wear is very small and smooth, without flaking of diamond film even after cutting for 90 min.

Milling an Al-18%Si alloy under wet condition

The influence of cutting speed on the tool life of diamond coating in milling an Al-18%Si alloy is summarized in Fig.12. The flank wear width of 0.2 mm was taken as the criterion of tool life. The work length is 107 mm. Cutting speeds were 300, 450, and 600 m/min, and a depth of cut and a feed rate were 2 mm and 0.1 mm/tooth respectively. Al-18%Si alloy has the structure with about 30 μm silicon particles dispersed uniformly in the aluminum matrix as shown in Fig.13. The thickness of

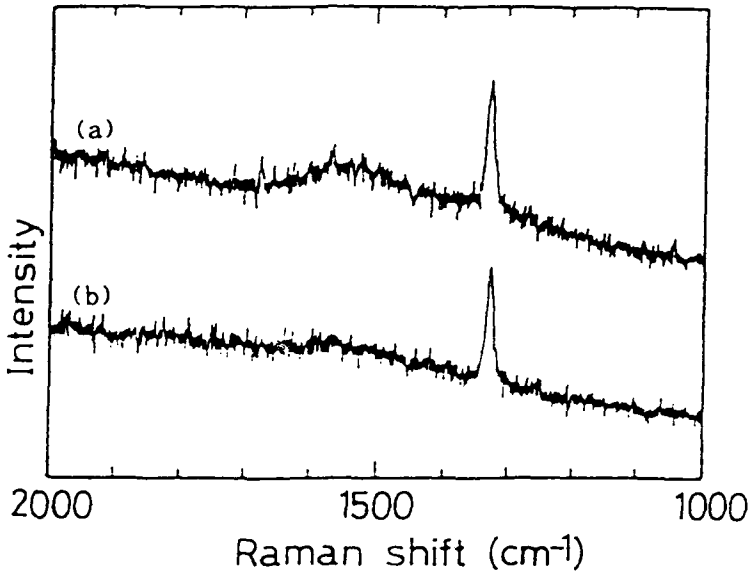

Figure 9. The micro-laser Raman spectrum analysis of diamond film on the cutting edge before and after cutting. (a) Before cutting. (b) After cutting for 60 min.

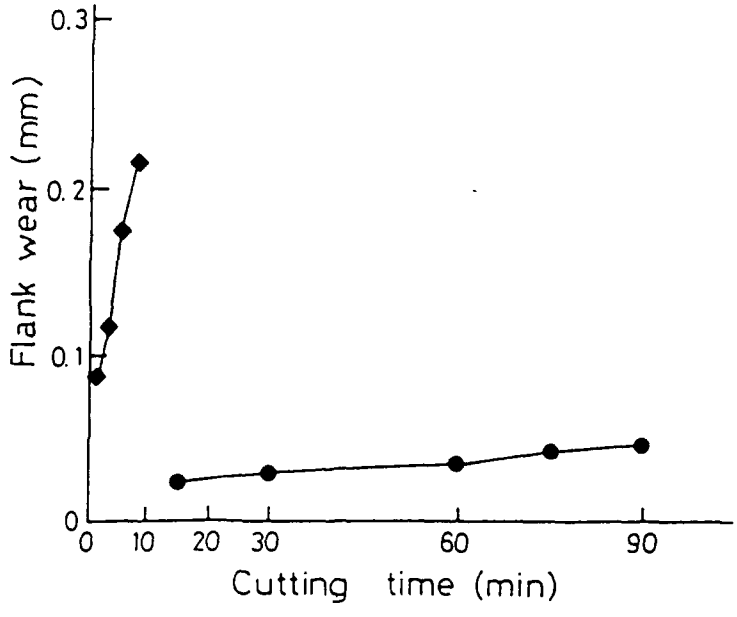

Figure 10. Flank wear in turning an Al-10%Si alloy. •:diamond coating on decarburized substrate. ♦:uncoated cemented carbide.

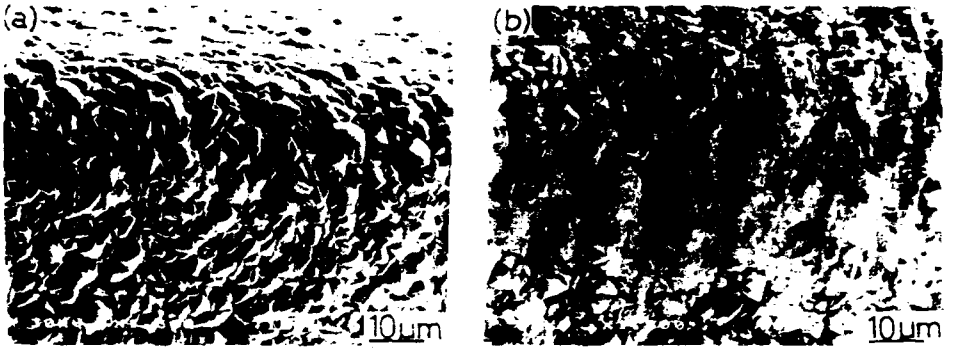

Figure 11. The cutting edge of diamond coating on decarburized substrate after turning an Al-10%Si alloy. (a) Before cutting. (a) After cutting for 90 min.

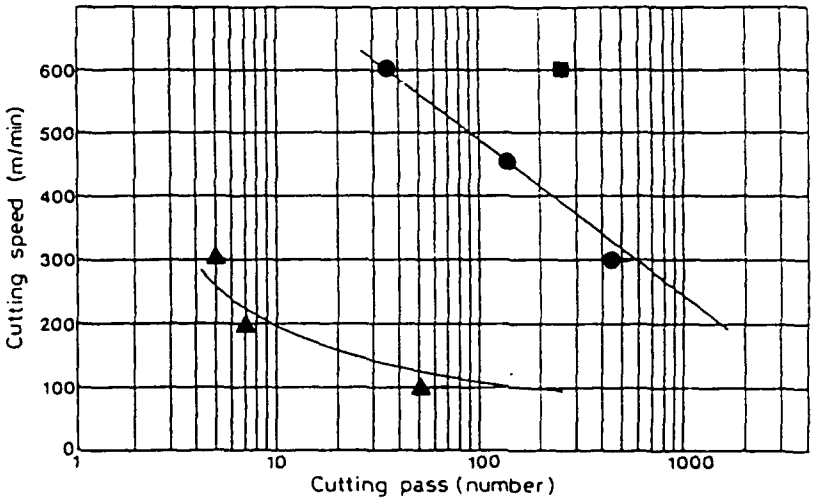

Figure 12. The influence of cutting speed to the tool life of diamond coating on milling an Al-18%Si alloy. ·:diamond coating on decarburized substrate. ▲:uncoated cemented carbide. ■:sintered diamond.

diamond film is about 6 μm. The damage to diamond film after cutting is shown in Fig.14. The results indicate that the tool life of diamond coating strongly depends on the cutting speed. At the cutting speed of 300 m/min, the damage to diamond film is characterized by smooth abrasive wear as shown in Fig.14(a). However, at the cutting speed of 600 m/min, the damage obviously changes to micro-chipping of the film, as shown in Fig.14(b).

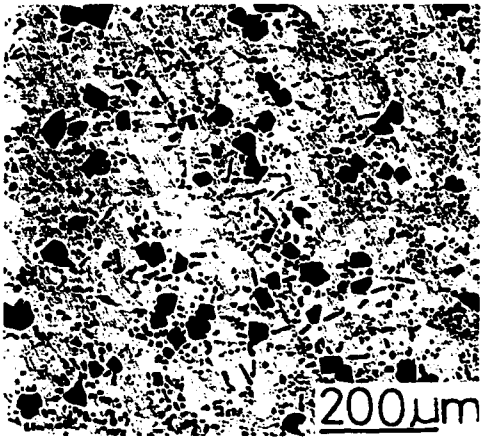

Figure 13. The structure of Al-18%Si alloy.

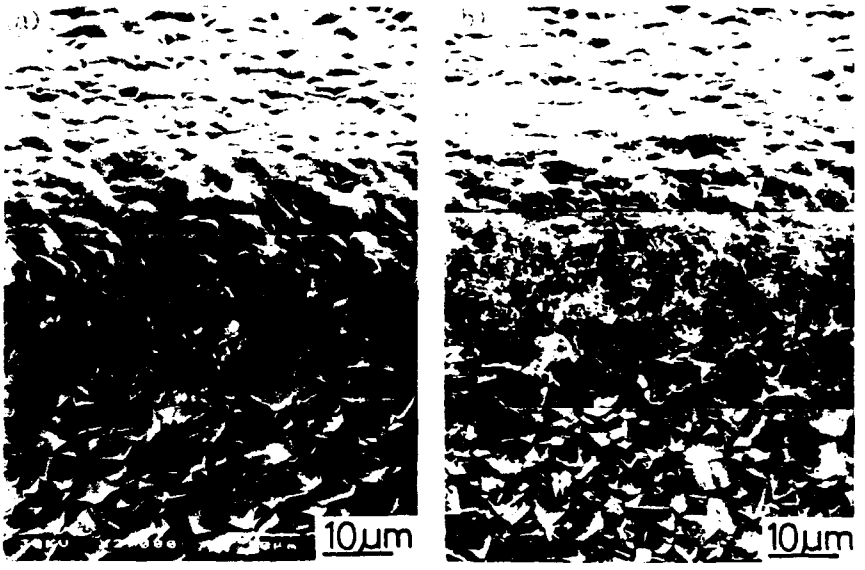

Figure 14. The damage to diamond film on the cutting edge after milling an Al-18%Si alloy. (a) 240 passes at 300 m/min. (b) 36 passes at 600 m/min.

The reason for the change in damage mechanism of diamond film is considered to be increased mechanical and thermal shock into the diamond film by collision of hard silicon particles with higher cutting speed, and as a result the diamond film is chipped at high cutting speed.

Figure 15. The damage to sintered diamond on the cutting edge after milling 260 passes at 600 m/min.

Figure 15 shows the damage of sintered diamond after cutting 260 passes with cutting speed of 600 m/min. It seems to be similar to the damage of diamond coating shown in Fig.14(b). In spite of the similar damage, the tool life of sintered diamond is much longer compared with that of diamond coating. It is caused by the difference in the thickness of diamond layers. The thickness of diamond layer on cutting edge of sintered diamond is much thicker than that of diamond film. From these results, in the case that the damage mechanism is dominated by smooth abrasive wear of diamond film, the present diamond coating shows excellent cutting performance.

CONCLUSION

The effects of surface decarburization of WC substrate on the adhesion of diamond film were investigated. Tungsten layer is formed on the surface of decarburized substrate, but it is completely carburized again during diamond coating, and very fine WC grains compared with original WC grains in the substrate are generated in the recarburized layer. As a result, remarkable increase in the adhesion of diamond film is obtained. The excellent cutting performance of the diamond coating is confirmed in cutting a hard carbon, Al-10% and 18% Si alloys.

ACKNOWLEDGMENTS

The authors are grateful to Prof. Echigoya of Tohoku University for the TEM observations and helpful discussions.

REFERENCE

1. Lux, B., and R. Haubner, VDI Berichte NR 762, p.61-84, (1989).

2. Kikuchi, N., and T. Komatsu, Materials Science and Engineering, A105/106, p.525-534, (1988).

3. Okuzumi, F., New Diamond 1990 (For Overseas Readers), Published by New Diamond Forum, p.80, (1990).

4. Ito, T., and N. Hayashi, New Diamond 1990, (For Overseas Readers), Published by New Diamond Forum, p.83-85, (1990).

5. Kamo, M., H. Chawanya, T. Tanaka, Y. Sato, and N. Setaka, Materials Science and Engineering, A105/106, p.535-541, (1988).

6. Kamo, M., Y. Sato, S. Matsumoto, and N. Setaka, Japan Journal of Crystal Growth, Vol.62, p.642, (1983).

7. Matsumoto, S., Y. Sato, M. Kamo, and N. Setaka, Japan Journal of Applied Physics, Vol.21, p.L18, (1982).

8. Spear, K.E., Journal of the American Ceramic Society, Vol.72, No.2, p.171-191, (1989).

9. Kawarada, M., K. Kurihara, K. Sasaki, A. Teshima, and N. Koshino, Program and Abstracts of 1st International conference on the New Diamond Science and Technology, p.42, (1988)

10. Hirose, Y., and M. Mitsuizumi, New Diamond 1990 (For Overseas Readers), Published by New Diamond Forum, p.27, (1990),

11. Ishibori, K., Y. Ohira, Program and Abstracts of 1st International conference on the New Diamond Science and Technology, p.104, (1988)

12. Sato, Y., S. Matsumoto, M. Kamo, and N. Setaka, Journal of Surface Science Society Japan, Vol.5, p.54, (1984).

13. Suzuki, H., H. Matsubara, and N. Horie, Journal of Japan Society of Powder Metallurgy, Vol.33, p.262, (1986).

14. Shibuki, K., M. Yagi, K. Saijo, and S. Takatsu, Surface and Coatings Technology, Vol.36, p.295-302, (1988).

15. Murakawa, M., S. Takeuchi, H. Miyazawa, and Y. Hirose, Surface and Coatings Technology, Vol.36, p.303-310, (1988).

16. Saijo, K., M. Yagi, K. Shibuki, and S. Takatsu, "The Improvement of Adhesion Strength of Diamond Films," Surface and Coatings Technology, in press, (1990).

17. Yagi, M., Program and Abstracts of 1st International Conference on the New Diamond Science and Technology, p.158, (1988).

MATERIALS & MANUFACTURING PROCESSES, 8(1), 75-82 (1993)

DIAMOND FILMS FROM CH_3OH SYSTEMS

L.J. Zhangzhan, M. Liying, S. Zhenwu, and F. Lili
Zhengzhou Research Institute for Abrasives and Grinding
Zhengzhou, Henan, China

ABSTRACT

Polycrystalline diamond films were obtained on silicon (111) substrates by the microwave plasma-assisted chemical-vapour-deposition (CVD) method from the CH_3OH+H_2 systems.When CH_3OH,CH_3COCH_3, H_2 were used as the source gases,the diamond epitaxial films were obtained on the synthesized single-crystal diamond (100), (110) and (111) substrates too. From the experimental results, we could discover that CH_3OH, CH_3COCH_3 and other hydrocarbon gases could also be used as suitable source gases for the growth of diamond films.

INTRODUCTION

Diamond is the hardest material in the world and has been widely used in industrial applications as cutting tools, as grinding tools, and as polishing powders. Diamond is expected to be an attractive material for electronic and optical devices which operate under severe conditions, such as at high temperatures and in strong irradiation environments. It is expected that diamond films will have a vast area of application, particularly in the field of electronics. During the past few years, great progress has been made in experimental techniques for synthesizing diamond and diamond like carbon films by the decomposition of hydrocarbon gases. Some investigators have reported that diamond films could be grown from CH_3OH and hydrogen systems by filament activity method and from $CH_4+H_2+H_2O$ systems by microwave plasma CVD method (1). The experimental processes had been emphasized in their papers (2).

Since using CH_4+H_2 systems to using CH_3OH+H_2 systems, now many investigators are using C/H/O, C/F/O, C/O systems, to greatly enhance the qualities of diamond films and the diamond growth rate. Recently, we reported the possibility of the growth of polycrystalline diamond films from CH_3OH+H_2 system by microwave method (3). In this paper, we will report the dependence of morphology

and crystallinity on substrate orientation and carbon concentration in the microwave plasma CVD method. Using $CH_3COCH_3/CH_3OH/H_2/O_2$ as source gases, we could obtain rather thick high-quality polycrystalline diamond films and epitaxial films which have smooth surfaces and no graphitic component. The dependence of epitaxial temperature on the plane density tells us that all of the crystal materials such as MgO, cBN, SiC, LiF and Cr crystal could be used as suitable heteroepitaxial growth substrates of diamond films as well.

EXPERIMENTAL DETAILS

The experimental apparatus is shown in Fig.1. The substrates were placed on a silica glass heating operator (made by ourselves), and placed in a quartz reaction tube 40 mm in diameter. Microwaves (2.45 Ghz) were transmitted to the reaction tube through a set of waveguides, a three-stub tuner and power monitor. The power of the microwave was varied in the range from 0 to 5000 W. As the microwave supplied power was lower than 600 W, the heating operator could be used for increasing the substrate temperature.

Hydrogen (99.5%), CH_3OH (99.5%), CH_3COCH_3 (99.5%) and oxygen (99.0%) were used for the source gases. After the reaction tube was evacuated, a gaseous mixture of hydrocarbon, hydrogen and oxygen was introduced into the tube though three ways. The concentration of carbon was varied in the range from 0.8% to 1.0% (volume ratio). The concentration of oxygen was varied in the range from 0.1% to 0.3%. The pressure in the reaction tube was maintained at 4.0 KPa when the deposition reaction was carried out. Single crystal silicon wafers with (111) face (22 mm in diameter) and single crystal diamonds with (100), (110) and (111) face (1.2x1.0x0.8 mm^3) were used as substrates. Polycrystalline diamond films were obtained on silicon substrates, 3.14x11 mm^2 in area and 30 μm thick. Silicon substrates were polished with diamond powders of 1, 3, 7, 10, 20 μm for 10-30 min in order to increase the nucleation density of diamond. Single crystal diamond substrates were treated with water and acetone. Epitaxial diamond films were obtained on the diamond substrates with 6 μm in thick and 1.0x1.0 mm^2 in area.

After the reaction tube was evacuated below 10^{-3} torr by a pump, H_2 gas was then introduced into the reactor at the rate of 1000-2000 ml/min and microwave radiation of 1500 W was supplied at the same time. The plasma was spontaneously turned on when the gas pressure reached a few Torr. The gas pressure was finally adjusted and maintained at 4.0 KPa. When the silicon wafers were used as substrates for deposition, hydrogen, oxygen and hydrocarbon gases were introduced into the reactor at the same time. If the single crystal diamonds were used for the epitaxial growth, the substrate diamonds were treated for 10-30 min in a H_2 plasma and then one of the hydrocarbon gases was mixed with H_2 feed. The growth of diamond films was carried out for 4 h in every experiment. The substrate temperature was 750°C as polycrystalline diamond films were deposited on the silicon (111) face, measured by an optical pyrometer and a thermo-couple. When the diamond substrates were used for epitaxial growth, the substrate temperatures were 1050°C for diamond (100) face,

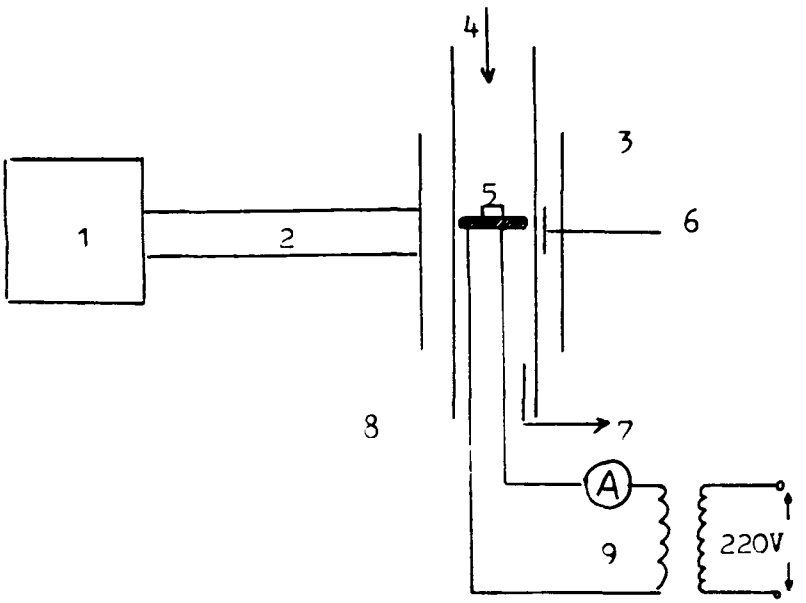

Figure 1. Schematic drawing of MW deposition system. 1. magnetron 2. wave guide 3. sleeve 4. gas inlet 5. substrate 6. plunger 7. pump 8. quartz tube 9. heating operator

900°C for diamond (111) face and 780°C for diamond (110) face as measured by an optical pyrometer (the estimated error is 40°C). The crystallinity of the films was examined by reflection electron diffraction (RED) and scanning electron microscopy. Micro Raman spectra and Raman spectra were recorded by backscattering from the samples at room temperature. The surface morphology of the diamond films was examined by optical microscopy too.

RESULTS AND DISCUSSION

The surface morphologies of polycrystalline diamond films determined by scanning electron microscopy are shown in Fig.2. When the silicon substrate temperature was 750°C, the high quality diamond films could be obtained (see Fig.2a). Under these reaction conditions (substrate temperature was 750°C, the concentration of carbon in the MW plasma was 1.2%, the total flow rate was 2000 ml/min, the MW power was 2400 W, and the oxygen concentration was 0.1% (volume ratio) in the plasma), the formed polycrystalline diamond films had (111) plane orientation as upper face and the growth rate of the films was 0.3 μm/h. When the substrate temperature was 1100°C (see Fig.2b), the great diamond polycrystalline ball could be obtained. In this case, the microwave power was 600 W and the heating operator had been used to increase the substrate temperature. The growth rate of the

Figure 2. *Scanning electron micrographs of diamond films grown on Si (111) face.* (a, *left*) 750°C, (b, *right*) 1100°C.

diamond polycrystalline ball could reach as higher as 20 μm/h, and the biggest diamond ball was 100 μm in diameter.

Scanning electron micrographs of homoepitaxial diamond films grown on single-crystal diamond (100) face are shown in Fig.3. At carbon source/hydrogen source=2.0% (volume ratio) and substrate temperature 1050°C, the homoepitaxial orientation growth (see Fig.3a), epitaxial growth spirals (see Fig.3b) and epitaxial steps (see Fig.3c) could be obtained from the differential reaction when depositions were carried out for 4, 7, 8 hours, respectively. At carbon source/hydrogen source=1.6% (volume ratio), substrate diamond (100) face temperature 1050°C and reaction time was 14.5 h, we could get an epitaxial single-crystal diamond film with 6 μm thick and 1.0x1.0 mm^2 in area (see Fig.3d). From the results of analysis of the epitaxial films microscopies, we found that the homoepitaxial growth rate is 0.3-0.4 μm/h. Figure 4 shows an SEM picture of the epitaxial film grown on diamond (110) substrate under the condition which carbon source/hydrogen source=1.6% (volume ratio), substrate temperature was 780°C and the reaction was carried out for 8.0 h. In this microscopy, you can find some circle-growth spirals and a lot of moon-knife like crystal defects.

Figure 5 shows micro Raman spectra of diamond epitaxial films (a), and Raman spectra of polycrystalline diamond films (b), in this figure, we can find that there are no other forms of carbon in the diamond epitaxial films, but there are other forms of carbon in the polycrystalline diamond films. Because there are not Raman absorptions in the region of 1580 cm^{-1} in the Fig.3a, but there are absorptions in the

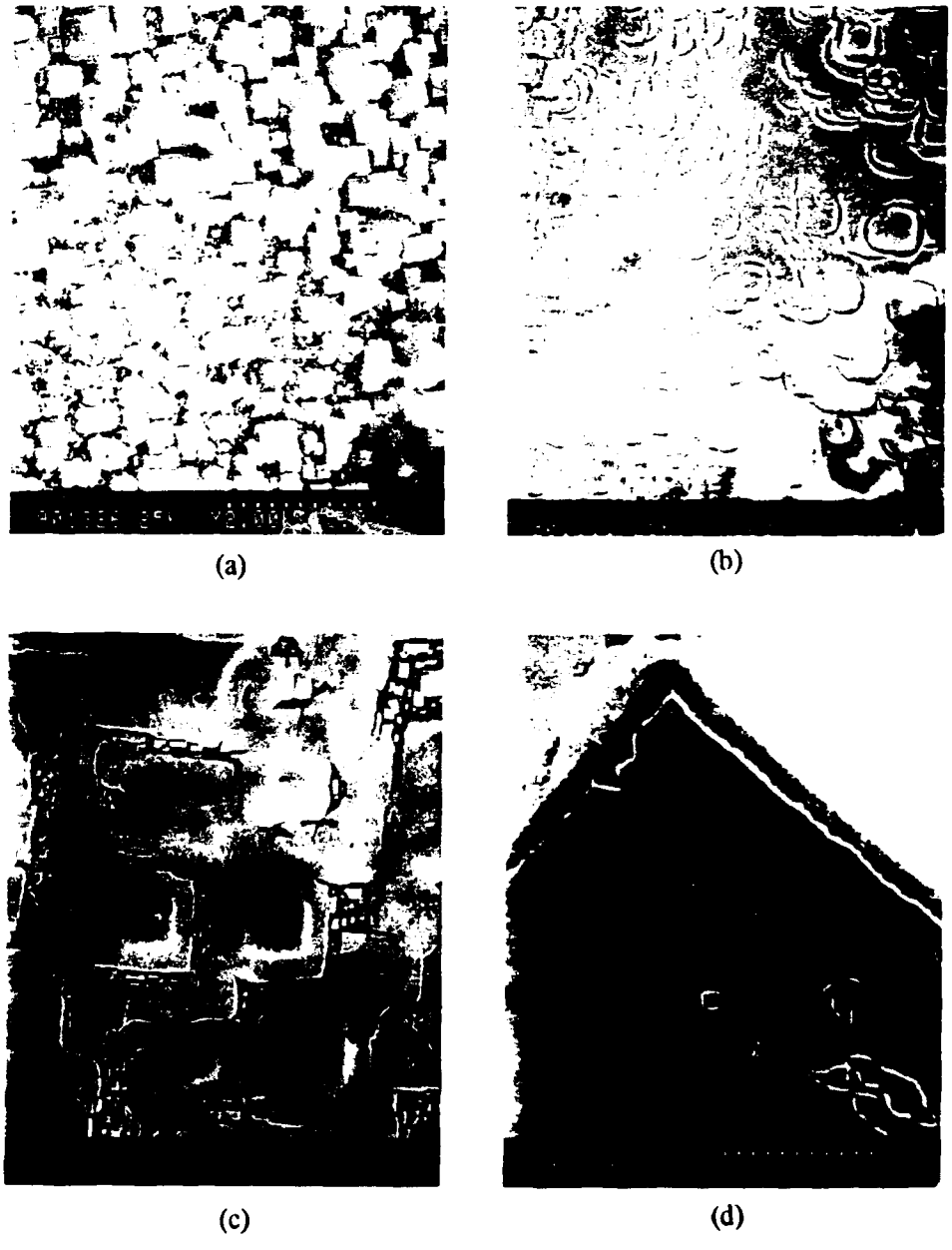

Figure 3. Surface morphology of the epitaxial diamond films by SEM. The films were grown on diamond (100) substrates, (a) orientation growth, (b) growth spirals, (c) steps, (d) single-crystal films.

Figure 4. Surface morphology of the epitaxial diamond film by SEM. The diamond film was grown on diamond (110) substrate.

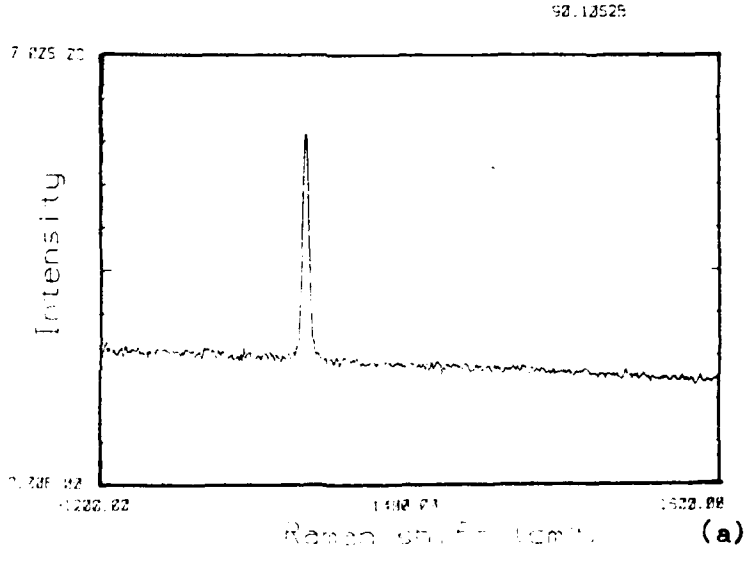

Figure 5a. Micro Raman spectra of epitaxial films.

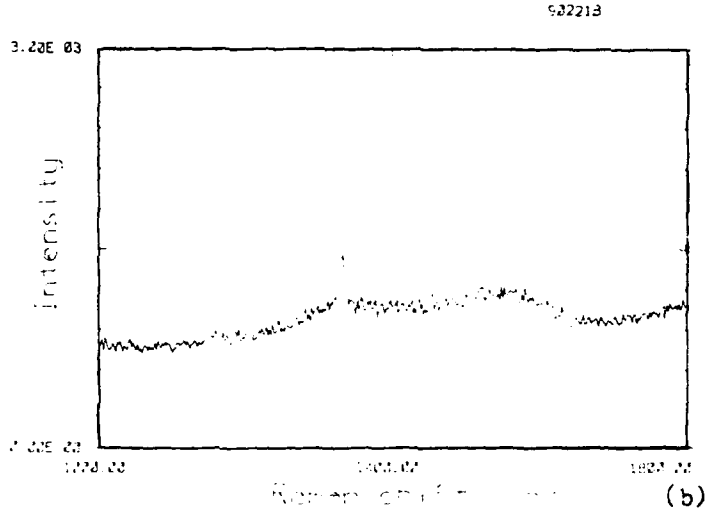

Figure 5b. Raman spectra of polycrystalline film.

Figure 6. RED pattern of the epitaxial diamond film grown on diamond (100) substrate for 14.5 h.

Fig.3b. The RED pattern of the epitaxial diamond film grown on diamond (100) substrate for 14.5 h is shown in Fig.6. Clear diffraction points with low background illumination indicate good crystallinity. Figure 7 shows the dependence of the epitaxial temperature on the plane density. With this relationship, the calculated results show that all of the crystal material such as MgO (the atomic density of (110) face is 0.160 n/A^2), cBN ((100):0.153 n/A^2; (110):0.217 n/A^2; (111):0.177 n/A^2),

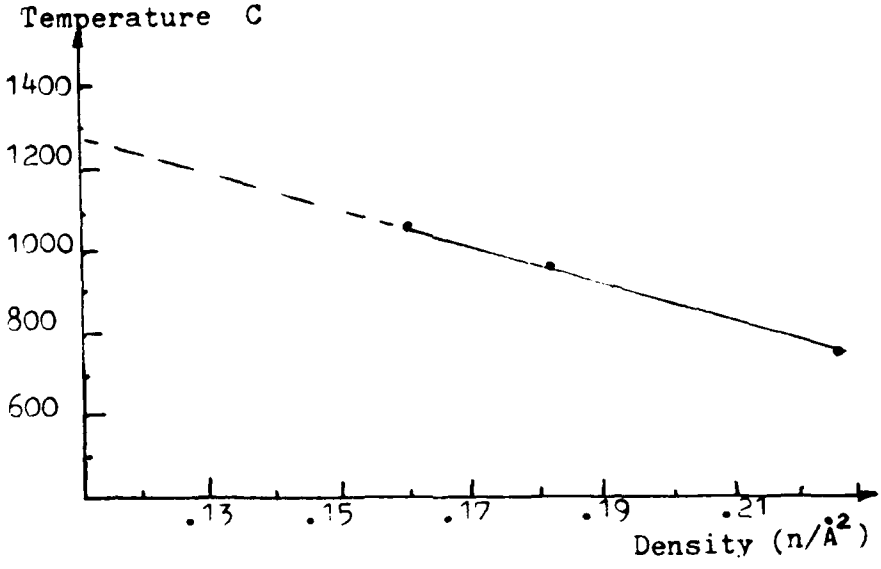

Figure 7. The dependence of the epitaxial temperature on the plane density.

SiC ((110):0.149 n/A^2) and LiF ((110):0.175 n/A^2) could be used as suitable heteroepitaxial growth substrates of diamond film.

CONCLUSIONS

We investigated diamond films grown on Si (111), diamond (100), (110) and (111) substrates using microwave plasma-assisted CVD method from CH_3OH, CH_3COCH_3, H_2, O_2 systems. In this paper, the experimental processes had been emphasized. From the experimental results, we could discover that CH_3OH, CH_3COCH_3 could be used as suitable source gases for the diamond films growth. Using micro Raman spectra method, we analyzed the contents of graphite and other forms of carbon in the diamond films. The experimental results shown that there were no other forms of carbon in the epitaxial diamond films. Analysis results of RED shown that epitaxial diamond films were single-crystal diamond films.

REFERENCES

1. Fujimori, N., T. Imai, and A. Doi, Vacuum, Vol.36, p.99, (1986).

2. Shiomi, H., Japanese Journal of Applied Physics, Vol.29, p.34, (1990).

3. Zhangzhan, L.J., and M. Liying, Abrasives and Grinding, Vol.1, p.8, (1990).

MATERIALS & MANUFACTURING PROCESSES, 8(1), 83-98 (1993)

DEPOSITION OF DIAMOND FILM BY A MAGNETIZED DC PLASMA JET

W.K. Kim and K.W. Whang
Department of Electrical Engineering
Seoul National University, San 56-1
Shinrim-Dong Kvanak-Ru, Seoul 151-742, Korea

ABSTRACT

A low pressure DC plasma jet has been used to obtain diamond films from a mixture of CH_4 and H_2 with high deposition rate (>1 m/min). The effects of the deposition conditions such as the torch geometry, substrate temperature, gas mixing ratio, chamber pressure, axial magnetic field on the diamond film properties such as the morphology, purity, uniformity of the film and deposition rate, etc. have been examined with the aid of Scanning Electron Microscopy, X-Ray Diffraction, and Raman Spectroscopy. Both the growth rate and particle size increase with the substrate temperature but the morphology changes from the faceted to the unshaped when the temperature deviates from its proper range. The growth rate increases rapidly for low methane concentrations but it saturates and the morphology changes from the octahedral to cubic structure when the concentration exceeds 1.0% Higher growth rates (>1.5 m/min) can be obtained by applying an axial magnetic field to the DC plasma jet. Diamond obtained from the magnetized plasma jet also shows a sharp peak at 1332.5 cm^{-1} in the Raman Spectra and this result implies that higher growth rate with a good quality diamond films can be obtained by applying an external magnetic field to the plasma jet

INTRODUCTION

A variety of deposition techniques have been used to synthesize diamond films from the gas phase at low pressure (1). These techniques are hot filament assisted CVD (2), MW plasma CVD (3), RF plasma CVD (4), Electron Assisted CVD (EACVD) (5), Laser Induced CVD (6), DC plasma CVD (7), RF induction thermal plasma CVD (8), ECRCVD (9), DC plasma jet CVD (10), Hollow Cathode CVD (11), ion-assisted deposition (12), arc discharge plasma CVD (13), combustion flame deposition (14), MW plasma torch CVD (15), etc. Among these techniques, the DC thermal plasma jet reported the highest growth rates (16), but little has been known about the quality of the film and optimum process conditions (17). In this work, the

dependence of the surface morphology, film quality and growth rate of the DC thermal plasma enhanced diamond coatings on the process parameters, especially on the external magnetic field, has been studied.

EXPERIMENTAL

A schematic drawing of our DC thermal plasma jet system is shown in Fig.1. The plasma torch is composed of the cylindrical cathode and conical anode. The cathode is 8 mm in diameter and made of W-2%ThO_2. The anode is made of oxygen-free copper and its shape is conical where the plasma gas can flow into the 8 nozzle easily. Hard cooling of the anode is necessary because the evaporated Cu can perturb the plasma jet and contaminate the deposited film, which degrades the quality of the diamond film. A magnet is placed around the torch to generate an axial magnetic field. Before the deposition, the chamber is evacuated down to 10^{-3} Torr by a mechanical booster pump and a rotary pump and the plasma gas is introduced into our non-transferred type DC thermal plasma torch to produce a plasma jet. When the plasma jet becomes stable and the jet flame is in its proper condition, a shutter on the substrate can be removed to initiate the deposition on the Mo substrate which has been abraded by diamond powder and cleaned by acetone and methanol before the deposition.

The substrate temperature during the deposition is measured by an optical pyrometer and a thermocouple. The substrate temperature can be varied from 700°C to 1100°C by changing the arc power, substrate cooling rate, etc. In our experiment, the shape of the jet flame, which in a standard condition is usually about 50 mm in length and 10 mm in diameter, and the position of the substrate in this flame are very important factors to produce high quality and high growth rate diamond films. The chamber pressure can be varied from 1 Torr to 760 Torr by controlling the gas flow rate and the throttle valve. Magnetic fields are calculated numerically and confirmed by the Gauss-Meter measurements. The field configuration is shown in Fig.2. The maximum magnetic field strength is 2600 Gauss at the center of the bobbin and 1200 Gauss at the nozzle of the torch. As the external magnetic field increases, the shape of jet flame becomes large and the light emission becomes more intense, The relations between the arc voltage and the magnetic field at various chamber pressures are shown in Fig.3. It shows that the arc voltage increases with the increase of the external magnetic field strength. Experimental conditions are listed in Table 1.

RESULTS AND DISCUSSION

The Effects of the Substrate Temperature

The substrate temperature is one of the most important factors in the deposition of the diamond film by the DC plasma jet, The effects of the substrate temperature

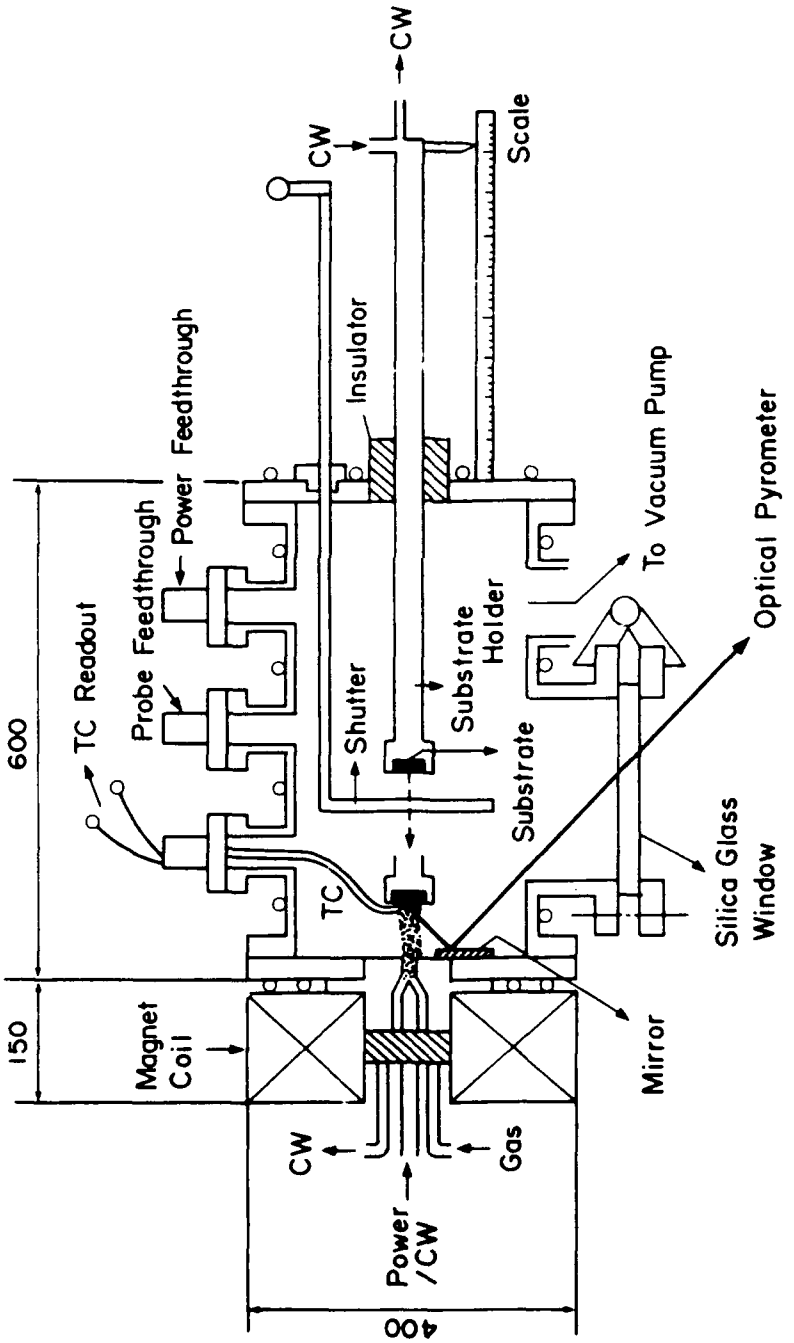

Figure 1. Schematic drawing of DC thermal plasma system.

TABLE 1
Experimental conditions

Arc Voltage 15~30 (V)	Ar Flow Rate 3~5 (SLM)
Arc Current 100~300 (A)	H_2 Flow Rate 1~2 (SLM)
Spraying Distance 10~30 (mm)	CH_4 Flow Rate 5 ~15 (SCCM)
Substrate Temp. 850~1050°C	Pressure 50~200 (Torr)
Magnetic Field O~900 (Gauss)	Deposition Time 30 (min)

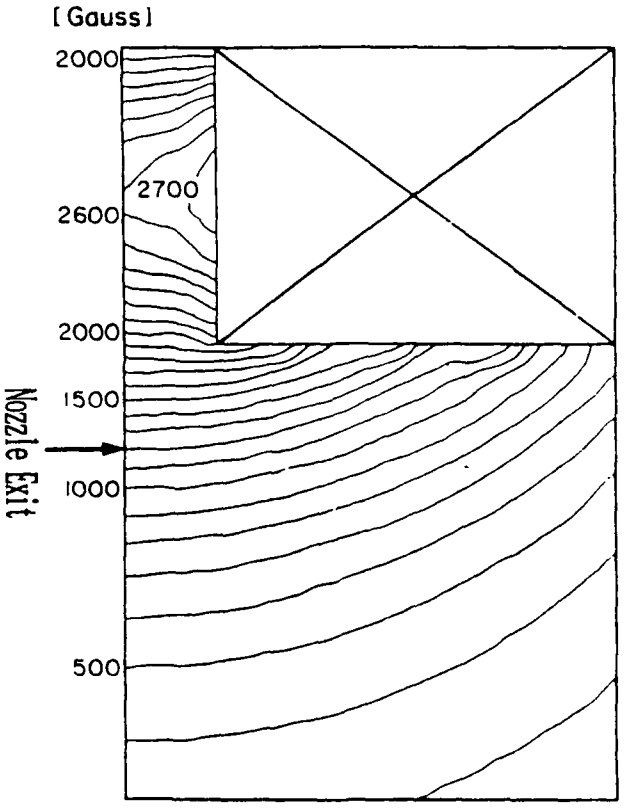

Figure 2. B field configuration.

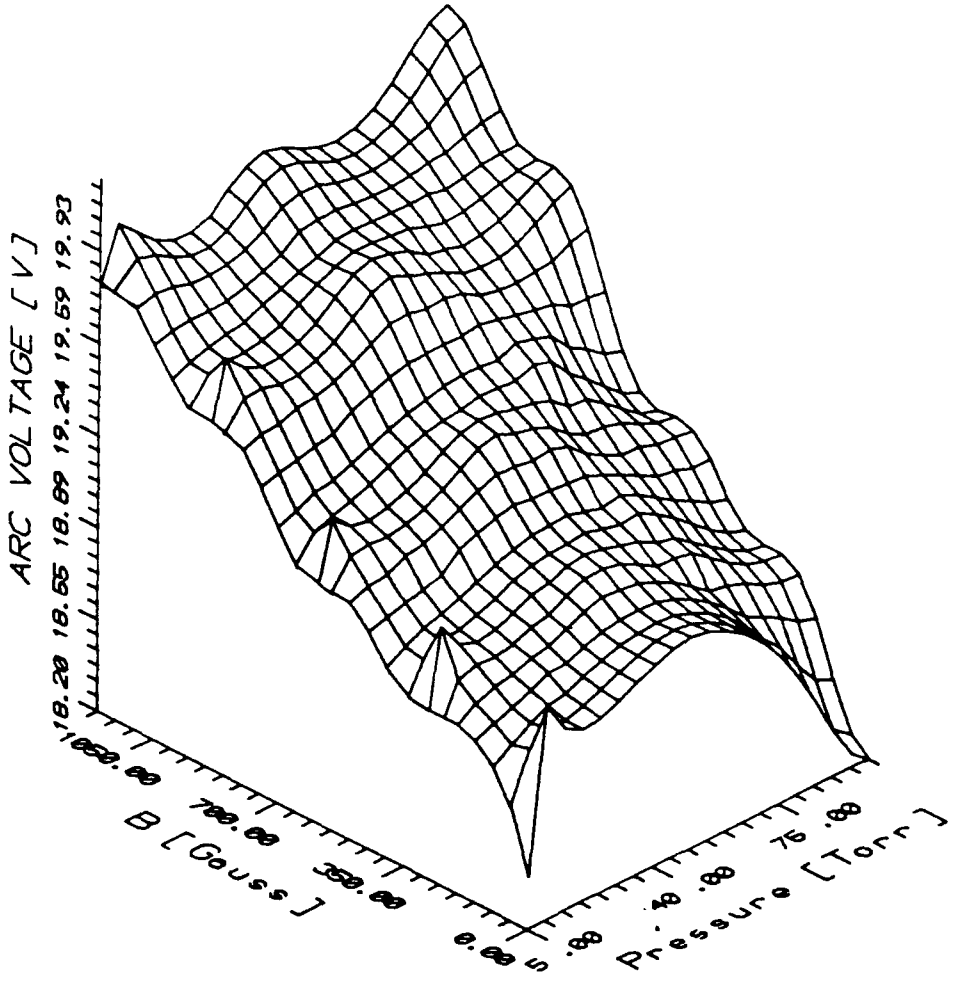

Figure 3. The relations between arc voltage and magnetic field at various chamber pressures.

on the particle morphology are shown in Fig.4. The growth rate and the particle size increase with the temperature but the morphology changes from the faceted to the unshaped when the temperature exceeds 1050°C. The growth rate measured for each substrate temperature is shown in Fig.5.

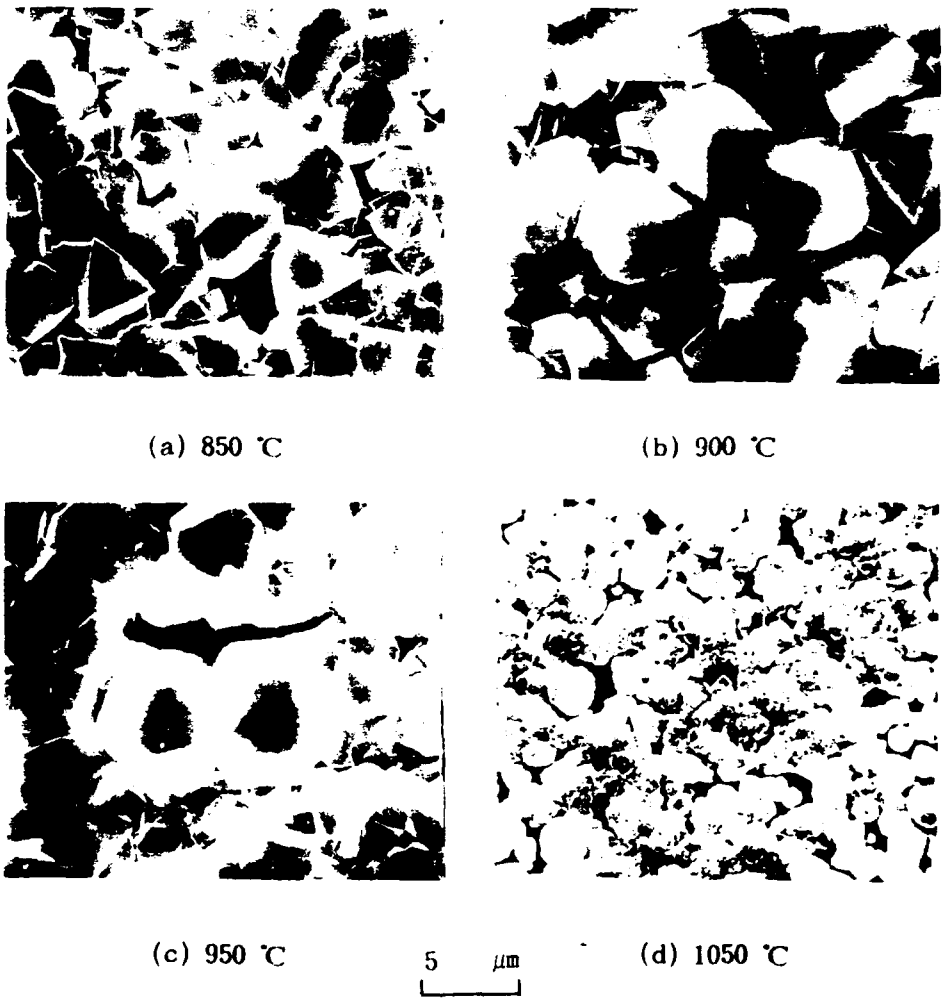

Figure 4. The effect of the substrate temperature (CH_4/H_2 = 0.5%, Chamber pressure: 50 Torr, Deposition time: 30 min.).

It increases from 0.7 μm/min to 1.0 μm/min when the substrate temperature changes from 800°C to 1000°C. X-ray diffraction pattern for a successively deposited sample is shown in Fig.6. When the deposition was done for 10 minutes, XRD pattern of the sample shows that the film contains not only Mo and diamond but Mo_2C, too. When the deposition time is 15 minutes, only small peaks due to Mo_2C appear. When the deposition time is more than 20 minutes, only diamond and Mo peaks appear and no other peak is observed. The observed values of interplanar spacings of deposited diamond films are in a good agreement with the values reported in ASTM data. From this result, we can conclude that a Mo_2C interlayer is

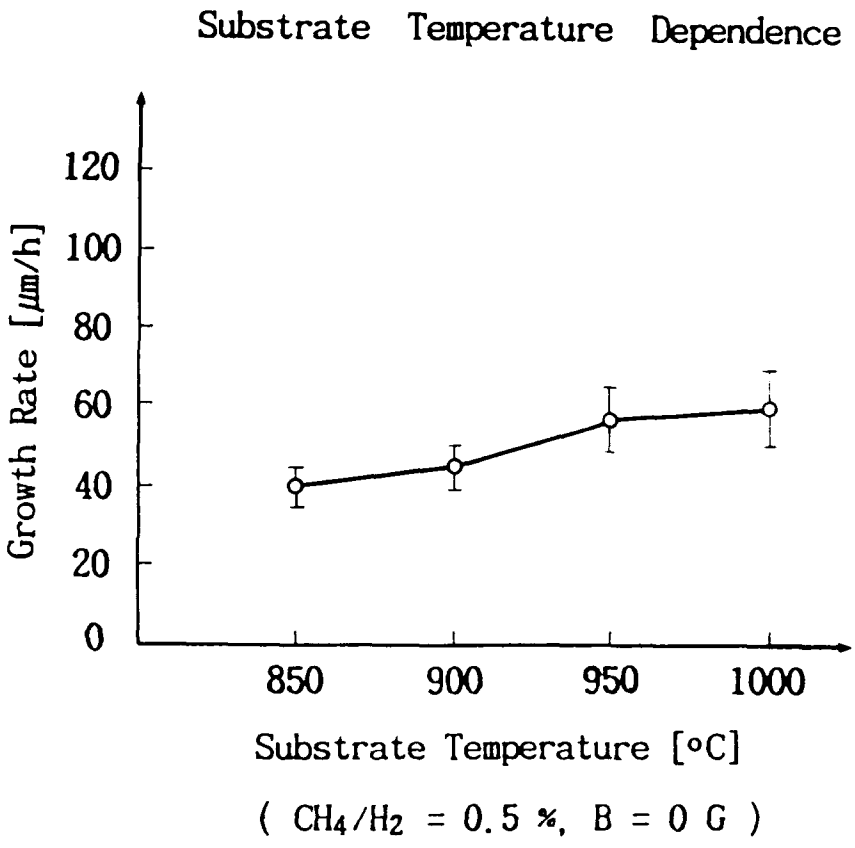

Figure 5. Film growth rate vs. substrate temperature.

formed onto which pure diamond is deposited. Raman spectra of diamond films obtained at three different substrate temperatures are shown in Fig.7.

It shows that the sharp peak at 1332.5 cm^{-1} due to diamond is observed at 950°C but the broad peak centered around 1560 cm^{-1} due to the graphitic structure dominates when the temperature deviates from its proper range of 900 ~ 950°C.

The Effects of the Methane Concentration

The methane concentration change is the other important factor, and its effect is shown in Fig.8. The morphology of the film is quite different for each different condition of the methane concentration. It changes from the octahedral to cubic structure and the area of <100> planes increases as the methane concentration increases. The growth rate dependence on the methane concentration is shown in Fig.9.

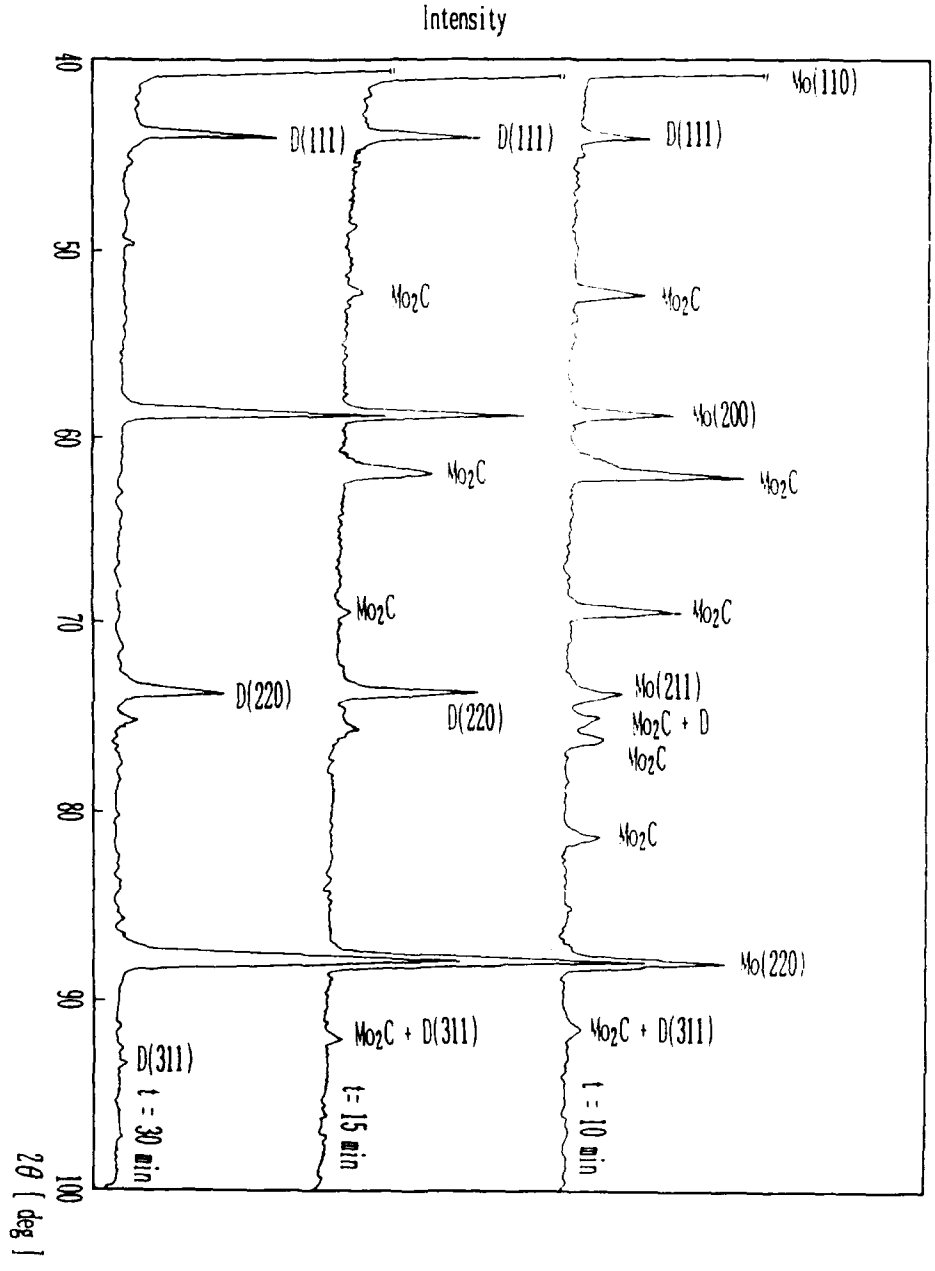

Figure 6. X-ray diffraction patterns of deposited diamond films on Mo substrate (Substrate temperature: 950°C. CH_4/H_2 = 0.5%, 50 Torr, Deposition time: 10/15/30 min.).

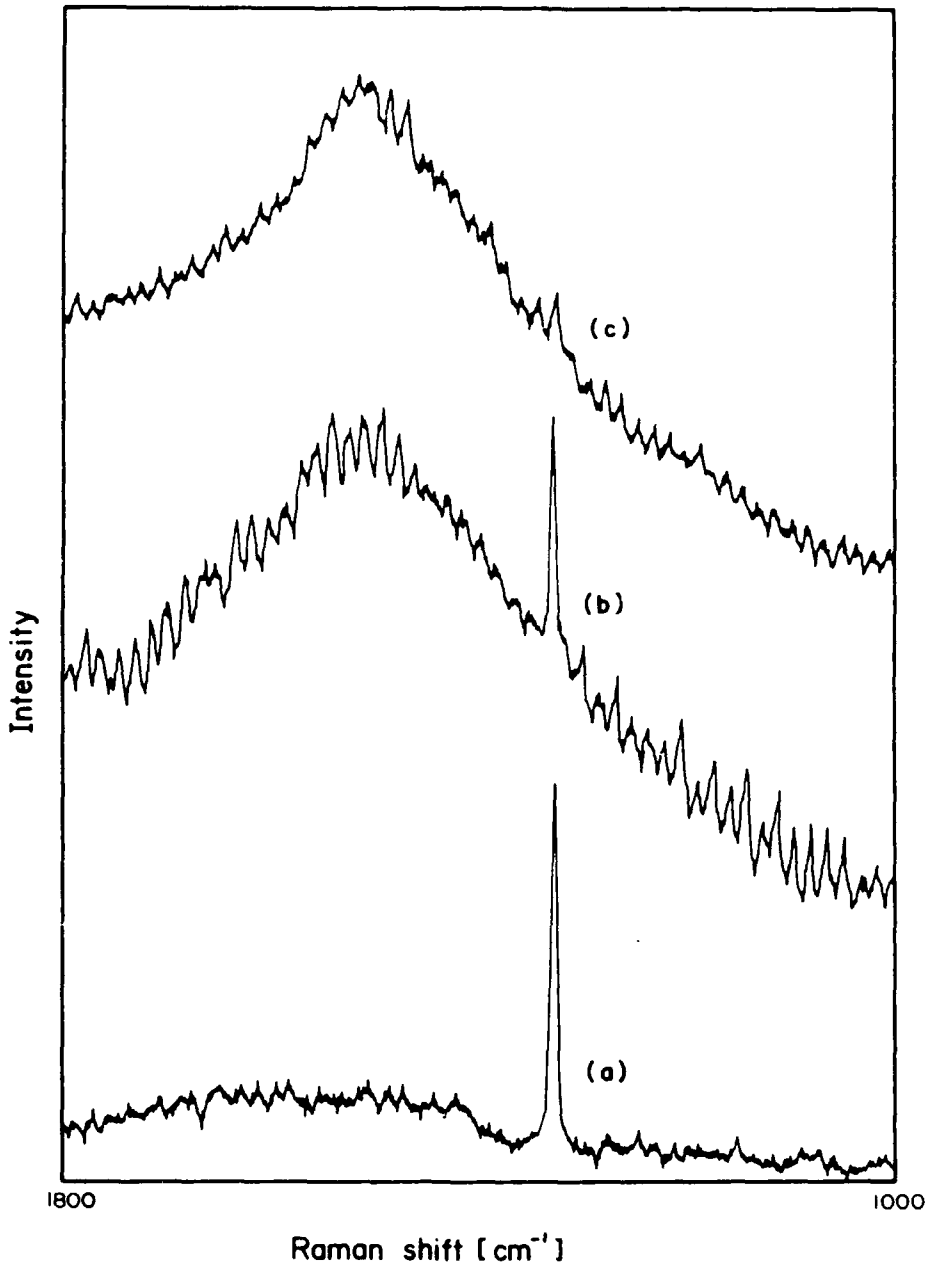

Figure 7. Raman spectra of diamond films. The substrate temperature is (a) 950°C (b) 850°C (c) 1050°C (CH_4/H_2 = 0.5%, Chamber pressure: 50 Torr).

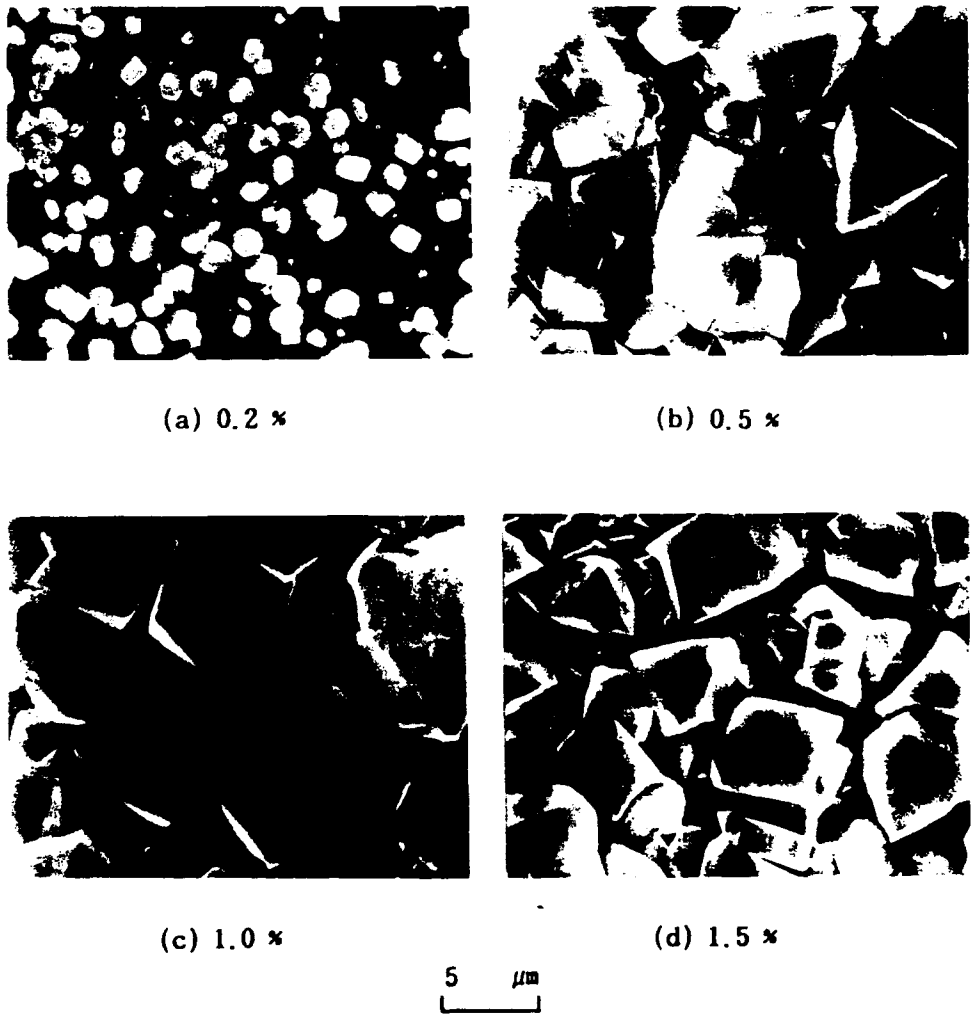

Figure 8. The effects of gas mixing ratio (CH_4/H_2) (Substrate temperature: 900°C. 50 Torr, 30 min.).

It shows that the growth rate increases rapidly for low methane concentrations but saturates when the concentration exceeds 1.0%. Raman spectra of the diamond films at different methane concentrations are shown in Fig.10. It shows that all deposits have the sharp diamond peak of 1332.5 cm^{-1}, but the broad peak due to the graphitic structure increases with the methane ratio.

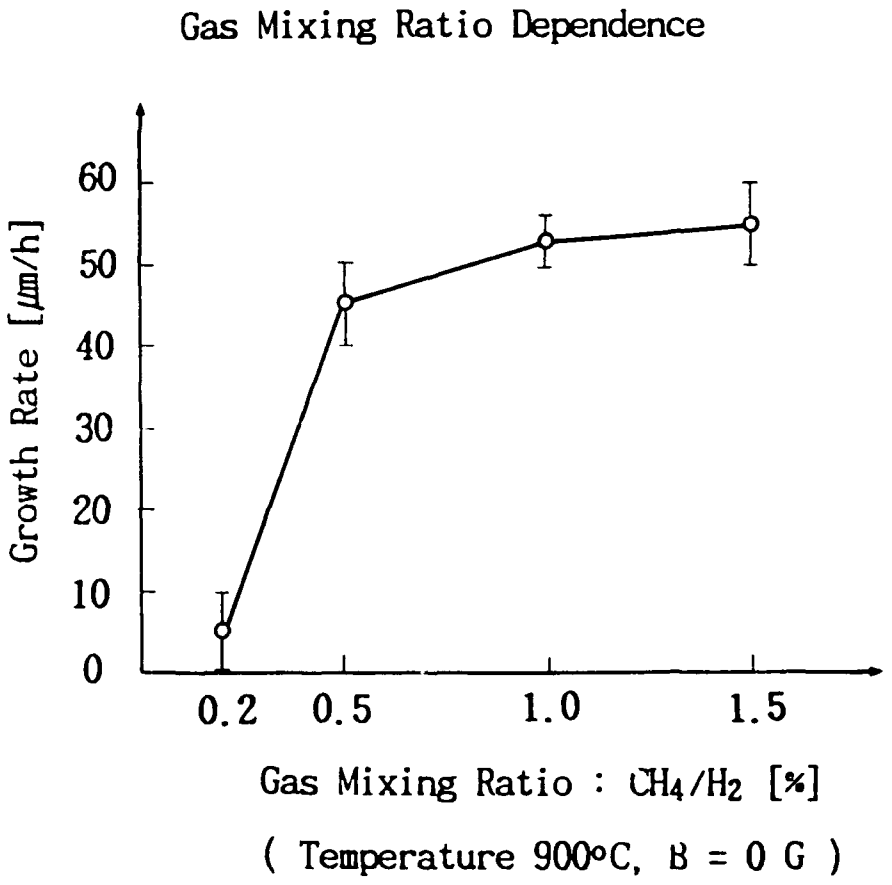

Figure 9. Film growth rate vs. gas mixing ratio.

The Effects of the Chamber Pressure

By lowering the chamber pressure, higher velocity and higher enthalpy plasma jet can be obtained. As is shown in Fig.3, the maximum arc-sustaining voltages appear at about a few tens of Torr. The volume of the jet flame increases as the chamber pressure decreases, which results in a larger deposition area. Thus in our experiment, low chamber pressures (~50 Torr) have been chosen to deposit the high quality diamond films. As the chamber pressure increases (more than 100 Torr), diamond films could also be obtained but the uniformity and bonding strength of the deposited films degraded. X-ray diffraction patterns and Raman spectra of these films are similar to those of the deposited films at 50 Torr.

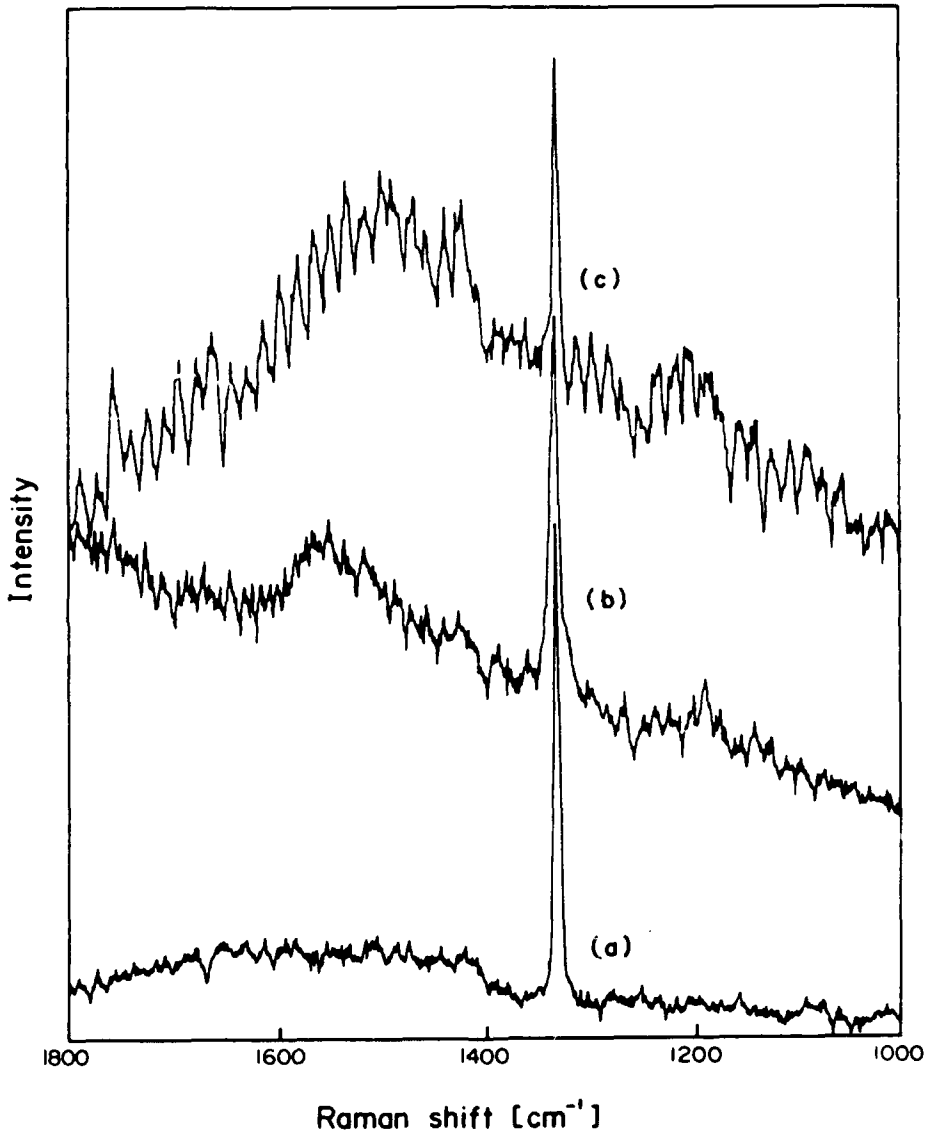

Figure 10. Raman spectra of diamond films (CH_4/H_2: (a) 0.5%, (b) 1.0% (c) 1.5%, (Substrate temperature: 900°C. Chamber pressure: 50 Torr).

The Effects of an External Magnetic Field

As an external, axial magnetic field was applied to the torch, the arc voltage increased and the arc discharge became more stable. The plasma density and the plasma temperature is thought to be higher in the presence of the magnetic field. Thus more intense, stable plasma jet can be obtained by applying an external

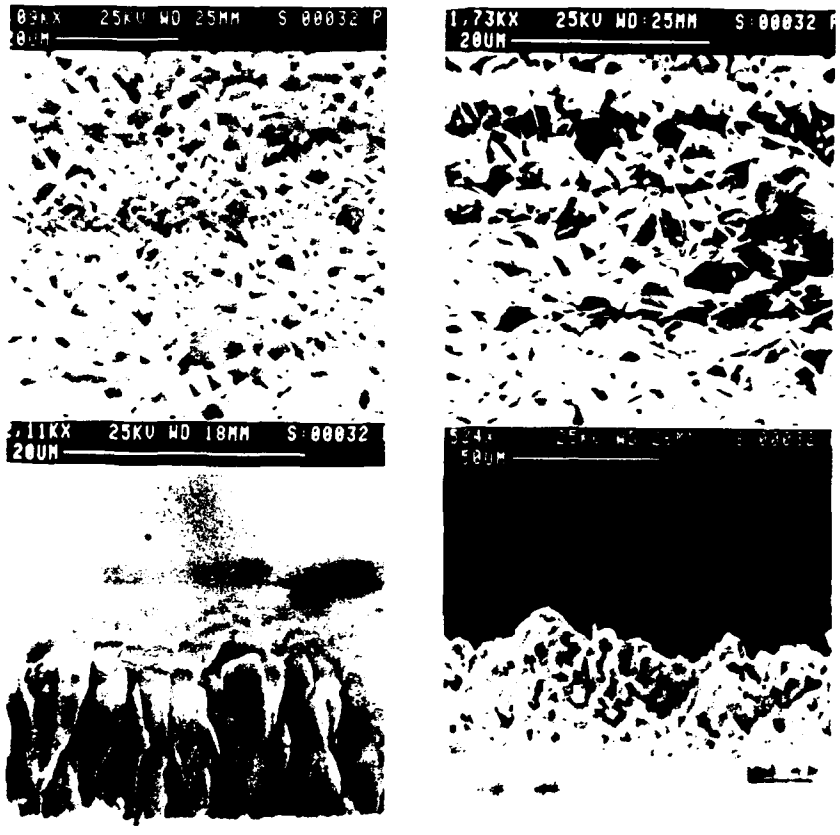

(a) (b)

Figure 11. Surface and cross-sectional microstructures of diamond films. The magnetic field is (a) 0 Gauss, (b) 600 Gauss, (Substrate temperature: 900°C, CH_4/H_2: 0.5%, Chamber pressure: 50 Torr, Deposition time: 30 min.).

magnetic field. The effect of the magnetic field on the surface and cross sectional microstructures of the diamond films is shown in Fig.11.

The growth rate measured for each different magnetic field condition is shown in Fig.12. It shows that the grain size and deposition rate increase with the magnetic field strength. The growth rate increases from 1 μm/min to 1.5 μm/min but the film uniformity seems to be degrading. Raman spectrum of the deposited film with the magnetic field of 600 Gauss is shown in Fig 13.

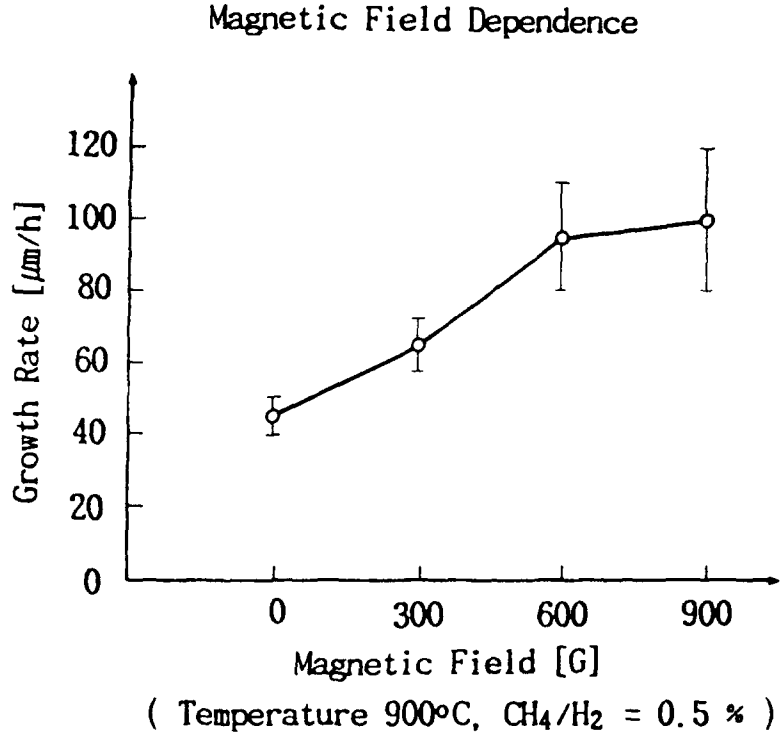

Figure 12. Film growth rate vs. magnetic field strength. (Substrate temperature: 900°C, CH_4/H_2 = 0.5%).

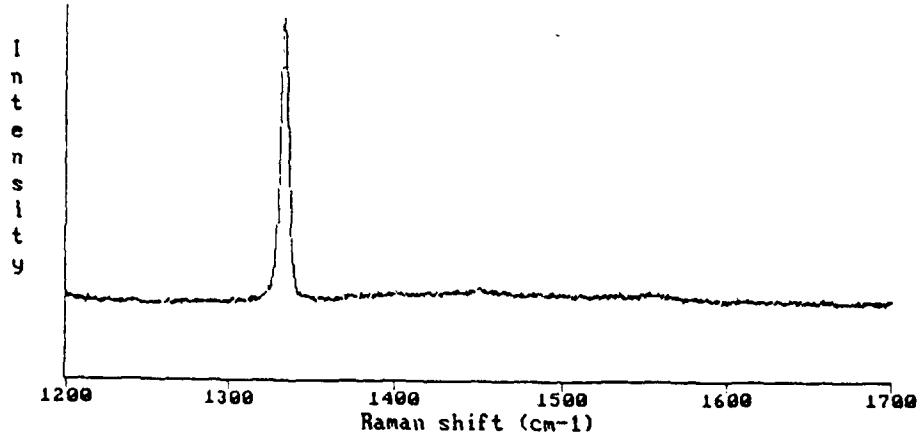

Figure 13. Raman spectrum of the deposited diamond film with the magnetic field of 600 Gauss (Substrate temperature: 900°C, CH_4/H_2: 0.5%, Chamber pressure: 50 Torr).

It shows a sharp peak at 1332.5 cm^{-1} due to diamond and this result implies that a good quality of diamond film with higher growth rates can be realized by applying an external magnetic field to the plasma jet.

CONCLUSION

The effects of the deposition conditions such as the substrate temperature, gas mixing ratio, chamber pressure, external magnetic field on the diamond film properties have been examined. Both the growth rate and particle size increase with the substrate temperature, but the morphology changes from the faceted to unshaped when the temperature deviates from its proper range. The growth rate increases rapidly with the methane concentrations but it saturates and the morphology changes from the octahedral to cubic structure when the concentration exceeds 1.0%. The growth rate increases from 1 μm/min to 1.5 μm/min and high quality diamond films are obtained when a magnetic field is applied to the plasma jet.

REFERENCES

1. Matsumoto, S., Proceedings of the 1st International Symposium on Diamond and Diamond-Like Films, Pennington, p.50, (1989).

2. Matsumoto, S., Y. Sato, M. Tsutsumi, and N. Setaka, Journal of Materials Science, Vol.17, p.3106, (1982).

3. Kamo, M., Y. Sato, S. Matsumoto, and N. Setaka, Journal of Crystal Growth, Vol.62, p.642, (1983).

4. Matsumoto, S., Journal of Materials Science Letters, Vol.4, p.600, (1985).

5. Sawabe, A., and T. Inuzuka, Applied Physics Letters, Vol.46, No.2, p.146, (1985).

6. Kitahama, K., K. Hirata, H. Nakamatsu, and S. Kawai, Applied Physics Letters, Vol.49, No.11, p.634, (1986).

7. Suzuki, K., A. Sawabe, H. Yasuda, and T. Inuzuka, Applied Physics Letters, Vol.50, No.12, p.728, (1987).

8. Matsumoto, S., M. Hino, and T. Kobayashi, Applied Physics Letters, Vol.51, No.10, p.737, (1987).

9. Suzuki, J., H. Kawarada, K. Mar, J. Wei, Y. Yokota, and A. Hiraki, Japanese Journal of Applied Physics, Vol.28, No.2, p.27, (1989).

10. Kurihara, K., K. Sasaki, M. Kawarada, and N. Koshino, Applied Physics Letters, Vol.52, No.6, p.437, (1988).

11. Singh, B., O.R. Mesker, A.W. Levine, and Y. Arie, Applied Physics Letters, Vol.52, No.20, p.1658, (1988).

12. Kitabatake, M., and K. Wasa, Journal of Vacuum Science and Technology, Vol.A-6, No.3, p.1793, (1988)

13. Akatsuka, F., Y. Hirose, and K. Komaki, Japanese Journal of Applied Physics, Vol.27, No.9, p.L1600, (1988).

14. Hirose, Y., S. Amanuma, K. Komaki, Journal of Applied Physics, Vol.68, No.12, p.6401, (1990).

15. Mitsuta, Y., T. Yoshida, and K. Akashi, Reviews of Scientific Instruments, Vol.60, No.2, p.249, (1989).

16. Ohtake, N., and M. Yoshikawa, Journal of the Electrochemical Society, Vol 137, No.2, p.717, (1990).

17. Stalder, K.R., and R.L. Sharpless, Journal of Applied Physics, Vol 68, No.12, p.6187, (1990).

MATERIALS & MANUFACTURING PROCESSES, 8(1), 99-102 (1993)

BOOK REVIEW

ADVANCED MATERIALS SOURCEBOOK

edited by
J. Binner, P. Hogg and J. Sweeney

Elsevier Advanced Technology, Oxford
367 pages, hardcover, 1991

Three active workers in materials research have joined forces to prepare this extensive collection of information on advanced industrial materials. The three editors have each been responsible for a chapter of the book and they deal with ceramics, plastics and composites. The source material has been taken from the Elsevier Advanced Technology's international newsletters, which are the Advanced Ceramics Report, the Advanced Composites Bulletin and High Performance Plastics. The three chapters are cross-referenced and each includes a list of contact names and addresses for the organizations referred to. The result is a very comprehensive collection of information in which the editors highlight and comment upon trends in fundamental and applied research, new materials and processes, novel applications, company news and emerging markets. The fourth and final chapter is a very short presentation of conclusions, which although short (less than two pages) is still very useful.

The first chapter on ceramics consists of fifteen sections and one hundred and fifty one pages, and it deals with monolithic ceramics as well as ceramic matrix composites and their constituents including whiskers and fibres. Ceramic coatings are also dealt with including functionally graded coatings where the composition of a coating changes gradually from 0% at the substrate (100% substrate) to 100% (0% substrate) at the outer surface. This approach minimizes abrupt interfaces between phases of different composition and allows stresses created by differences in thermal expansion coefficient to be accommodated throughout a greater volume of material and thus to reduce stress concentrations. Another interesting section deals with diamond-like thin films.

One of the longest sections in this chapter, consisting of twenty one pages, is on superconductivity, and this is included because of the fairly recent discovery of mixed oxide ceramics which superconduct at temperatures in the region of 90°K, and which therefore can be held in a superconductive state using liquid nitrogen (boiling point

77°K) rather than the much more expensive liquid helium. Because of the enormous industrial potential of these materials there has been a rapid increase in the amount of published technical information dealing with them. This review makes no pretence to being complete but it provides an easy-to-read primer with information on the four main material systems involved, their properties, and their processing in bulk form, as wires or as thin films.

The chapter on ceramics, like the ones on plastics and composites, deals primarily with the practical aspects of the business rather than with theoretical and scientific concepts, and it concentrates heavily on industrial applications, processing and production methods, news of company developments and alliances, and business opportunities. Coverage is fairly comprehensive and it includes information on work in progress in at least fourteen countries, with information on work in Japan, the United States and United Kingdom predominating. This reviewer found the information to be interesting and he is likely to use the book quite frequency during the next five to ten years. Because of the rapidly changing nature of the business, the book is unlikely to be very useful beyond this time span.

The term high performance plastics may refer to organic materials with outstanding mechanical properties, high resistance to harsh chemical environments, high resistance to high temperatures or fire, or unusual electrical properties. In this book high performance simply implies either a new material, a new processing method, or a novel application. The chapter on plastics is shorter than that on ceramics, being less than one hundred pages, and it consists of ten sections. The three largest sections deal with new engineering plastics, processing methods and areas of application, and there are supporting sections on low-friction and non-stick plastics, reinforcement fibres and toughening agents, composite matrix materials, structural composites and pre-pregs, and market and company news.

News of North American and European companies and products appears to predominate this chapter, with numerous mentions of DuPont, GE Plastics, Bayer, BASF, CibaGeigy and ICI. There are however some product lines such as reinforcing fibres where Japanese companies have a very strong presence, and regardless of country there are many small companies with unique product lines.

The section on new engineering plastics deals with polymers intended to replace metals in high stress applications and therefore it concentrates on materials with improved fracture toughness, creep resistance, and high temperature performance. Several new grades of nylon are described including nylon 1212 from DuPont, nylon 46 from Unitika, and several nylon alloys including Triax 1180 from Monsanto and Grilon BT40X from Emser Industries. Comparisons are provided of the properties of these materials with those of the materials they are expected to replace, but users must still compare these new materials against each other to determine which would be most suitable for his own application. This section also covers liquid crystal polymers which achieve high strength by developing oriented polymer chains during the molding process, while a subsequent section on processing covers polymer chain orientation and the achievement of high strength by mechanical means. This latter

section also contains a very interesting review of surface modification techniques for plastics, which includes technology developed in Bulgaria where ion bombardment is involved and a process developed in the US where the deposition of any metal, alloy, ceramic or semiconductor is achieved by a low temperature arc vapor deposition process (LTAVD).

Ion bombardment is possible using gases, non-metals or metals, and the use of carbon allows the synthesis of new phases on polymer surfaces, while the use of silicon allows thin heat-resistant coatings to be produced. The LTAVD process is non-line-of-sight and therefore it can be used to deposit hard wear or erosion resistant coatings on the inside and outside of plastic tubes or pipes. Many other novel applications are described for both processes.

The third chapter on composites is the shortest of the three main chapters and it consists of seven sections and eighty seven pages, including ten pages of addresses. The three longest sections of this chapter deal with new materials, processing and applications, and of the twenty three pages devoted to applications, eighteen deal with aerospace applications. This emphasis reflects the fact that aerospace still sets the pace in the development of new high performance products and processes, while yesterday's aerospace technology is adopted by other industries as practical experience is gained and after production capacities have increased and costs reduced.

The chapter deals with thermosets, thermoplastics, carbon-carbon composites, and both ceramic and metal matrix composites, and even though several of these material types have been dealt with in the preceding chapters there appears to be no duplication of information.

The focus of effort on thermosets appears to be towards toughened materials which retain high strength under hot/wet conditions, while cost is a major concern with thermoplastics and therefore lower cost materials and processes are the goal. Health and safety issues associated with the processing of several thermosets are still of some concern, and therefore the chemical stability of thermoplastics gives them an advantage.

Ceramic and metal matrix composites appear far less well advanced than organic matrix composites, although they appear to be the focus of a great deal of development effort. Several countries including Japan, Korea, the United Kingdom and Sweden have national programs to develop these materials, and there is still a great deal of work in the US under defence sponsorship. Because of the extremely high processing temperatures required for these materials, compatibility between fibre and matrix is a problem of general concern, and the development of new types and forms of fibres is being actively pursued. Work is reported on new ways to produce Si_3N_4 in fibre and whisker form, and a new process from Japan to produce titanium boride whiskers is also reported. The high strength, high heat resistance, hardness approaching that of diamond, and a melting temperature of almost 3000°C, suggest that these titanium boride whiskers will find many applications in metal-

matrix composites once they become commercially available. At the moment the SiC-Al composites developed by DWA Composite Specialties of California are among the few metal matrix composites available commercially.

Perhaps the most striking information in this chapter is the intense activity in the development of teaming relationships which involves companies in different countries, where the aim is to secure a strong market share by an established company in a remote but industrially powerful geographical region, as well as companies within a country. Examples are provided of this latter type where aerospace companies have teamed with companies in the automobile industry and where there is therefore the opportunity for transfer of technology between the partners.

In conclusion, this book will be extremely useful to managers and researchers in industry, government laboratories and funding agencies where the individual must not only be conversant with the science and engineering involved, but must also understand the market opportunities and business risks. It will not be useful to students or teachers who are concerned primarily with the fundamental and theoretical concepts of materials science and engineering. The title of the book describes its contents fairly well. It is a source of information that readers would consult for general information on specific topics, and not the sort of book that would be read from cover to cover.

W. Wallace
Head, Structures and Materials Laboratory
Institute for Aerospace Research
National Research Council of Canada
Building M-4
Ottawa, Ontario, K1A 0R6

MATERIALS & MANUFACTURING PROCESSES, 8(1), 103-106 (1993)

BOOK REVIEW

HANDBOOK OF TRIBOLOGY
Materials, Coatings, and Surface Treatments

by
B. Bhushan and B.K. Gupta

McGraw-Hill Publishing Company
1221 Avenue of the Americas
New York, NY 10020, USA
1168 pages, Hardbound, 1991

This is an impressive piece of authorship by Drs. Bhushan and Gupta, covering practically every pertinent aspect of the subject of tribology. A mere quick scan of the table of contents reveals the enormity of the information contained in this excellent handbook, and detailed reading only cements the initial impression that this is an extremely well-written, comprehensive and authoritative book on a subject that every equipment designer, mechanical engineer, materials scientist and student of tribology must read.

The book contains sixteen chapters that cover the whole gamut, from the fundamentals of friction, wear and lubrication to the physics, chemistry, metallurgy and technologies of surface modification that deal with the tribological applications in the modern age of materials. The senior author of the book, Dr. Bharat Bhushan, is an internationally recognized expert in this field, and this book indeed reflects his vast expertise and his ability to hold forth on a subject of enormous implications in the age of conservation and environmentally-conscious manufacturing. The fundamental belief of the authors -that tribology cannot be comprehended without a clear understanding of the materials, their properties, microstructures, synthesis techniques and measurement techniques, and their inter-relationships - is underscored by the organization of this book and the selection of the subject matter.

The book begins with an overview of lubricants from a historical perspective, and provides a quick summary of the variety of materials that can be, and have been, used for lubrication. The basic precepts of friction and wear are covered in chapter 2, which also provides a glimpse into the methods of reducing wear by various methods, and the role of lubrication in conserving material and energy in moving components of industrial machinery.

The essential element of the tribological phenomena is the surface. The properties of surfaces in contact determine what kinds of interactions will occur between them. The authors have dealt with this aspect in the next chapter, by providing a concise treatment of the physics and chemistry of solid surfaces. The concepts of surface energy, surface defects, the phenomena of physi-sorption and chemi-sorption, microstructural characteristics and phase equilibria as applied to the development of surface properties are dealt with concisely but lucidly.

Chapters 4 and 5 deal with materials. Metallic and ceramic materials, such as pure metals, ferrous and non-ferrous alloys, ceramics, cermets, compounds and composite materials are described in chapter 4 which, together with chapters 3 and 5 captures the essence of Materials Science 101. Chapter 5 deals with solid lubricants and self-lubricating solids, including polymers and polymer composites.

Next, the authors tackle the subject of modifying the behavior of surfaces by various means. Chapter six gives an excellent overview of the wide range of coating techniques, such as hard-facing, vapor deposition, spray techniques, lithography, conversion coatings, sol-gel techniques, and the like. It also addresses various surface heat treatments, such as carburizing, nitriding, boriding, chromizing, flame and induction hardening, and ion implantation, to name just a few. Criteria for selecting a coating/deposition/surface-treatment scheme are given, based on the type of wear encountered.

Adhesion is as fundamentally essential a property of a coating as wetness is of water. The surface science that underlies the development of adhesion of a coating on to a substrate must be well-understood if the gains to be achieved by applying the coating are to be realized. Thus, the authors provide a welcome treatment of the subject of surface preparation techniques for coating deposition. The various methods of cleaning by aqueous solutions, mechanical methods such as roughening, and techniques of monitoring the cleanliness and roughness are briefly dealt with. To be sure, the treatment of these topics in this book is rather sketchy, but this should not lull the reader into discounting its importance, because this is a very important aspect, as anyone who makes a living by depositing adherent coatings on surfaces knows only too well. There are other comprehensive treatises on this subject which the reader can refer to as needed.

The next three chapters go into more details of the various coating deposition methods. Chapter 8 deals with hard-facing techniques, and provides a comprehensive summary of such methods as thermal spray, welding and cladding. Chapter 9 deals with the vapor phase deposition methods. Various physical vapor deposition techniques, such as evaporation, ion plating and sputtering are described, and the microstructural and other properties of coatings deposited by these methods are briefly dealt with. Chemical vapor deposition, and its various modifications, as well as the rapidly growing field of plasma-enhanced chemical vapor deposition are treated in some detail. A nice touch rounds out this chapter, with appendices dealing with glow-discharge plasmas and vacuum systems used in vapor deposition processes. It is almost tempting to suspect that one, or perhaps both, of the authors may be

secret aficionados of the CVD/PVD technologies, even though their avowed profession is tribology.

Chapter 10 describes the inevitable "miscellaneous" techniques, which defy stereo-typical classification, and are indicative of the innovative spirit of man. Spray coatings of various flavors, electrochemical deposition techniques, sol-gel and lithography techniques, chemical methods, conversion coatings and the like are briefly covered, as are the types of materials which can be deposited by these techniques. Chapters 11 and 12 provide details of the principles and practices of various surface treatment techniques mentioned earlier, with an entire chapter devoted to ion implantation technique and materials treated thereby.

Soft lubricating coatings are discussed in chapter 13, including layered and non-layered lattice coatings, polymer coatings, soft metallic coatings, and binder materials used in the application of these coatings. Hard coatings are the subject of the next chapter, which covers ferrous and non-ferrous metallic coatings, ceramic oxide, carbide, nitride, boride and silicide coatings, as well as diamond and carbon coatings. It is a useful account of how the methods of synthesis, structure and properties of hard, tribological coatings are intimately correlated, giving the reader an appreciation of the "materials science" behind the design and application of various machine components.

The methods by which the various properties of significance in tribological applications are measured, are described in the next chapter which covers the techniques of physical examination such as hardness, density, surface roughness, internal stress, electrical properties etc. The tribological tests, such as friction, wear and corrosion, are also treated in some detail. The final, sixteenth, chapter of the Handbook is devoted to tribological applications. The various machinery components which experience tribological environment are described, such as bearings, seals and gears, cams, tappets and piston rings, electrical brushes, metal-cutting tools and components used in gas turbine, fusion reactors and magnetic storage media.

Thus, this treatise provides a well-balanced and complete erudition of the world of tribology. The text is very well-written, and the diagrams, photographs and tables are well done. One of the strengths of this book is the vast bibliography at the end of every chapter, which demonstrates the thorough and painstaking effort by the authors to acknowledge the work of hundreds of researchers in this field.

Therefore, to quote the authors: "This book is intended for graduate student of tribology, mechanical engineering, materials science, physics, and chemistry, for research workers who are active or intend to become active in materials aspects of tribology and coating technology, and for industrialists and practicing engineers who need state-of-the-art information on materials, coatings, and surface treatments that are required to improve tribological performance." This reviewer could not agree more. For the serious practitioner of the art, this book is well-worth the investment,

and McGraw-Hill deserves to be applauded for facilitating the publication of this Handbook.

D.G. Bhat
Manager
Advanced Coatings Development
GTE Valenite Corporation
Troy, Michigan 48084

MATERIALS & MANUFACTURING PROCESSES, 8(1), 107-109 (1993)

BOOK REVIEW

HANDBOOK OF INCINERATION SYSTEMS

C.R. Brunner

McGraw-Hill, Inc.
1221 Avenue of the Americas
New York, New York 10020
432 pages, hardcover, $72.50, 1991.

This handbook contains 25 chapters covering a multitude of subjects, including: waste classification, regulations, definitions, thermodynamics, various technologies for incineration and destruction, pollution control, and more. This handbook provides sufficient information to determine equipment selection, sizing, and parameters of operation for incineration equipment that burns a variety of wastes generated by industry. Numerous detailed examples are presented, which benefit the reader considerably. These sample calculations provide the method and pertinent data required to achieve a certain design.

The author has over 20 years experience in the incineration field. His area of expertise includes: design, operation, and evaluation of systems. The author has written several textbooks, several technical articles, and computer programs for the analysis of thermal disposal systems. The author's experience is manifested by a comprehensive bibliography present at the end of each chapter, permitting the interested reader further resources of specific interest.

The chapters discussing waste classification are thorough and definitive. The Standard Industrial Classification (SIC) is presented for industrial type wastes, along with typical waste generating processes. Criteria for establishing the presence of hazardous material is presented. Examples of these materials are tabulated and their Hazard Codes and Hazardous Waste Number are included. Tables are provided for identifying Acute Hazardous and Toxic wastes. However, the author did not include the levels of expose required to achieve gene mutation or death.

Regulatory requirements are discussed in regards to emissions. Federal and State regulations and National Ambient Air Quality Standards are briefly presented. State limits are tabulated for CO_2 emissions and smoke exhaust opacity.

The chapters dealing with thermodynamics and heat transfer are very basic and serve as primer for calculations for covering incineration. Moisture content and combustion calculations are presented in an informative manner. These chapters are not adequate to gleam knowledge on thermodynamics or heat transfer, but merely serve to introduce the use of these tools for system design. The reader does benefit from this presentation by not having to consult an additional handbook for these type calculations.

Air pollution control and emissions calculations are discussed fully. These discussions include NOx and SOx and COx, efficiencies of combustion, and types of smoke emitted. Numerous sample calculations are provided as engineering examples. These examples include combustion products due to incineration of sludges, liquids, and gases. Combustibility characteristics for a large assortment of materials are provided.

This reviewer was particularly interested in the chapter on incineration of radioactive waste. The author presented some generic discussion on transuranic material and the volume of waste generated in the United States. Several typical incineration methods are briefly discussed and flow diagrams for these systems are included. One very informative table lists the US incinerators used for treating radioactive wastes providing: location, application, capacity, and operating temperature. Some incinerators used outside the US for treatment of radioactive wastes are listed, also. This chapter should be expanded in the future revisions to assist the environmental engineer. In years to come this application will be of greater concern due to public interest and concern for general welfare.

The format is well thought out and the information is pertinent in today's environmental focus. The examples provided offer the environmental engineer a concise handbook of data and information. The information includes: heat transfer charts, thermodynamic data, BTU content of various combustibles, and listings of incinerator contractors and manufacturers. The author has elected to include numerous schematics, sketches, and flow diagrams. These figures enhance the discussions of the various subjects. The handbook is very concise, the examples and figures take the place of "a thousand words" many times over.

The final chapter is entitled, "Comprehensive Design Example". This design analysis walks the engineer through all the required steps for the design of an incinerator system. The author does not employ any "hand waving" as students so often complain during classes. The index is more than adequate and is quite complete, covering all the aspects of the book. The same is true for the glossary located at the end of the book. It is comprehensive and not verbose, but concise. There are no tables or charts as appendices, rather, this information is situated within the pertinent chapter juxtapose the numerical examples. This type format enhances the numerical analysis of the book, but it does disrupt the readability. However, the main premise is to provide a working handbook for the design engineer, in which case, the present format is best suited.

The manner in which the information is presented would allow the book to be used as an undergraduate introductory course in Waste Management. This reviewer is of the opinion that the handbook is not suited to be used in graduate level courses, but would enhance the book shelf of environmentally concerned engineers (and, therefore, the engineer's knowledge).

W. Reitz
Environmental Engineer / Metallurgist
Babcock & Wilcox
3225 Old Forest Rd
Nuclear Environmental Services, Inc.
Lynchburg, VA 24501

MATERIALS & MANUFACTURING PROCESSES, 8(1), 111-114 (1993)

BOOK REVIEW

HIGH TEMPERATURE SINTERING
New Perspectives in Powder Metallurgy
Vol. 9: Fundamentals Methods and Applications

edited by
H.I. Sanderow

Metal Powder Industries Federation
105 College Road East
Princeton, New Jersey
419 pages, hardcover, 1991.

This book is essentially the first available compilation that covers various aspects of high temperature sintering. It would be judicious to point out that the term "high temperature" in this book refers to relatively high temperatures compared to the normal sintering temperatures that are used for sintering ferrous materials. It is not meant to indicate very high sintering temperature in the absolute sense, i.e. sintering temperatures say in excess of 2000°C. For this book, the term high temperature denotes temperatures in excess of 2100°F, but it would be limited to temperatures below the melting point of the ferrous materials. The conventional mesh belt type sintering furnaces have a maximum temperature capability of around 2100°F. To use temperatures greater than 2100°F requires alternative furnace designs such as a pusher, vacuum, or walking beam mechanism. Sintering in these furnaces and the effect of such sintering on the final properties of the ferrous parts, forms the chapters of this book.

It had been determined that sintering of ferrous parts at temperatures of 2100°F instead of the conventional 2000°F always resulted in higher and more predictable properties. Though the added expense for using high temperature sintering can prove to be a deterrent for a number of ferrous part manufacturers, the advantages that have been gained from this cannot be ignored. High temperature sintering proved to be the key in processing low alloy steels with improved properties and fully dense tool steel parts, and in optimizing the properties of magnetic and stainless steel parts. With this effective form of sintering opening broader horizons in the area of sintered ferrous materials, intense research and development efforts were soon underway. This

book serves the critical function of compiling a large number of significant research and development papers in the area of high temperature sintering.

This book is presently the latest volume (Volume 9) in the series of books entitled "New Perspectives in Powder Metallurgy," that is published by Metal Powder Industries Federation. One of the unique feature of this book is that each of the seven sections of the book is preceded by a short introductory review by the editor. The long time experience of the editor in the area of high performance ferrous P/M parts makes the critical review and analysis extremely valuable to the reader.

As mentioned earlier, the book is divided into seven broad sections. They are:

Section I:	Overview	(2 papers)
Section II:	Stainless Steel	(3 papers)
Section III:	Tool Steel	(2 papers)
Section IV:	Magnetics	(2 papers)
Section V:	Steels (General)	(5 papers)
Section VI:	Steels (Chromium Bearing)	(3 papers)
Section VII:	Steels (Fatigue Properties)	(4 papers)

The total number of chapters in the book is 21, and the chapters are divided among the seven sections in the manner shown above. The first two chapters in the overview section provide an effective summary of the high temperature sintering process as applied to ferrous materials. The first chapter, by Volker Arnhold, offers four different reasons for high temperature sintering: (1) improved mechanical properties, (2) improved corrosion resistance, (3) ability to process reactive alloying elements, (4) and the ability to process certain alloys to full density. Specific examples are reviewed for each application area. The second paper, by Sanderow (also the editor), also reviews the advantages of high temperature sintering and briefly discusses the fundamentals of the sintering process. This paper also briefly addresses the process control requirements for high temperature sintering, which includes tighter control of the powder blend, the green density, and the sintering conditions.

The general conclusion was that high temperature sintering without the proper control system would not really be cost effective because the variation in the properties and the distortion of the parts will negate the advantages. The second section is a compilation of three papers in the area of stainless steels. One of the major factors hampering the growth of P/M stainless steels is its lower corrosion resistance compared to its wrought counterpart. Sanderow's paper describes how high temperature sintering can, in case of austenitic stainless steels, improve the strength and ductility for the same alloy density. This paper does not provide any information about the corrosion properties, but the fact that the material produced was used for valves indicates that it must have had acceptable corrosion properties. The paper by Lei, et al., however, deals extensively with the corrosion resistance of austenitic stainless steels. The authors also provide an excellent review of the past work. The last paper by Svilar and Ambs, recommends the use of low dew point gas

atmospheres or vacuum sintering atmospheres for producing parts with good corrosion resistance. An interesting case history analysis showed that a poor corrosion resistant 314 stainless steel part could regain its corrosion properties when it was resintered at 2200°F for 30 minutes in a $75H_2$:$25N_2$ atmosphere.

The third section, which deals with tool steels, consist of two papers. The first paper by Podob et al. describes a process known as FULDENS, where the sintering atmosphere is vacuum and the sintered part does not require any post- sintering hot deformation operation. Some of the AISI alloys processed by this technique have been outlined. The contributions of a very small amount of liquid formation and low temperature solid diffusion have been identified as the important parameters. The second paper, by Bee, et al., describes the sintering response of M2 and T15 grades of tool steels with and without the presence of liquid phase. For both type of steels, the sintering temperature plays a major role. Close to the optimum sintering temperature, the densification can be extremely rapid, with full densification requiring the presence of a small amount of liquid phase. For T15 grade, the optimum sintering temperature is 1260°C, and the optimum sintering temperature for the M2 grade is 1243°C. The available sintering window for the T15 grade was found to be greater than its M2 grade counterpart.

The two papers on magnetic alloys provide the reader with an insight into the processing conditions that affect the properties of these alloys. High temperature sintering in general improves the magnetic response due to the greater homogeneity, reduction of the interstitial impurities such as carbon, oxygen, and nitrogen, and an increased grain size. The paper by K.H. Moyer clearly shows the advantages of sintering magnetic materials at 2300°F instead of the conventional sintering temperature of 2050°F. The second paper, by Lall and Baum, also recognizes the importance of high temperature sintering in improving the mechanical and magnetic properties of sintered ferrous magnetic materials. The paper also identifies metal injection molding as a process that could significantly improve the properties.

The next three sections deal with various aspects of steels in general. The first section contains a variety of topics: the properties of a high strength Ni-Mo-P steel, the effect of high temperature sintering in nitrogen atmospheres, the effect of high temperature sintering in an endogas and a $95\%N_2 + 5\%H_2$ gas mixture, high pressure compaction of ferrous parts, and the effect of alloying additions on the properties of partially prealloyed powders. The next section has three papers on chromium bearing steels. The work by Zapf and Dalal describes the use of complex carbides as alloying constituents. The sintering was carried out at 1280°C in a walking beam furnace. The sintering process for chromium and manganese added P/M steels have been the subject of discussion in the next paper, by Tengzelius et al. For these alloys, it was found that conventional sintering temperatures did not result in adequate homogenization. Sintering at 1250°C, however, yields excellent mechanical properties for a Fe-2Cr-2Mn-4C material. The final paper by Sanderow, et al., discusses the sintering of an oil atomized prealloyed steel powder with 1Cr and 0.8Mn. This powder when vacuum sintered at 2350°F for 2 hours, provided materials

with excellent properties. The last section deals with the fatigue properties of steels, an extremely important topic for demanding applications.

The paper by Sonsino and his co-workers discussed the influence of sintering temperature on the homogeneity and the fatigue design of a copper and copper-nickel containing steels. The next paper, by Christian and co-workers, investigates in detail the fatigue properties of two standard P/M alloys using a designed test matrix that varied the powders, sintering atmospheres, and sintering temperatures. The higher sintering temperature affects the fatigue properties depending on the alloy composition. In case of the solid state sintered alloy, the use of higher sintering temperature improved the fatigue properties due to the faster diffusion of nickel and better homogenization of the alloy. However, in case of the liquid phase sintered material, higher sintering temperatures could degrade the properties due to pore coarsening. The next paper, by O'Brien, also discusses the dynamic properties of pressed and sintered ferrous powder metallurgy parts. The last paper, by Lindqvist, examines the effects of powder characteristics, nickel content, density, and sintering temperature on the properties of a copper, nickel, molybdenum, and carbon containing ferrous alloy. The author concludes that the large pores are detrimental to the fatigue properties. Increased density, which results in finer pores, improves the fatigue properties.

The readers can glean a great deal of information about the pros and cons of high temperature sintering of a number of specific ferrous alloy systems. A more detailed discussion on the high temperature sintering equipment would have been a good addition to the book. This book provides an excellent reference source for high temperature sintering of conventional ferrous powder metallurgy parts. The book also provides a subject and author index for easy reference. The book is a must for engineers associated with the production and development of ferrous powder metallurgy parts.

A. Bose
Senior Research Engineer
Southwest Research Institute
San Antonio, Texas

MATERIALS & MANUFACTURING PROCESSES, 8(1), 115-117 (1993)

BOOK REVIEW

LASER MICROFABRICATION THIN FILM PROCESSES AND LITHOGRAPHY

edited by
D.J. Ehrlich and J.Y. Tsao

Academic Press, Inc.
1250 Sixth Avenue, San Diego, CA 92101
587 pages, hard cover, 1989

Interest in laser microfabrication processes especially based on laser-induced thin film chemistry, has undergone tremendous growth. This growth was generated by scientist and engineers from various disciplines including surface science, electronics, chemical physics, microelectronics and materials science. This multidisciplinary nature of laser microfabrication has lead it to sustained growth in past decade.

The present book compiles a review on this vast subject put together by the experts in the field from several reputed academic, research and commercial organizations. In this attempt authors have presented information by dividing the volume in three parts: 1) Technology, 2) Fundamentals and, 3) Reactions. Part I on the technology reviews in a convenient format the fundamental scientific knowledge on laser-stimulated surface chemistry which could serve as a starting point for students and researchers to learn about the field. Part II compasses a description on state-of-the-art in the technology of these processes. Such description is very useful to application engineers. Part III is a compilation of up-to-date reference data on process parameters, thermochemical constants, photodissociation cross-sections etc. obtained from many scattered sources. It therefore is useful for the active researcher in the field.

Part I comprises of one chapter which introduces to the knowledge on optical considerations useful for laser microfabrication, state-of-the-art microfabrication systems and some instrumental design parameters. The chapter further reviews a selected number of coherent and noncoherent sources useful for microprocessing. In addition, some useful nonlinear optical techniques such as harmonic generation and stimulated Raman scattering for visible and UV generation are discussed. A reader will confront with a discussion on optical considerations relevant to focused laser-beam technology, in which a scanning visible or UV laser such as argon-ion and

krypton-ion lasers, or high-repetition-rate, pulsed solid-state YAG lasers are frequently employed. Parameters such as spatial mode-structures, Gaussian beam propagation, focusing, depth of focus, collimation and beam shaping, modulation, and monitoring are dealt with. Several state-of-the-art laser direct-write systems for interconnections are reviewed. This part of the volume concludes with broad-beam projection technology in which an excimer laser source properties, the author reviews important consideration such as image formation, coherent effects, resolution, modulation transfer function, depth of field, as well as other practical constraints such as source life, cost and reliability.

Photochemistry is usually considered as a means for carrying out molecular or even mode-selective chemical processes for chemical synthesis and purifications, isotope enrichments, and chemical fabrications of microelectronic and microchemical devices. Chuang (in Chapter 2) discusses fundamentals of these processes in description on the interaction of laser photons with the gaseous, adsorbed species and the solid substrate. Detailed classification and discussion of basic types of laser excitation, which depend on the chemical system, the optical arrangement and the laser wavelength, are given in this chapter. This chapter has also thoroughly examined the fundamental surface processes and basic interaction mechanisms involved in adsorption, surface reaction, and desorption affected by the laser radiation. In the following chapter a reader is walked through an information on spectroscopic and photochemical properties of a large number of molecules used in laser-induced thin film deposition or etching processes. Such information is important for designing of a successful laser-induced process as it hinges on a judicious selection process that matches the appropriate ambient molecule with the right laser. Surface physical or chemical processes are influenced by laser light in variety of ways.

Chapter 4 focuses on the primary photoexcitation of the solid substrate in the sequence of events a) light absorption by the solid, b) thermal relaxation of carriers, c)carrier recombination and carrier diffusion into the bulk, d) heat diffusion into the bulk. There are two extremes of behavior, depending on the partitioning of absorbed energy into the available electronic or vibrational degrees of freedom. In the first group of processes the laser is merely a spatially localized heat source enhancing the rate of a thermally activated chemical reaction where as second group comprises of processes in which photogenerated electrons and holes participate directly in chemical reaction. The degree to which processes fall at one or other extreme depends both on the partitioning of the absorbed energy into the available electronic and vibrational degrees of freedom and on the processes that transport energy away from the surface. Authors have, in this chapter, discussed the photophysics and thermophysics of these partitioning and energy transport questions from a laser microfabrication point of view. It is widely recognized that an important and unique feature of laser-beam processing is shortness of the time scale of the laser surface interaction. Because of this, the nature and kinetics of the surface processes can be very different from those that govern ordinary surface processes. This aspect was made more convincing by Zeiger, Ehrlich and Tsao in Chapter 5 through discussion on the fundamental mass-transport processes involved in laser-microchemical

reactions, with an emphasis on those strongly dependent on the size of the reaction zone.

Part III opens with a chapter on an overview of significant recent work on the laser etching of materials commonly used in microelectronic fabrication. The emphasis is on processes and parameters that control etch rates, resolution, and application. Even though, laser-induced deposition has been studied vigorously in last ten years, it has not been widely incorporated into manufacturing processes. This technology is very young, with many fundamental aspects yet poorly understood and much essential material and process characterization only beginning. The next two chapters discuss the underlying fundamentals and early experimental work on laser deposition respectively. Photochemical deposition, photochemically assisted chemical vapor deposition (CVD), localized photochemical deposition, laser-induced thermal deposition processes along with physical phenomena like surface temperature rise, thermochemistry and dynamic process are dealt with in these chapters. Thermally activated epitaxial growth is considered as a special case of thin-film deposition whereby a single crystal layer in vapor phase is deposited onto a single crystal substrate. These vapor phase epitaxial reactions are modified through photolytic and photothermal processes which result into a phenomenon called photochemistry. Chapter 9, explores the range of those photoepitaxial processes and the range of semiconductor materials successfully prepared by photoepitaxy. The volume concluded with a Chapter 10 which deals with the use of photon beams to locally modify the structural and electronic properties of materials by the controlled introduction of a range of atomic species. Process such as laser doping and laser oxidation were explained through underlying mechanisms and their effects in specific materials.

In summary, the volume serves the purpose of being a comprehensive source on various aspects including principles, science and applications of laser microfabrication. It contains numerous references on recent scientific as well as commercial work conducted in the field. Chapters keep flow in the subject and a reader becomes more and more involved as well as interested in the subject matter irrespective of the fact whether he is familiar with the subject. The reviewer highly recommend the book to anybody who is interested in the subject.

N.B. Dahotre
Center for Laser Applications
University of Tennessee Space Institute
Tullahoma, Tennessee 37388

MATERIALS & MANUFACTURING PROCESSES, 8(1), 119-124 (1993)

BOOK REVIEW

POWER BEAM PROCESSING
Electron, Laser, Plasma-Arc

Proceedings of the International Power Beam Conference
May 2-4, 1988, San Diego, California, USA

edited by
E.A. Metzbower and D. Hauser

ASM International and the Edison Welding Institute
300 pages, hardcover, 1988.

This book contains the research papers that were presented at the International Power Beam Conference on May 2 - 4, 1988 in San Diego, California. It begins with an introduction to the power beam processes. There are two papers on the Plasma Arc Welding (PAW) process, twelve papers on Electron Beam Welding (EBW), and fourteen papers addressing Laser Beam Welding (LBW). In general, the papers are well written and cover a variety of topics. It appears that an effort was made to include research on the processes as they are used for fabrication and manufacturing, as well as characterization of the processes themselves. This reviewer has attempted to give a brief summary of the content of each study.

The book begins with a quick introduction by Johnson to the power beam processes, which are defined as those processes capable of producing energy densities greater than 10 kW\mm² and are therefore capable of deep "keyhole" penetration. It gives a brief description of Plasma Arc Welding (PAW) and how the arc is constricted to concentrate its power. There is a summary of some of the processes that PAW is used for; seam welding of tubes and low penetration weld surfacing are two examples that are described.

The article then gives a short review of the Laser Beam Welding (LBW) process. It tells about some industrial uses and gives a good description of the process as it is used to surface treat the inside of 4.7 in. diameter tank gun barrels. Some of the new equipment that is currently being manufactured is discussed in addition to some of the savings and advantages that are inherent to the LBW process.

Finally, the article examines the Electron Beam Welding (EBW) process and how it has evolved over the past twenty years. It discusses improvements that have

been made to power supplies and to electron guns. Most of the discussion is related to gun discharge, a phenomenon that occurs under normal operation.

The book continues with one article by Gittens and one abstract by Whitfield and Browning about the PAW process. The latter appears to have been an interesting idea; its omission was regretted. The former is an overview which describes the fundamentals of the PAW process, its applications in industry, and its impacts on productivity and quality. It gives some history of PAW and compares it to Gas Tungsten Arc Welding (GTAW), the process from which it was derived. The PAW process is used today in such areas as welding, cutting, surfacing, and gouging. A good description of arc fundamentals and process variables is given, along with the effects of changing some of these variables. Some of the major variations are accounted for; for example, different methods of plasma arc cutting are addressed. The article concludes with some fundamentals of the PAW process and some of its applications in today's welding environment.

The next twelve articles cover the topic of Electron Beam Welding (EBW), beginning with an overview of the process by Powers. This first article gives a very brief but thorough introduction to the EBW machine and some of the process parameters. It tells how the process was first used for the nuclear and aerospace industries, and how it was limited to these industries by the fact that a vacuum is required. However, as the high production industries (automotive, etc.) saw its potential, it was adapted for use without a high vacuum system, making the process faster. The article is more a history of the process than a summary of its technical capabilities.

Next is an article by Burns and Higgins describing a specific production application and how a second-hand EBW machine was purchased and subsequently modified to produce consistent high quality welds. It gives a good synopsis of their problem, and how they arrived upon the decision to upgrade a machine like this. The three main improvements that were made to the machine included the upgrading of the beam focus control (for spot definition), the beam current control, and the mechanical fixturing. These improvements resulted in improved machine control, and thus increased weld quality and yield. The article closes with a few paragraphs on the economic aspects of EB welding; specifically, it gives a biased comparison of EBW and LBW, explaining why EBW is advantageous.

A comparison of the EBW and the PAW processes is made in the next paper by Chen and Yeh. The weld shapes, microstructures, mechanical properties, and residual stresses resulting from each of these two processes are compared. Generally, PAW is a low cost alternative to EBW and is considered to be competitive when welding thin gauge metals. EBW is limited by the size of each machine's vacuum chamber and by the cost of tooling and joint preparation, which must be precise. However, for critical applications where high precision and repeatability are a must, EBW is the best choice.

The actual investigation compares the two processes as they are used to weld 17-4 PH stainless steel. All welding parameters are given and the results are discussed thoroughly. The typical heat inputs necessary to produce full penetration welds in base metal with a thickness of 3.2 mm are 400% higher for PAW, and the fusion zone is approximately 300% wider. This obviously means that the PAW process could cause more shrinkage and distortion. A fairly detailed discussion of the resulting microstructures follows, with the important point being the much higher levels of δ-ferrite that results from the PAW process. A study of the mechanical properties shows better values for yield strength, elongation, and impact toughness are obtained from EBW. Microhardness measurements reveal the presence of overtempered zones in PA welds, which result in double-necking and failure in tensile tests. The article closes with a list of experimental results in the Conclusion section, but fails to mention the real conclusion: EBW produces superior welds to PAW in 17-4 PH stainless steel based on studies of mechanical properties, microstructures, heat inputs, and microhardness measurements.

The next paper, by King and Hudson, describes a fabrication method for producing an improved Duplex Crack Arrest (DCA) specimen. EBW is used to join hardened 4340 steel, which serves as a crack initiator, to A533 grade B class 1 steel which has had a Submerged Arc Weld (SAW) produced on it. A crack is initiated in the 4340 steel, runs perpendicularly through the EB weld and travels into the actual test material. The resulting crack length is then measured. The welding was done in two passes, one from each side of the joint, and produced defect free welds with a minimum heat input. This minimized the tempering of the material in the heat affected zone on the 4340 side of the joint. By remelting the surface of the SAW using the electron beam, the surface was degassed and porosity was reduced in the EB weld. Photomicrographs reveal that excellent weld microstructures are the result, and show that this process could possibly be used for many materials that form porosity in EB welds.

3Cr-1.5Mo-.1V steel is used to characterize the EB welding of thick section ferritic steels in the next study by David, King, and Vitek. It tells how single pass, full penetration welds can be made in 102 mm thick steel. It describes the changes in microstructure and the effects welding has on mechanical properties. A post weld heat treatment is used to reduce the mechanical property variations.

The deep vapor channel phenomenon in EBW is discussed next in a paper by Leskov and Nesterenkov, which describes attempts to actually measure the vapor pressure in the channel. An ion manometer measures the vapor pressure in the channel and, subsequently, the ion current produced during welding. The ion current is a good indication of weld quality and process efficiency.

Next is an article by Zubchenko, et al. describing the construction of a 120 kW electron gun. Included is the development of a tungsten cathode to eliminate the problems caused by a lanthanum boride cathode. Also the design of the triode emission system is discussed. The gun is built in modules, which appears to make it serviceable and amenable to design modifications. The gun can be used with either

a tungsten or a lanthanum boride cathode, with conversion from one to the other being fairly easy. An all-brazed alumina high voltage insulator was also developed to ensure electrical integrity. This seems to be a very powerful gun and could be used to weld extremely thick sections.

The elimination of root defects formed in partial penetration EB welds is a common problem that is addressed in the next paper by Akopyants, et al. The problem is confronted by varying the beam scanning angle. Increasing the angle widens the root of the weld and decreases the chance of creating a void there. When the root of the weld is widened, it becomes more rounded, and cooling rates are decreased, allowing time for the molten metal to wet the weld root.

A summary of EB welding and repair procedures is the topic of the next article by Nazarenko and Kaidalov. It gives a very brief summary of many (24) different approaches to EB welding. None are treated in detail, but it lists several references to get details on each subject and could possibly be a good literature source.

The next paper by Paton, et al. describes a fairly new development in EB welding; EB cladding is used to improve the weldability of thick section structural steel welds. The process is described and calculations modelling the heat transfer details are shown. This appears to be a reliable, economical process since it uses existing equipment and can be used to refine metals that would otherwise be difficult to weld.

The last study addressing the EBW process, by Sanderson and Ribton, describes a detector that is designed to aid in seam tracking for the EBW process. The method described uses back-scattered electrons to keep the beam aimed at the joint. The advantages are listed as compared to other techniques, such as optical or mechanical alignment. Technical details are not given, but many figures are included and the system is thoroughly described.

The fourteen articles addressing the Laser Beam Welding (LBW) process begin with Lessman's brief history of the process and some of its evolution. It describes the tremendous growth in commercial and research activity related to LBW that has occurred since lasers were introduced to manufacturing in 1966. Many applications for using the laser as a metal working tool are discussed. Offering uses in cutting, welding, heat treating, brazing and soldering, cladding, and hardfacing, the versatility of the laser has allowed it to succeed despite the fact that it requires a hefty investment and offers very poor thermal efficiency. Many applications are described and pictured.

The second LBW paper, by Moon and Metzbower, describes a technique for measuring base metal temperatures near the weld using thermocouples. The temperatures were measured and tabulated using a computer program and, from these measurements, the laser welding efficiency was calculated to be ~66%.

An analytical approach to studying 3D heat flow during full penetration LBW is described in the next study by Tsai and Kou. The laser beam is treated as a non-uniform line heat source. Calculations are made for a uniform heat source; Beer-Lambert's law is used and is then modified to account for the laser being a non-uniform heat source. The solution can be used to predict several weld pool shapes, and some of their predictions are verified experimentally.

The next paper, by Metzbower, tells of another method of calculating heat flow efficiency for the LBW process. Temperature measurements are taken at various distances from the weld and are used to construct a temperature profile. The profile can then be extrapolated and used to find the proper heat input to reproduce itself. This article concludes that 50% of the beam energy is converted to heat, which indicates an even lower efficiency than is calculated in a previous paper in this book.

A practical approach describing a method of producing dual spot welds from one heat source via a fiber optic system is addressed ir the fifth LBW paper by Coyle, Webb, and Solan. A simple beam divider and system of optical fibers is used to produce matched spot welds. The beams are actually "homogenized" during their travel through the fiber to aid in obtaining identical welds. Several ideas for future study are mentioned, most involving efficiency and beam power losses. This study does not address the question of efficiency at all.

Pulsed ND:YAG laser welding is used to hermetically seal electromechanical relays, and this process is described in the next article, by Fuerschbach. It describes the development of the weld schedule and how the final assembly is tested for airtightness. It also describes a problem encountered in production; porosity began to appear in the weld. This was found to be the result of having Type 304 stainless steel inadvertently substituted for Type 304L, and was thought to be the result of a carbon/oxygen reaction that does not occur with the low carbon alloy. This is a good paper describing a real production investigation.

The next paper, by Norris, is a study of the LBW process as it is used to weld thick section structural steels. A high power (>10kW) welding machine is used. The study characterizes the impact toughness behavior of autogenous laser welds and investigates techniques for adding filler metal. Weld microstructures, hardness, and toughness properties were investigated. Welding speed is reported to have a significant effect on these properties. Adding filler metal had a good effect, producing low hardness weld metal with good toughness properties. There were a lot of porosity problems encountered with the welds that had filler metal added.

Next is a short paper by Gnanamuthu and Moores describing laser welding of the 8090 Aluminum-Lithium alloy. Autogenous welds are explored and preparation techniques are discussed. Welding parameters are varied and the effects on the weld are examined. This article could have been more in-depth; it seems to have a lot of good information.

The effect of polarization on penetration in CO_2 LBW is addressed in the next paper by Garashchuk and Kirsey, which studies the effect of varying the angle between the electric intensity vector and the direction of travel, and also studies the angle of incidence of the laser beam. Depths of penetration are calculated theoretically and then verified with actual welding procedures. The results seem to be quite accurate.

The next paper, by Tönshoff and Emmelman, discusses the laser as it can be used to process ceramic materials. The effects of the laser on the machined surfaces is examined, along with the effects of thermal stresses. It discusses the appearance of the cut surfaces and some of the effects of the different laser types (ND:YAG, CO_2, and excimer).

The casting of metal powder into shapes using the laser beam is addressed next in a paper by Whitlow and Bruck. The process is used to build up near net shape components from existing substrates. Layers of the cast material are melted on top of each other to produce the final thickness. High volume production is demonstrated with the results verified microstructurally.

The next paper, by Xiao-yeng, et al., discusses the problem of obtaining a uniform composition in the fusion zone of a laser weld used for surface alloying. It is found that the composition uniformity strongly depends on the shape coefficient of the fusion zone. The shape coefficient is defined as the diameter ÷ height of the weld, and is dependent on the power density and interaction time.

The last paper, by Tönshoff and Semrau, discusses the variation of process parameters in LBW and the addition of water to the gas used in laser cutting. This paper concludes that the addition of water causes processing points to become processing ranges, thus making the process more forgiving.

In closing, this book should serve as a good reference to anyone investigating the high power density welding processes. The research papers that are presented and the references quoted in each one are all excellent sources of information. I recommend it for researchers involved with these processes.

J.M. Kalinowski
Research Engineer
Sverdrup Technology
2001 Aerospace Parkway; MS 49-3
Brook Park, Ohio 44142

MATERIALS & MANUFACTURING PROCESSES, 8(1), 125-128 (1993)

FORTHCOMING MEETINGS

APRIL 1993

12-16 **MRS Spring Meeting**: San Francisco, CA. M. Geil, Materials Research Society, 9800 McKnight Rd., Pittsburgh, PA 15237. (412) 367-3003; fax (412) 367-4373.

13-17 **9th International Conference on Wear of Materials**: San Francisco, CA. Wear of Materials Secretariat, COMST, P.O. Box 415, 1001 Lausanne 1, Switzerland. 41 (21) 234 886; fax 41 (21) 234 972.

19-23 **International Conference on Metallurgical Coatings and Thin Films**: San Diego, California. Gregory J. Exarhos, Pacific Nothwest Laboratory, Battelle Blvd., P.O. Box 999, MS K2-44, Richland, WA 99352. (509) 375-2526; fax (509) 375-2186.

20-22 **8th International Conference on the Mechanics of Composite Materials**: Riga, Latvia. International Conference MCM-93, Institute of Polymer Mechanics, 23 Aizkraukles Street, Riga 226006, Latvia. 97-0132-551149.

20-23 **Computer Methods and Experimental Measurements for Surface Treatment Effects**: Southampton, U.K. Sue Owen, Conference Secretariat, Wessex Institute of Technology, University of Portsmouth, Ashurst Lodge, Ashurst, Southampton, SO4 2AA, U.K. (44) 703 293223; fax (44) 703 292853.

21-23 **International Conference on Hot Isostatic Pressing**: Antwerp, Belgium. R. Peys, K VIV-HIP 93, Desguinlei 214, B-2018 Antwerpen, Belgium. 32-3-216-09-96; fax 32-3-21-06-89.

MAY 1993

6-8 **Fift Annual 1993 International Industrial Symposium on the Super Collider (IISSC) and Exhibition**: San Francisco, CA. Ms. Regina Borchard, Martin Marietta Energy Systems, Inc., HAZWRAP, P.O. Box 2003, MS 7606, Oak Ridge, TN 37831-7606; (615) 435-3425; fax (615) 435-3523.

16-21 **Electrochemical Society Meeting:** Honolulu, Hawaii. Electrochemical Society, Inc., 10 South Main St., Pennington, NJ 08534.

17-18 **Mesostructural and Mesomechanics in Composite Materials:** Ontario, Canada. Dr. M.R. Piggot, University of Toronto, 215 Huron Street, Toronto, Ontario M5S 1AI, Canada. (416) 978-4745.

24-28 **13th International Plansee Seminar '93: Refractory Metals and Hard Materials - Key to Advanced Technologies:** Dr. mont. Ralf Eck, Metallwerk Plansee GmbH, A-6600 Reutte, Austria.

JUNE 1993

3-6 **Scientific and Technical Conference: Anodic Aluminum Oxide Films:** Tatarstan, Applied Physics and Chemistry Department, K. Marx Str 10, Interanode-93, Kazan Aviation Institute, 420111 Kazan, Tatarstan. 39-08-01; fax 843 236 9393.

7-9 **Engineering Solutions to Industrial Corrosion Problems:** Sandefjord, Norway. Prof. R.N. Perkins, c/o NACE UK Representative, P.O. Box 47, Godalming, Surrey GU7 1TD, U.K. 44 (0) 483-418299; fax 44 (0) 483 418928.

8-14 **8th International Conference on Fracture:** Kiev, USSR. ICF8 Secretariat, Karpenko Physico-Mechanical Institute of the UkrSSR Academy of Sciences, 5 Naukova Street, LVIV 290601, USSR. 7(044) 2276016; fax 7(044) 2680486.

13-18 **21st Biennial Conference on Carbon:** Buffalo, NY. D. Chung, Composite Matenals Research Lab., Fumas Hall, SUNY, Buffalo, NY 14260; (716) 636-2520; fax (716) 636-3875.

14-18 **5th International Conference on Welding and Melting by Electron and Laser Beams:** Conference Secretariat, 5 eme CISFFEL, c/o Institut de Soudure, 32 boulevard de la Chapelle, F-75882 Paris Cedex 18, France.

JULY 1993

12-15 **Powder Metallurgy World Congress '93:** Kyoto, Japan. JPMA, Tamagawa Building 2-16, Iwamoto-chu 2-Chome, Chiyoda-ku, Tokyo 101, Japan.

12-16 **Cryogenic Engineering Conference/International Cryogenic Materials Conference (1993 CEC/ICMC):** Albuquerque, New Mexico. Coordinator Jan C. Hull, Los Alamos National Lab, Protocol Office, MS P366, Los Alamos, NM 87545. (505) 667-6574; fax (505) 667-7558.

AUGUST 1993

25-27 **Applied Diamond Conference: Second International Conference on the Applications of Diamond Films and Related Materials**: Saitama, Japan. M. Murakawa, Program Committee Chairman, Department of Mechanical Engineering, Nippon Institute of Technology, 4-1 Gakuendai, Miyashiro, Minami-Saitama-Gun, Saitama 345, Japan. 81-480-34-4111 Ext 409; fax 81-480-34-2941.

SEPTEMBER 1993

5-10 **44th ISE Meeting**: Berlin, Germany. Prof. W. Plieth, Institut of Physical & Theoretical Chemistry, Free University of Berlin, Takustrasse 3, D-1000 Berlin 33, Germany.

6-9 **International Conference on Computer-Assisted Materials Design and Process Simulation - COMMP '93**: Japan. Iron and Steel Institute of Japan, Secretariat, COMMP '93, Keidanren Kaikan, 3rd Floor, 1-9-4 Otemachi, Chiyoda-ku, Tokyo 100, Japan. fax (81) 3-3245-1355.

12-15 **Progress in Electrolysis - Theory and Practice**: Ferrara, Italy. Prof. S. Trasatti, Department of Chemistry & Electrochemistry, Via Venezian 21, 20133 Milan, Italy.

19-24 **12th International Corrosion Congress**: Houston, TX. NACE Membership Services Department, P.O. Box 218340, Houston, TX 77218. (713) 492-0535; fax (713) 492-8254.

26-30 **International Symposium on Structural Intermetallics**: Champion, PA. Dr. R. Darolia, GE Aircraft Engines, Mail Drop M-89, Cincinnati, OH 45215; (513) 243-4509; fax (513) 243-3250.

27-29 **CANCOM '93 Second Canadian International Conference on Composite Structures and Materials**: Ottawa, Canada. Dr. W. Wallace, Co-chairman, CANCOM '93, Institute for Aerospace Research, National Research Council of Canada, Ontario, Canada K1A 0R6; fax (613) 993-7136.

27-29 **3rd International Conference on Near-Net-Shape Manufacturing**: Pittsburg, PA. ASM International, Materials Park, OH 44073-0002. fax (216) 338-4634.

OCTOBER 1993

14-15 **Adhesions**: Fort Worth, Texas. Dorothy Savini, Symposium Operations, ASTM, 1916 Race Street, Philadelphia, PA 19103, (215) 299-5529; fax (215) 299-2630.

NOVEMBER 1993

2-4 **3rd Pacific Rim Forum on Composite Materials**: Honolulu, Hawaii. Prof. Stephen W. Tsai, Department of Aeronautics and Astronautics, Stanford University, Stanford, CA 94305. (415) 725-3305; fax (415) 725-3377.

15-19 **40th Annual AVS Symposium**: Orlando, FL. American Vacuum Society, 335 E. 45 St., New York, NY 10017-3483; (212) 661-9404.

29-3 **MRS Fall Meeting**: Boston, MA. M. Geil, Materials Research Society, 9800 McKnight Rd., Pittsburgh, FIA 15237. (412) 367-3003; fax (412) 367-4373.

DECEMBER 1993

8 **Symposium on Case Studies of Wear-Related Failure Analyses**: Fort Worth, Texas. Chairman Floyd W. Wood, Rt.2, Box 2437, Melrose, FL 32666-8522, (904) 772-4519; after December 20, 1992 (904) 475-1056.

MARCH 1994

21-25 **APS March Meeting**: Pittsburgh, PA American Physical Society, 335 E. 45 St., New York, NY 10017-3483; (212) 682-7341.

APRIL 1994

11-15 **MRS Spring Meeting**: San Francisco, CA. M. Geil, Materials Research Society, 9800 McKnight Pld., Pittsburgh, PA 15237. (412) 367-3003. fax (412) 367-4373.

MAY 1995

22-24 **Zinc & Lead '95**: Sendai, Japan. M. Hino, Department of Metallurgy, Faculty of Engineering, Tohoku University, Aoba, Aramaki, Sendai, Japan 980. fax 81-22-268-2949, or J.E. Dutrizac, CANMET, 555 Booth Street, Ottawa, Ontario, Canada K1A 0G1. (613) 995-4823; fax (613) 995-9041.

Just Published . . .

1992 WORLD CONGRESS JUNE 21-26 / SAN FRANCISCO

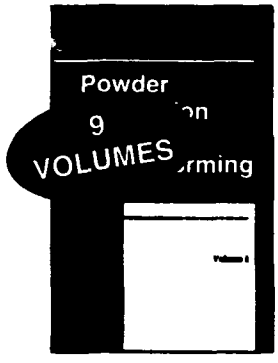

Advances in Powder Metallurgy & Particulate Materials - 1992

Proceedings of the
1992 Powder Metallurgy World Congress
June 21-26, San Francisco, California

Compiled by: Joseph M. Capus, Randall M. German

Largest ever compilation of papers on powder metallurgy and particulate materials:

- 90 Technical Sessions with 231 papers
- 4 Special Programs with 50 papers
- Poster Program with 27 papers

6" x 9", hardcover, 4576 pages
subject and author index
$1000 list price
$900 APMI Member price
$800 MPIF Member price
ISBN 1-878954-19-9

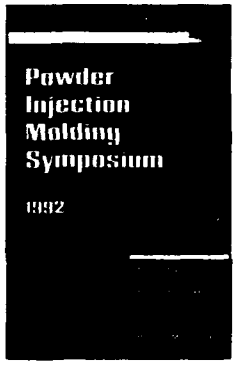

Powder Injection Molding Symposium - 1992

A separate, edited proceedings of the
1992 Powder Injection Molding Symposium
June 21-26, San Francisco, California

Edited by: Philip H. Booker, John Gaspervich, Randall M. German

One volume with 36 papers in the following subject areas: Powders • Binder Systems • Feedstock • Process Control • Material Systems • Molding • Debinding • Sintering • Flow Modeling • PIM Applications

6" x 9", hardcover, 528 pages
subject and author index
$135.00 list price
$121.50 APMI Member price
$108.00 MPIF Member price
ISBN 1-878954-18-0

Order From:
Metal Powder Industries Federation
105 College Road East
Princeton, N.J. 08540-6692
Telephone: (609) 452-7700
FAX: (609) 987-8523

In Europe
European Powder Metallurgy Association
Old Banks Bldgs., Bellstone
Shrewsbury, England
SY1 1HU
Phone: (0743) 64675
Fax: (0743) 62968

In Japan
Multi-Tech Research Corp.
Meguroeki Higashiguchi
Bldg. 3-1-5 Kamiosaki
Shinagawa
Tokyo 141 Japan
Phone: (03) 3449-0091
Fax: (03) 3445-8013

THE PREPARATION OF MANUSCRIPTS FOR DIRECT REPRODUCTION

A paper submitted for publication must be an original work that is not being considered for publication elsewhere.

DIRECTIONS FOR SUBMISSION

One original manuscript suitable for direct reproduction, carefully inserted in a folder, and three (3) copies of the manuscript must be submitted to one of the Editors:

T.S. Sudarshan — *Materials Modification, Inc.*
2929-P1 Eskridge Center, Fairfax, VA 22031

T.S. Srivatsan — *Department of Mechanical Engineering*
The University of Akron, Akron, OH 44325

FORMAT OF MANUSCRIPT

1. The general format of the manuscript should be as follows: title of article; names and full addresses of authors, abstract (maximum 150 words) and text discussion. All headings should be capitalized and centered. Allow three lines of space below the abstract before beginning the article. The text discussion should be divided into such major sections as INTRODUCTION, METHODS, RESULTS, DISCUSSIONS, ACKNOWLEDGEMENTS, and REFERENCES. These major headings should be separated from the text by two lines of space above and one line of space below. Main headings should be flush with the left margin, capitalized, and underscored; however REFERENCES heading must be capitalized and centered. Secondary headings, throughout the paper, should be flush with the left margin, underscored, and have the first letter of all main words capitalized. Only two levels of headings must be provided. Do not number headings. Leave two lines of space above and one line of space below secondary headings. The full reference listing, collected at the end of text, will be consecutively numbered in numerical order, and citings within text will be numbered in parentheses "( )". No footnotes should be included.

2. Paragraphs should start with a TAB character in the word processing file. Each page of manuscript should be numbered lightly at the bottom of the sheet with a light blue pencil.

TYPING INSTRUCTIONS

1. It is mandatory that authors submit a MS DOS formatted diskette containing their manuscript on either WordPerfect, Wordstar, Multimate software format or as an ASCII file. Diskette must be clearly marked with author name, file name, computer, and software used. The date submitted must be marked on the diskette, and on the first page of all copies of printed manuscripts.

2. The manuscript must be printed on good quality white bond paper measuring approximately 8½ x 11 inches (21.6 cm x 27.9 cm), with one inch margin on all sides.

3. The chapter title, abstract, tables, and references, and all other text discussion should be printed single-spaced. Prestige elite character (12 pitch) is recommended. Do not change font, TAB set, or line-spacing within the text.

4. Tables should be typed as part of the text, and must be separated from the text by a two-line space above and below the table. If using WordPerfect software, please use Tables option to create tables. Use Arabic numerals for the table number. Tables

MATERIALS AND MANUFACTURING PROCESSES

Volume 8, Number 1, 1993

Special Issue on Hard Carbon Films

CONTENTS

MARCEL DEKKER, INC. New York, Basel, Hong Kong

Contributions to this journal are published free of charge

should be inserted in the text as close to the point of reference, and authors must make sure that one table does not run over to the next page. Titles should be typed single-spaced preceded by the word TABLE. Use the full width of the type page for the table title. Use TABs (not spaces) to align columns in tables.

5. Graphs, and other numbered figures should be professionally drawn in black India ink or prepared using graphics software and printed on laser printer. They must be placed on separate sheets of white paper and placed at the end of the text. Two graphs or figures should be placed per page. Allowing for figure captions, each figure must fit within the size 5" width x 3" height. Figures should not be placed within the body of the text. Photographs must be glossy prints and must have micron markers. Photographs larger than 5" width x 3" height will be rejected. Figure numbers, name of senior authors, and arrow indicating "top" should be written in light blue pencil on the back or typed on a gummed label, which should be attached to the back of the illustration. A typewriter or lettering set should be used for all labels on the figures or photographs. For graphs, legend for symbols used (eg. $\oplus$, $\odot$, Δ) must be placed within each graph, and NOT in the caption. Captions for the figures should be typed single-spaced on a separate sheet, along the full width of the type page, and preceded by the word Figure and a number in Arabic numerals.

6. The reference list, consecutively numbered in numerical order, should be separated from one another by an extra line of space. References to journal articles should include (1) surname, first and middle initials, (2) journal, (3) volume number, (4) first page, and (5) year, in that order. References to books should include (1) author; surname, first and middle initials, (2) title of book, (3) editor of book (if applicable), (4) edition of book (if any), (5) publisher, (6) city of publication, (7) page reference, and (8) year of publication. A sample reference is given below:

> 18. Aselage, T., and K. Keefer, Journal of Materials Research, Vol. 3, No. 6, p. 1279, (1988).

Use Indent key in word processor after entering reference number. Expand all abbreviations such as "Proc.", "Inst.", "J.", etc.. For the first author, enter last name first. For journal articles, the issue MUST BE specified in the format: "Vol. 37, No. 2, p. 81, (1990)."

7. All quantities should be expressed in SI units.

8. All papers must have a list of 15 Key Words listed on a separate sheet of paper, one per line and first letter capitalized. The list must also be included in the diskette submitted.